ISTANBUL TECHNICAL UNIVERSITY ★ GRADUATE SCHOOL

THIOL-DIBROMOMALEIMIDE POLYMERIZATION: A SIMPLE STRATEGY FOR EASILY DEGRADABLE AND MODIFIABLE POLYTHIOETHER SYNTHESIS

M.Sc. THESIS

Gülşah İlayda TEZCAN

Department of Chemistry

Chemistry Programme

MAY 2025

ISTANBUL TECHNICAL UNIVERSITY ★ GRADUATE SCHOOL

THIOL-DIBROMOMALEIMIDE POLYMERIZATION: A SIMPLE STRATEGY FOR EASILY DEGRADABLE AND MODIFIABLE POLYTHIOETHER SYNTHESIS

M.Sc. THESIS

Gülşah İlayda TEZCAN
(509231259)

Department of Chemistry

Chemistry Programme

Thesis Advisor: Prof. Dr. Hakan DURMAZ

MAY 2025

İSTANBUL TEKNİK ÜNİVERSİTESİ ★ LİSANSÜSTÜ EĞİTİM ENSTİTÜSÜ

TİYOL-DİBROMOMALEİMİD POLİMERİZASYONU: KOLAY PARÇALANABİLİR VE MODİFİYE EDİLEBİLİR POLİTİYOETER SENTEZİ İÇİN BASİT BİR STRATEJİ

YÜKSEK LİSANS TEZİ

Gülşah İlayda TEZCAN
(509231259)

Kimya Anabilim Dalı

Kimya Programı

Tez Danışmanı: Prof. Dr. Hakan DURMAZ

MAYIS 2025

Gülşah İlayda TEZCAN, a M.Sc. student of ITU Graduate School student ID 509231259 successfully defended the thesis/dissertation entitled "THIOL-DIBROMOMALEIMIDE POLYMERIZATION: A SIMPLE STRATEGY FOR EASILY DEGRADABLE AND MODIFIABLE POLYTHIOETHER SYNTHESIS", which she prepared after fulfilling the requirements specified in the associated legislations, before the jury whose signatures are below.

Thesis Advisor :	**Prof. Dr. Hakan DURMAZ** Istanbul Technical University	.....
Jury Members :	**Assoc. Prof. Dr. Ufuk Saim GÜNAY** Istanbul Technical University	.....
	Prof. Dr. Emrah ÇAKMAKÇI Marmara University	.....

Date of Submission : 08 May 2025
Date of Defense : 20 May 2025

To my family,

FOREWORD

As I reach the end of this two-year master's journey, which has been full of challenges, growth, and valuable experiences, I feel incredibly grateful to everyone who supported, encouraged, and stood by me throughout this period. This process has not only contributed to my academic development but also shaped me personally, and I will always cherish the memories and lessons it brought.

First and foremost, I would like to express my heartfelt and sincere gratitude to my thesis supervisor, Prof. Dr. Hakan DURMAZ, for the invaluable opportunity to complete my M.Sc. thesis under his guidance. It has truly been a privilege to collaborate with him throughout this journey. I also wish to thank Assoc. Prof. Dr. Ufuk Saim GÜNAY for his support. I am particularly grateful to Dr. Gökhan SAĞDIÇ, as this work would not have been possible without his experience and expertise.

I would also like to thank my lab-mate and one of my best friends, Oğuzhan ASLANTÜRK, who, while pursuing his M.Sc., acquired nearly as much laboratory experience as one would typically gain during a Ph.D. He not only accumulated this wealth of knowledge but also took the time to share it with me. Whenever I faced challenges, he was always there to assist, responding to my calls and offering invaluable support.

I would like to extend my sincere gratitude to my dear friend and Research Assistant Emre Can UYSAL, whose continuous motivational support throughout the course of my research played a significant role in sustaining my determination and progress. I am also thankful to my friends Meltem FİLİZ and Zeynep ACUN for their kindness, encouragement, and friendship throughout this journey.

I am deeply thankful to my beloved mother Fatma TEZCAN and my father Yüksel TEZCAN for their unwavering support. My sincere thanks also go to my cousin, whom I consider a sister, Fatma TOKSOY, as well as to my brother Arin Tuna TEZCAN and his wife Özge GÖKSU, who is like a sister to me, for their constant encouragement and presence throughout this journey.

This work was supported by the Research Fund of the Istanbul Technical University (Project Number: 2024-46265).

May 2025

Gülşah İlayda TEZCAN
(Chemist)

TABLE OF CONTENTS

ABBREVIATIONS

^{1}H NMR **:** Hydrogen Nuclear Magnetic Resonance Spectroscopy
^{13}C NMR **:** Carbon Nuclear Magnetic Resonance Spectroscopy
ATRP **:** Atom transfer radical polymerization
$CHCl_3$ **:** Chloroform
DABCO **:** 1,4-diazabicyclo[2.2.2] octane
DBM **:** 2,3-Dibromomaleimide
DBU **:** 1,8-diazabicyclo[5.4.0]-undec-7-ene
DIPEA **:** *N*,*N*-diisopropylethylamine
DMAc **:** *N*,*N*'-dimethylacetamide
DMF **:** *N*,*N*'-dimethylformamide
DMSO **:** Dimethyl sulfoxide
DSC **:** Differential Scanning Calorimetry
FTIR **:** Fourier Transform Infrared Spectroscopy
GPC **:** Gel Permeation Chromatography
HDT **:** 1,6-hexanedithiol
NMP **:** *N*-methyl-2-pyrrolidone
PFCP **:** Perfluorocyclopentene
PPM **:** Postpolymerization modification
PS **:** Polystyrene
RAFT **:** Reversible addition fragmentation chain transfer polymerization
ROMP : Ring Opening Metathesis Polymerization
TEA **:** Triethylamine
THF : Tetrahydrofuran
TMG : 1,1,3,3-tetramethylguanidine

SYMBOLS

%	**:** Percentage
°C	**:** Degree Celcius
cm^{-1}	**:** Wavenumber
δ	**:** Chemical shift
Đ	**:** Dispersity
kDa	**:** Kilodalton
M_w	**:** Weight average molecular weight
T_g	**:** Glass transition temperature

LIST OF TABLES

Page

LIST OF FIGURES

Page

THIOL-DIBROMOMALEIMIDE POLYMERIZATION: A SIMPLE STRATEGY FOR EASILY DEGRADABLE AND MODIFIABLE POLYTHIOETHER SYNTHESIS

SUMMARY

In this work, 2,3-dibromomaleimide (DBM) and multiple dithiol monomers were polymerized into linear poly(maleimide thioether)s through the thiol-dibromomaleimide (thiol-DBM) reaction. Numerous dithiols with varying structural characteristics reacted with DBM to produce a range of polymer structures under optimized conditions. These polymerizations proceeded via a substitution mechanism, allowing the formation of new polymer backbones carrying unsaturated maleimide units along the main chain and free imide N−H functional groups in the side chains. The produced polymers were isolated in high yields, and their molecular weights ranged from 7.3 to 68.2 kDa, thereby opening up a wide range of applications.

Following polymerization, an imide-yne click reaction using different propiolates was employed to modify the free N-H groups in the polymers' side chains. The 1,4-diazabicyclo[2.2.2]octane (DABCO) organocatalyst was effectively utilized to carry out this modification process, resulting in notable changes in the structural characteristics of the polymers. All synthesized poly(maleimide thioether)s exhibited a wide range of glass transition temperatures (T_g) depending on the structure of the dithiol used, indicating that the thermal properties of the material can be adjusted according to the desired applications.

In addition, it was experimentally demonstrated that the obtained poly(maleimide thioether)s could be easily degraded in the presence of a monothiol. For this purpose, detailed degradation studies were carried out on a model polymer and a cross-linked network using an excess amount of 1-propanethiol in the presence of triethylamine (TEA). Degradation experiments revealed that the formation of chemically inducible degradable structures, enabling the design of recyclable or biodegradable materials.

As a result, the method developed in this study draws attention in terms of its practical applicability, time and energy savings, and high structural flexibility. The findings are expected to make significant contributions to future studies on polymer synthesis, functionalization strategies, and controlled degradability.

TİYOL-DİBROMOMALEİMİD POLİMERİZASYONU: KOLAY PARÇALANABİLİR VE MODİFİYE EDİLEBİLİR POLİTİYOETER SENTEZİ İÇİN BASİT BİR STRATEJİ

ÖZET

Maleimidler, eşsiz reaktivite özellikleri ve geniş kullanım alanları sayesinde malzeme bilimi, organik kimya, polimer bilimi ve biyokonjugasyon gibi alanlarda büyük ölçüde ilgi görmüş bileşiklerdir. Maleimidin çekirdek yapısı, konjuge olmuş ve elektron bakımından fakir bir çift bağa sahip beş üyeli bir imid halkasından oluşur. Bu elektron eksikliği, yapıda yer alan iki karbonil grubundan kaynaklanmakta olup, maleimidlerin nükleofillere ve dienlere karşı son derece reaktif hale gelmesini sağlar. Bu özellikleri sayesinde maleimid ve türevleri; Michael katılmaları, sikloadisyon reaksiyonları ile radikal ve anyonik polimerizasyonlar gibi çeşitli kimyasal tepkimelerde geniş bir uygulama alanı bulmaktadır. Ek olarak, maleimid-tiyol kimyası kullanılarak çeşitli organik ve inorganik nanomalzemelerin yüzey modifikasyonları sağlanmış ve biyomoleküller ile ilaçların kovalent bağlanması gerçekleştirilmiştir. Ancak, mevcut olarak kullanılan yüzey modifikasyon yöntemlerinin çoğu; zaman alıcı, karmaşık ve çok adımlı prosedürler gerektirmektedir.

Maleimidlerin aksine mono- ve dihalomaleimidler (maleimide türevleri) farklı davranışlar sergiler. Monobromomaleimid; geçtiğimiz on yılın başında, seçici sistein reaksiyonları ve tiyol geri kazanımında rol almak gibi çok fonksiyonlu özellikler gösteren bir bileşik olarak ortaya çıkmıştır. Bu bileşikler; tiyol gruplarıyla klasik katılma reaksiyonları yerine nükleofilik sübstitüsyon tepkimeleri gerçekleştirirler ve bu şekilde sahip oldukları çift bağı korumuş olurlar. Aynı şekilde dihalomaleimid türevleri de iki eşdeğer tiyol ile kolayca reaksiyona girerek monobromomaleimidlere benzer bir reaksiyon mekanizması oluştururlar. Bu türevleri arasında, diiyodomaleimid en hızlı reaksiyon hızına sahipken, dikloromaleimid en yavaş reaksiyon hızına sahiptir. 2,3-dibromomaleimid ise, özellikle ayrılan grubun yeteneği ile belirlenen, orta düzeyde bir reaktiviteye sahiptir.

DBM ve benzer yapıya sahip bileşikler polimer kimyasına; RAFT ajanları, ATRP başlatıcıları ve monomerik fonksiyonel gruplar olarak dahil edilmiştir. İlk ATRP başlatıcılarının kullanımı yönündeki girişimler başarısızlıkla sonuçlanmış olsa da, Haddleton'un grubu ditiyofenol maleimidleri bromoisobutirat grubuyla fonksiyonlandırarak başarılı bir şekilde sentezlemiş ve bu yapıların ATRP için etkili başlatıcılar olduğunu göstermiştir. Ayrıca, Jiang ve ekibi, yapısında DBM grubu taşıyan norbornene monomerlerini sentezlemiş ve bu monomerleri halka açılma metatez polimerizasyonu (ROMP) ile polimerleştirerek, her tekrarlayan birimde iki reaktif merkez içeren polimerler elde etmişlerdir. Ross ve ekibi, yüzeye polimerize edilen bir DBM monomerini kimyasal buhar biriktimre yöntemi ile geliştirmiş ve bu yöntemle tiyol-fonksiyonlu biyomoleküllerin immobilizasyonu ve salımı sağlanmıştır.

DBM'nin kendine özgü reaktivitesi, polimer yapılarının modüler şekilde oluşturulmasına imkan tanımaktadır. Ayrıca, dibromomaleimid ve türevleri kullanılarak tiyol uçlu hidrofilik polimerler ile yapılan nükleofilik substitüsyon reaksiyonları ile post polimerizasyon modifikasyonları gerçekleştirilmiştir. Bu yöntem sayesinde miktoarm star polimerler gibi farklı fonksiyonel yapıların tasarımına olanak sağlanmıştır.

Jennings ve ekibi son yıllarda, perflorosiklopenten kullanarak politiyoeterler sentezlemişlerdir. DBM'nin kullanımı ile ilgili çeşitli literatür örnekleri, polimerizasyon reaksiyonlarının verimli bir şekilde gerçekleştirilmesini sağlamıştır. Ayrıca You ve takımı, DBM'nin ditiyol ile polimerizasyonunu gerçekleştirmiş ve bu reaksiyon ile bir dizi kontrollü polimer elde etmişlerdir. Bu çalışma, DBM'nin tiyol grupları ile olan etkileşimini detaylı bir şekilde inceleyerek, lineer politiyoeterlerin sentetik yollarını geliştirmiştir.

Bu bağlamda, DBM ve türevlerinin yüksek reaktivitesi; post polimerizasyon modifikasyonları ve polimer yapılarının fonksiyonelleştirilmesi açısından büyük bir potansiyel taşımaktadır.

Bu çalışmada, tiyol-dibromomaleimid (tiyol-DBM) polimerizasyon reaksiyonunun koşulları sistematik olarak optimize edilerek, bu yöntem ile elde edilen polimerlerin yapısal özellikleri detaylı bir şekilde değerlendirilmiştir. Öcelikle, model ditiyol olarak seçilen 1,6-hekzanditiyol ile DBM'nin 1:1 molar oranda reaksiyona sokulmasıyla başlatılan optimizasyon çalışmaları; çözücü, baz türü, sıcaklık ve derişim gibi parametrelerin reaksiyon verimi üzerindeki etkilerini ortaya koymuştur. Elde edilen veriler, özellikle NMP gibi polar aprotik çözücülerin reaktanların çözünürlüğünü artırdığını ve bunun yanı sıra zincir büyümesini destekleyici bir ortam sağladığını göstermiştir. Reaksiyon ortamında baz olarak kullanılan trietilaminin (TEA), hem oluşan HBr'nin nötralizasyonunu sağladığı hem de polimer zincirlerinin kararlılığını artırdığı anlaşılmıştır. Kullanılan TEA bazının miktarındaki değişimler ise, zincir büyüme hızında ve nihai moleküler ağırlık üzerinde doğrudan etkili olmuş, fakat belirli bir eşdeğerin üzerinde ilave baz kullanımının etkisinin ise sınırlı kaldığı gözlemlenmiştir.

Reaksiyonun başlangıcında gözlenen hızlı viskozite artışı ve ekzotermik tepkime, sistemin oldukça hızlı ilerleyen bir zincir büyümesine olanak tanıdığını göstermektedir. Ancak sıcaklığın düşürülmesiyle birlikte zincir büyümesinin yavaşladığı ve ürünün daha düşük moleküler ağırlıkta kaldığı görülmüştür. Bu durum, reaksiyonun termodinamikten ziyade kinetik olarak kontrol edildiğini, yani ortam koşullarının moleküler düzeyde belirleyici olduğunu ortaya koymaktadır. Alternatif bazların kullanımıyla yapılan karşılaştırmalı deneylerde ise özellikle daha güçlü bazların, kısa vadede yüksek moleküler ağırlıklı ürünler oluştursa da zamanla zincir uçlarıyla etkileşerek sistemde depolimerizasyonu tetikleyebileceği anlaşılmıştır. Bu nedenle TEA'nın tercih edilmesi, reaktivite ve kararlılık açısından daha dengeli bir sistem sağlamıştır.

Elde edilen polimerlerin yapısal analizleri sonucunda, dibromomaleimid biriminin tiyollere karşı seçici ve verimli şekilde reaksiyona girdiği, bu sırada halkasal yapının korunduğu gözlemlenmiştir. Bu durum, başlangıç maddelerinin kimyasal stabilitesinin sürdürülebilirliği ve modifikasyonlara açık olması açısından önemli bir avantaj

sağlamaktadır. Ayrıca zincir yapısındaki ditiyol köprülerinin reaksiyon boyunca korunması, sentezlenen polimerlerin daha sonra yapılacak fonksiyonelleştirme çalışmalarına uygunluk taşıdığını göstermektedir. Bu bağlamda, sistemin yalnızca iyi tanımlı, doğrusal polimer yapıları üretmekle kalmayıp aynı zamanda ileri uygulamalara açık, reaktif platformlar sunduğu söylenebilir.

Çalışmanın ilerleyen aşamalarında farklı ditiyol bileşikleri kullanılarak sistemin uygulanabilirliği daha kapsamlı bir şekilde test edilmiş ve bu yapıların reaktiviteye etkisi incelenmiştir. Zincir uzunluğu, fleksibilite ve yapısal özellikler dikkate alındığında, bazı ditiyollerin molekül içi halkalaşmaya daha yatkın olduğu ve bu durumun moleküler ağırlık üzerinde sınırlayıcı bir etki yarattığı anlaşılmıştır. Özellikle daha kısa zincirli ditiyollerden elde edilen polimerlerin bu eğilimi daha fazla gösterdiği gözlemlenmiştir. Buna karşın daha uzun ve esnek zincirli ditiyollerin, polimer zincirleri arasında daha efektif bir köprüleme sağladığı ve sonuç olarak daha yüksek moleküler yapılara olanak verdiği ortaya konmuştur.

Sonuç olarak, bu çalışma ile 2,3-dibromomaleimid ile gerçekleştirilen polimerizasyonun yüksek verimlilikte, kısa sürede ve oldukça kontrollü şekilde gerçekleşebileceği gösterilmiştir. Kullanılan kolay erişilebilir başlangıç malzemeleri ve hafif reaksiyon koşulları sayesinde, bu sistemin hem temel polimer sentezi hem de sonrasında uygulanacak modifikasyonlar için güçlü ve esnek bir platform sunduğu söylenebilir. Yüksek moleküler ağırlıkta elde edilen polimerlerin, kontrollü yapıları ve reaktivite özellikleri, bu yaklaşımın çeşitli uygulamalar için büyük bir potansiyel taşıdığını göstermektedir. Polimerlerin fonksiyonelleştirilebilirliği, yüzey kaplama teknolojileri, biyomedikal uygulamalar ve çevresel sürdürülebilirlik açısından önemli avantajlar sunmaktadır. Ayrıca, dibromomaleimid biriminin kimyasal stabilitesi sayesinde farklı fonksiyonel gruplar polimer yapısına başarıyla entegre edilebilmekte ve bu da sonraki modifikasyon süreçlerini destekleyerek polimerlerin farklı fonksiyonel özellikler kazanmasına olanak tanımaktadır.

Tüm bu bulgular, tiyol-dibromomaleimid polimerizasyonunun, hem temel araştırmalarda hem de ticari uygulamalarda kullanılabilecek geniş bir potansiyele sahip olduğunu ortaya koymaktadır. Özellikle miktoarm star polimerlerin sentezinde kullanılan bu tür stratejiler, çok fonksiyonlu malzemelerin tasarımı ve üretimi için kritik bir adım olarak öne çıkmaktadır. Gelecekteki çalışmalar, bu polimerlerin özelliklerini daha da iyileştirecek modifikasyon stratejileri ve reaksiyon koşulları üzerine odaklanarak, daha yüksek verimli ve daha stabil polimer yapıları üretme potansiyelini araştırabilir. Ayrıca, çevresel etkilerin azaltılması ve geri dönüşüm süreçlerinin iyileştirilmesi için de bu polimerlerin biyolojik olarak bozunabilir özellikleri incelenebilir. Bu çalışmanın, dibromomaleimid temelli polimerizasyonun uygulama alanlarını genişletme potansiyeline sahip olup, malzeme bilimi ve mühendislik alanlarında önemli bir referans noktası olacağı düşünülmektedir.

1. INTRODUCTION

Maleimides are multifunctional compounds that have received considerable attention due to their unique reactivity and broad utility in materials science, organic chemistry, polymer science, and bioconjugation [1-4]. Maleimide scaffold consists of a five-membered imide ring annulated to a conjugated, electron-deficient double bond. Electron deficiency due to the presence of carbonyl groups renders the maleimide molecule very reactive towards nucleophiles and dienes. Therefore, they have been extensively employed in Michael additions [5-16], cycloaddition reactions [17-30], and radical and anionic polymerizations [31-40]. Scientific reports have identified a wide range of organic and inorganic nanomaterials that use maleimide-thiol chemistry for surface modification and the covalent linkage of (bio)molecules and drugs (Figure 1.1). However, most existing methods for modifying the surface with maleimides include complex multistep procedures that require considerable time.

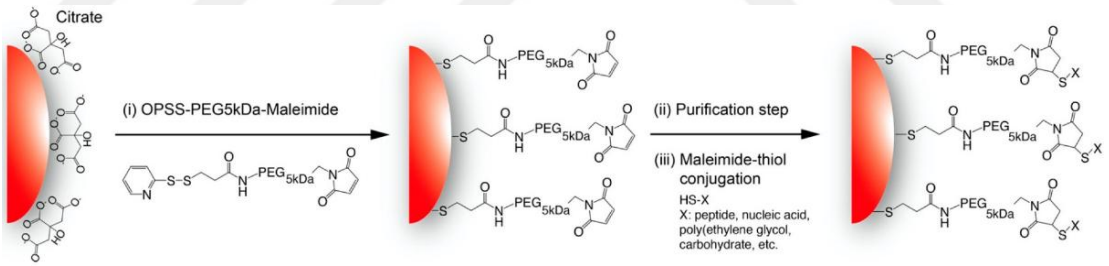

Figure 1.1 : Schematic representation of surface modification of nanomaterials via maleimide functionalization.

In contrast, mono- and dihalomaleimides exhibit very different behavior. Monobromo maleimide appeared at the start of the last decade and developed as a multifunctional compound capable of selective cysteine reactions (Figure 1.2) as well as thiol regeneration [41].

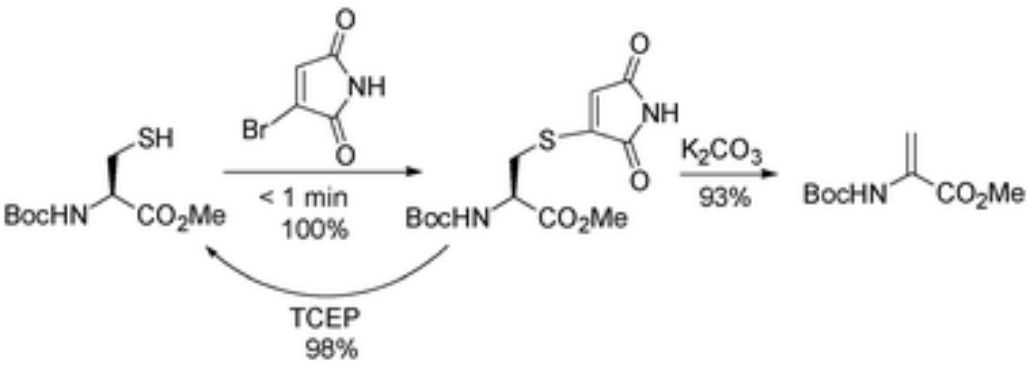

Figure 1.2 : Schematic illustration of selective cysteine modification and thiol regeneration using monobromomaleimide.

Rather than engaging in normal addition, they proceed via nucleophilic substitution reactions with thiol groups, preserving the double bond [4, 41-43]. This is distinct from the saturated succinimide product formed through the addition of maleimide to a thiol.

Caddick and Baker showed that dihalomaleimide analogs readily and efficiently react with two equivalent thiols, establishing a mechanism that parallels monobromo maleimides [42]. Among these analogs, diiodomaleimide was found to have the fastest reaction rate, dichloromaleimide had the slowest, and 2,3-dibromomaleimide had an intermediate reactivity, which was determined mainly by the leaving group's ability [43]. In their research, dibromo- and dithiomaleimides were successfully employed for biomolecular coupling, targeted protein modification, and rapid reformation of disulfide bonds when a reducing agent was present, overcoming frequent issues related to disulfide reduction, including protein denaturation, aggregation, and scrambling of disulfide bonds.

Thanks to their selective and efficient reactivity towards thiols, DBM analogs have found increasing application in polymer chemistry, serving as RAFT agents [44] (Figure 1.3), ATRP initiators [45,46] (Figure 1.4), and monomeric functional groups [47–49].

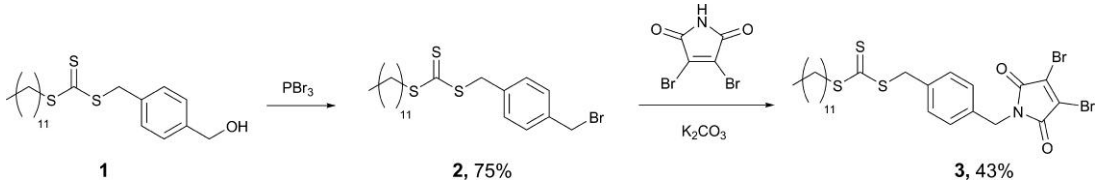

Figure 1.3 : Synthesis of DBM functional RAFT agent.

These applications have been largely enabled by the ease of disulfide cross-linking and the versatility of post-polymerization modifications. Although initial attempts to employ DBM derivatives as ATRP initiators were unsuccessful due to undesired radical addition to the maleimide moiety [45], Haddleton and co-workers later developed dithiophenol maleimides bearing a bromoisobutyrate group, which proved to be effective initiators (Figure 1.4).

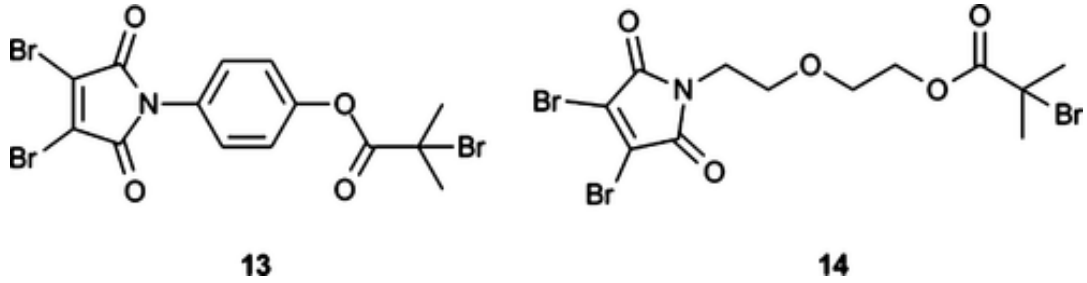

Figure 1.4 : Synthesized dibromomaleimide ATRP initiator.

Jiang and colleagues created norbornene monomers containing DBM group, which, following polymerization using ring-opening metathesis polymerization (ROMP), formed two reactive sites per repeating unit, allowing for postpolymerization modifications (Figure 1.5).

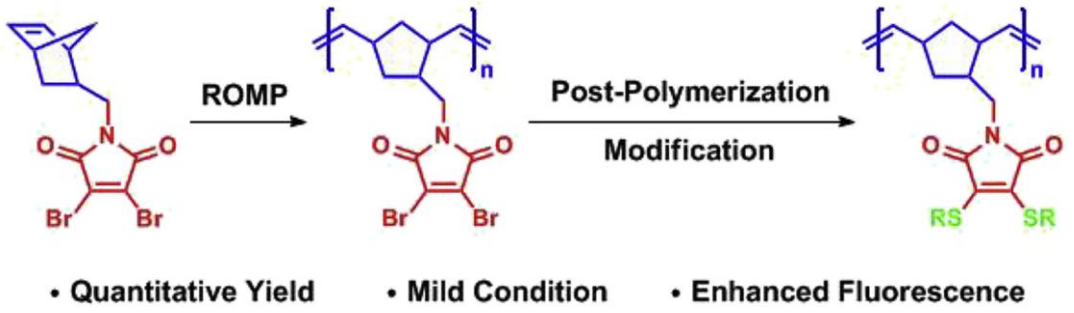

Figure 1.5 : ROMP polymerization of a DBM-functionalized monomer followed by postpolymerization modification via a DBM–thiol reaction.

In addition to these studies, several other groups demonstrated unique utilizations of DBM derivatives in surface polymerization and polymer architecture design. In their research, Ross et al. developed a monomer bearing a DBM, which was primarily polymerized onto a surface utilizing the chemical vapor deposition approach. This method produced surfaces with DBM functionality, enabling immobilization and release of thiol-functionalized biomolecules [50]. The A_2B-type miktoarm star polymer was developed through a copper-catalyzed Azid-alkyne cycloaddition reaction using N-alkyl azide-functional DBM with thiol end groups utilizing polymer coupling [51]. Furthermore, the DBM core's specific reactivity facilitated postpolymerization modification via thiol substitution reaction, enabling the modular

formation of multifunctional polymer structures [60]. Published reports have shown that chemical analogs enable an akin reaction mechanism. Baker and Chudasama concluded that cysteine residues and aniline analogs could be bioconjugated using 4,5-dibromopyridazine-3,6-dione derivatives. In their research, it was observed that in the presence of an extremely reactive thiol, the thiol linkages could be degraded (Figure 1.6) while the C-N bond remained stable [52].

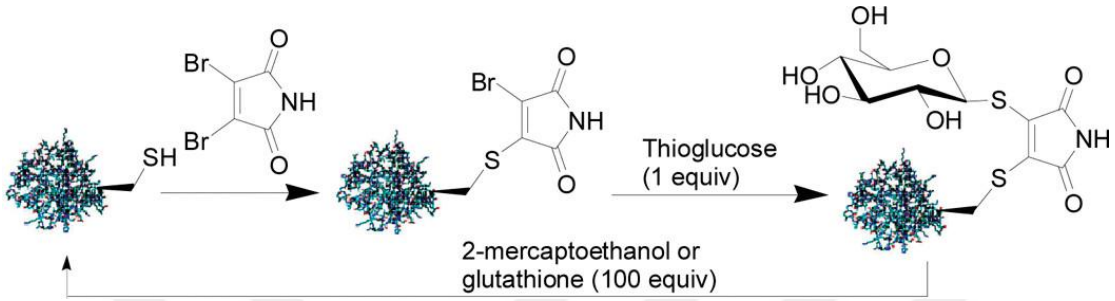

Figure 1.6 : Representation of selective thioether bond cleavage in the presence of excess thiol, with preserved C–N connectivity.

In recent years, Jennings et al. synthesized perfluorinated polythioethers (Figure 1.7) using perfluorocyclopentene, which shows their simple chemical creation and remarkable thermal stability [53].

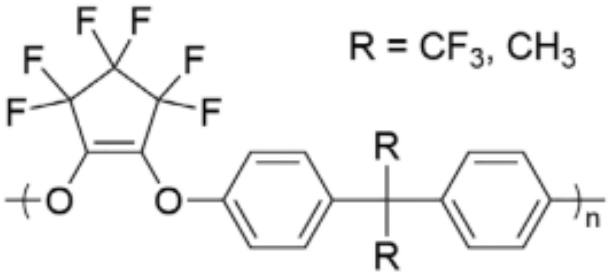

Figure 1.7 : Synthesized Perfluorocyclopentene (PFCP) poly(aryl ethers).

The representative examples of the utility of DBM in the literature are summarized in (Figure 1.8).

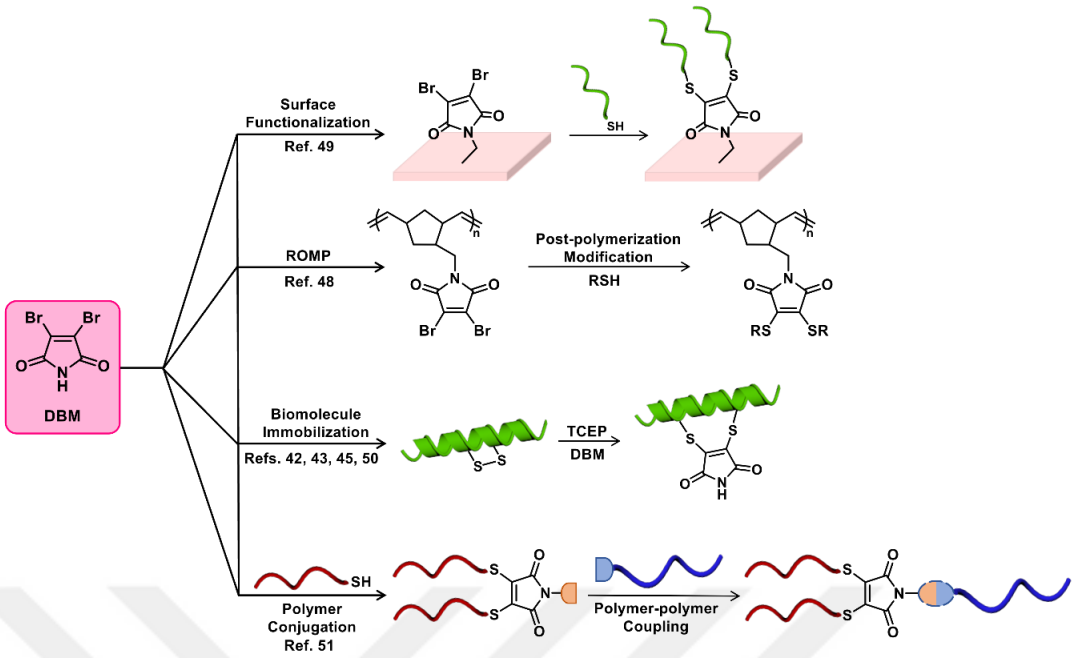

Figure 1.8 : Schematic representation of DBM and its use in various applications in the literature.

So far, only one research study has demonstrated the polymerization reaction between DBM and dithiol. In the study conducted in 2013, You and his team demonstrated that the synthesis of sequence-controlled polymers was achieved via the variant of dithiols derived from a thiolactone molecule, followed by the in situ addition of DBM to the prepared dithiol reaction mixture [54]. The result of this one-pot method was a polymer with a molecular weight of 8.5 kDa. The extraordinary reactivity of DBM towards thiols encouraged us to conduct a detailed investigation of this molecule to develop a linear polythioether synthesis. In this contribution, we employed DBM as a monomer and reacted it with various aliphatic and aromatic dithiol compounds to obtain poly(maleimide thioether)s. General scheme of the polymerization reaction between DBM and dithiols (Figure 1.9) is presented below. Due to the easily cleavable Csp^2-S bond in the resulting polymers, a degradation study was performed in the presence of a competing thiol. Pendant imide N-H bonds were further utilized for postpolymerization modification (PPM) through imide-yne click reaction, similar to the study reported by Durmaz et al. [55].

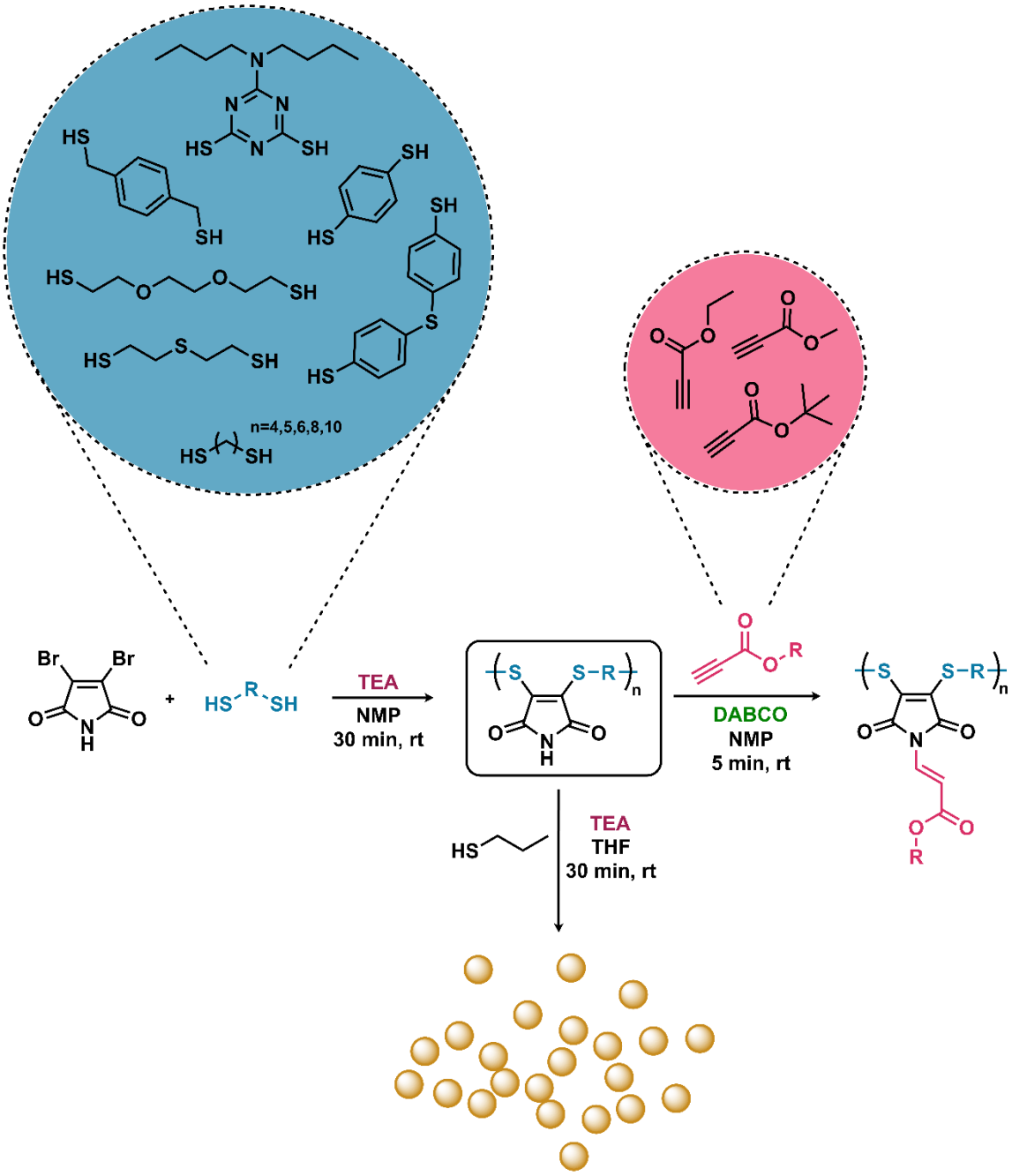

Figure 1.9 : Outline of the study: Polymerization of DBM with various dithiols, postpolymerization modification (PPM) of a model polythioether through imide-yne click reaction with various propiolates, and degradation of the same model polythioether in the presence of excess 1-propanethiol.

2. THEORETICAL PART

2.1. Surface Functionalization

One of the most common uses for 2,3-dibromomaleimide and its derivatives is surface functionalization, especially for the reversible and selective attachment of biomolecules (Figure 2.1) [41–43, 49, 50].

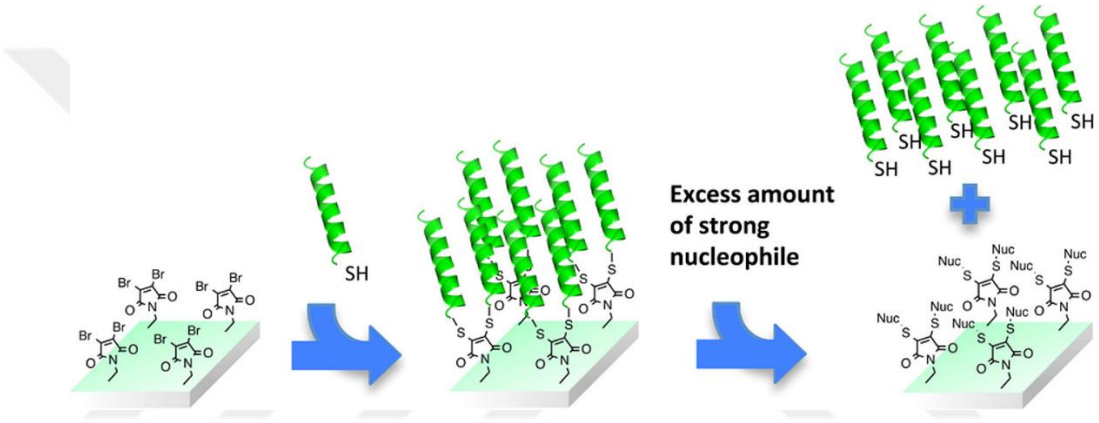

Figure 2.1 : Schematic representation of surface functionalization with a DBM derivative.

This feature is particularly useful in biomedical fields such as biosensors and diagnostic tools. Ross et al. have extensively covered this in their study. The thiol groups attached to dibromomaleimide provide strong and specific binding via Michael addition. This property enables biomolecules to remain conjugated to the surface and allows the reversal of these bonds later with strong nucleophiles, such as tris(2-chloroethyl) phosphate (TCEP) [49]. Consequently, such surface modifications offer a flexible and controlled method for targeted binding and release of biomolecules [49].

This surface functionalization process first starts with the synthesis of 4-(3,4-dibromomaleimide)[2.2]paracyclophane (1) (Figure 2.2a). This synthesized compound is then converted into a polymer structure by chemical vapor deposition (CVD) (Figure 2.2b). The compound can be transformed into the polymer poly[4-(3,4-dibromomaleimide)-p-xylylene-co-p-xylylene] (2) through CVD polymerization. The

obtained polymer (2) provides a suitable platform to effectively control the binding and release of biomolecules to surfaces [49].

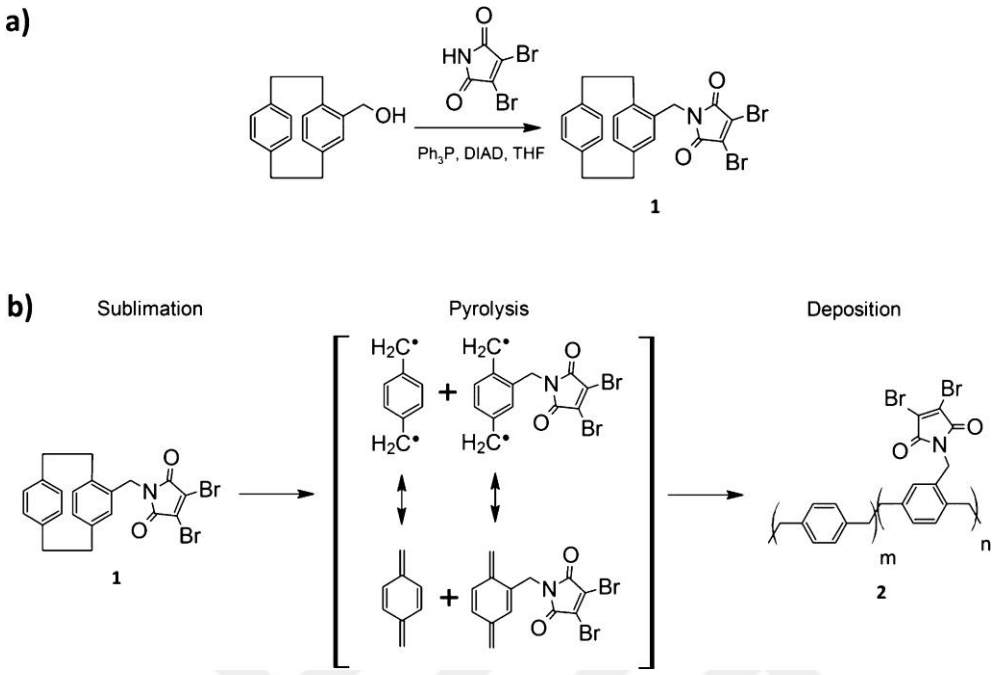

Figure 2.2 : (a) Synthesis of 4-(3,4-Dibromomaleimide)[2.2]paracyclophane (1) and (b) Chemical vapor deposition polymerization of precursor 1 into Poly[4-(3,4-dibromomaleimide)-p-xylylene-co-p-xylylene] (2)

Chemical vapor deposition polymerization is an ideal method for integrating dibromomaleimide groups onto surfaces. Polymerization through chemical vapor deposition enables the formation of thin polymer coatings on a wide range of substrates (Figure 2.3a). The resulting coatings are well-suited for the controlled attachment and release of thiol-containing biomolecules on surfaces [49]. Furthermore, the fact that polymer coatings easily adapt to surface morphology creates a great advantage in biotechnology and biomedical applications [49].

The differences in polymer thickness observed on the surface after the coating process directly reflect the selectivity and homogeneity of this process (Figure 2.3b). Such control enables the biomolecules to be placed in the desired order on the surface, providing high sensitivity in functional biosensor designs [49].

Fluorescent microscopy images have clearly confirmed that biomolecules functionalized with thiol groups have been successfully immobilized on the surface (Figure 2.3c). These functionalized surfaces play a crucial role in achieving reliable analytical results in biosensor applications by allowing for the controlled placement and release of proteins and peptides as needed [49, 61].

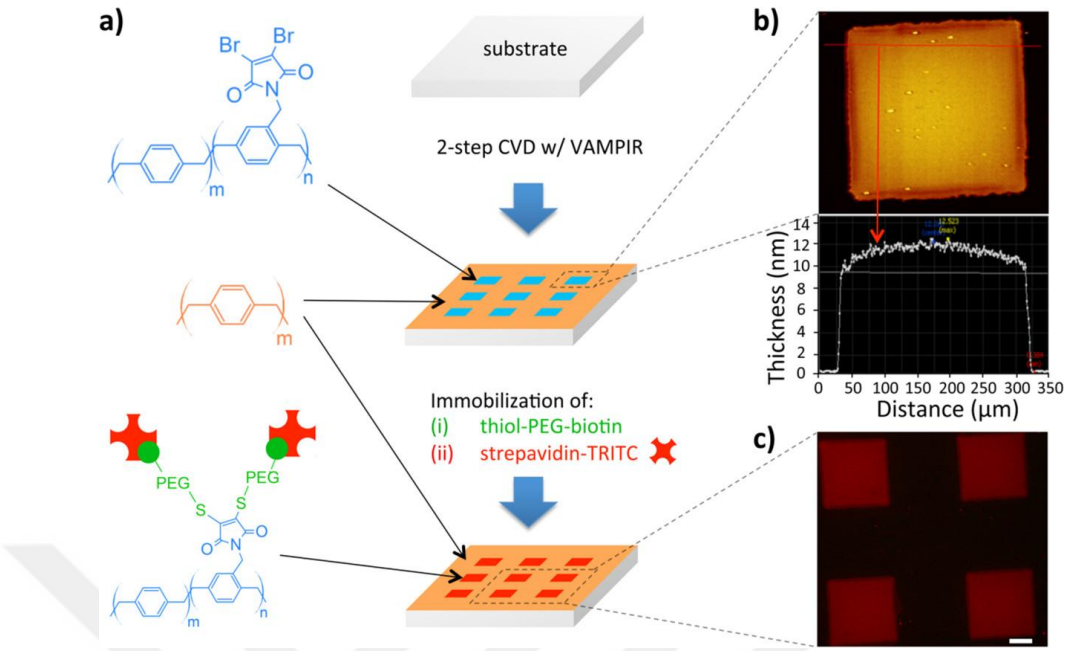

Figure 2.3 : (a) Schematic diagram illustrating the immobilization of thiol-PEG-biotin and streptavidin-TRITC on a patterned polymer film prepared using the VAMPIR (vapor-assisted micropatterning in replica structures) technique. (b) Thickness profile depicting the difference in thickness of polymer coatings selectively deposited on a substrate surface across two different areas. (c) Fluorescence micrograph obtained after the immobilization of thiol-PEG-biotin and streptavidin-TRITC on the patterned polymer film. Scale bar: 100 µm.

Finally, the reversible binding capacity of dibromomaleimide groups provides flexibility in biomolecule immobilization; thus, the bound biomolecules can be released from the surface according to the application need. Taking into account all these advantages, developing dibromomaleimide-containing polymers offers significant opportunities for biomedical applications. These polymers constitute a reliable platform for biotechnological solutions such as biosensors and diagnostic systems [49].

2.2. ROMP & Post Polymerization Modification

The efficient synthesis of functional polymers is greatly enhanced by utilizing the DBM molecule and its derivatives in postpolymerization modifications and Ring-Opening Metathesis Polymerization (ROMP) [48]. ROMP is an extremely effective technique for generating polymers with controlled chain lengths and low polydispersity index. This method is used in the polymerization of cyclic monomers

such as norbornene derivatives and can be performed with high yields using Grubbs catalysts. DBM allows the production of polymers that can be modified, especially by reacting with thiol groups [48].

In the study conducted by Jiang and his colleagues, new functional polymers were obtained by synthesizing DBM-containing polynorbornene through the ROMP method and then modifying it with thiol groups. ROMP monomer 2 was synthesized in two sequential reaction steps (Figure 2.4). In the first step, DBM was reacted with methylchloroformate (MCF) and N-methylmorpholine (NMM) to yield the reactive intermediate 1. In the second step, intermediate 1 was reacted with 5-norbornene-2-methylamine (NMA) to form the ROMP monomer 2. The overall yield of this two-step procedure was reported to be 79%. This approach enables the efficient and controlled synthesis of DBM-based monomers [48].

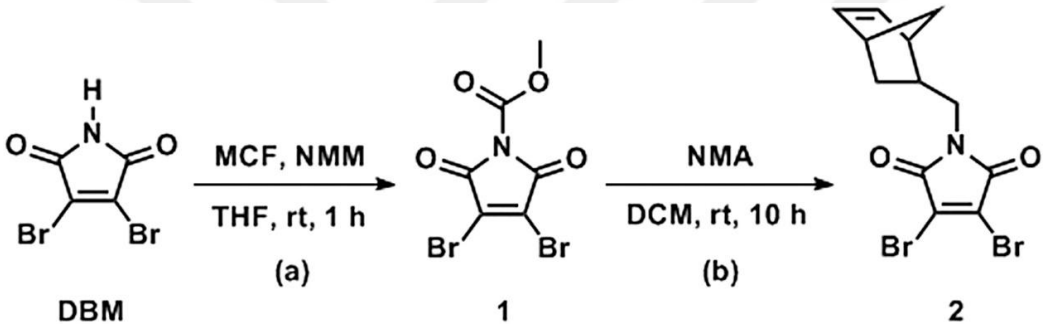

Figure 2.4 : DBM-based monomer synthesis.

The obtained monomer 2 was converted to polynorbornene P0 through ROMP (Figure 2.5). Subsequently, the P0 polymer was reacted with a stoichiometric amount of 1-butanethiol or benzyl mercaptan in DMF solvent to yield thiol-substituted polymers P1 and P2. The rapid change of the solution to a bright yellow color during the reaction indicates that the thiol groups underwent nucleophilic substitution with the DBM units, demonstrating the successful modification [48].

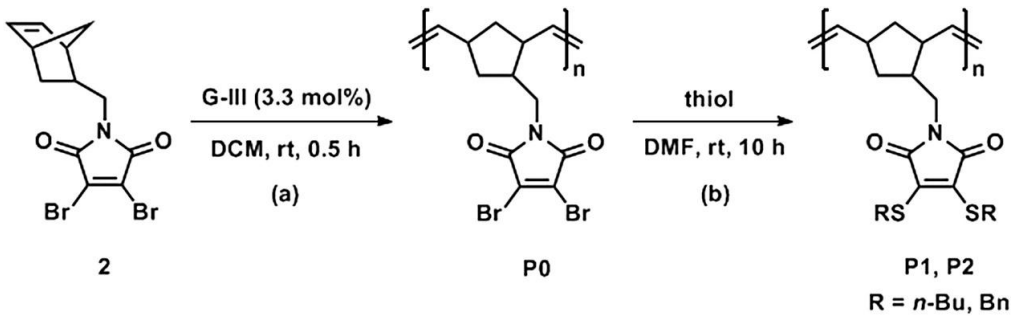

Figure 2.5 : ROMP and DBM-thiol reaction.

Postpolymerization modifications offer considerable flexibility in tailoring polymer properties through the incorporation of functional groups. In particular, thiol-based modifications facilitate the facile adjustment of polymer structural characteristics and the introduction of new functionalities, such as optical properties. For instance, thiol-substituted maleimides exhibit intrinsic fluorescence, allowing for the development of polymers with tunable photophysical features. The nature of substituents on the polymer backbone markedly affects both fluorescence intensity and the maximum emission wavelength, as demonstrated in Figure 2.6 [48]. These adjustable optical properties render such polymers promising candidates for applications including gene delivery systems, nanomedical technologies, and biomolecule conjugation. Consequently, postpolymerization thiol modifications represent a powerful strategy for enhancing polymer performance and expanding their applicability in advanced biomedical and material science fields [48].

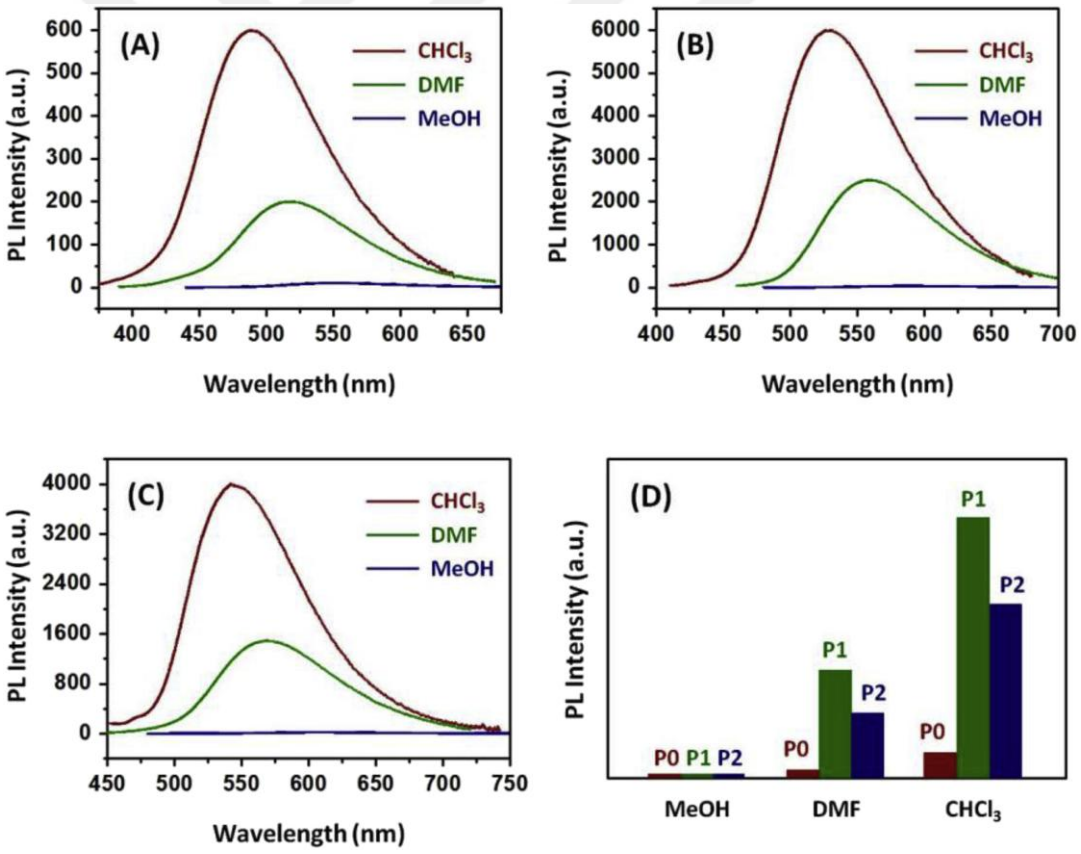

Figure 2.6 : (A)–(C) Fluorescence spectra of P0, P1 and P2 in different solvents at 2μM concentration. (D) Comparison of the intensities of P0, P1 and P2 in different solvents.

Thermal stability and mechanical properties of the polymers were also evaluated, as shown in Figure 2.7. The TGA curves of P0–P2 polymers (Figure 2.7a) indicate that

the polymers are stable at high temperatures. The endothermic DSC thermograms (Figure 2.7b) were used to analyze the glass transition temperatures and melting behaviors of the polymers [48].

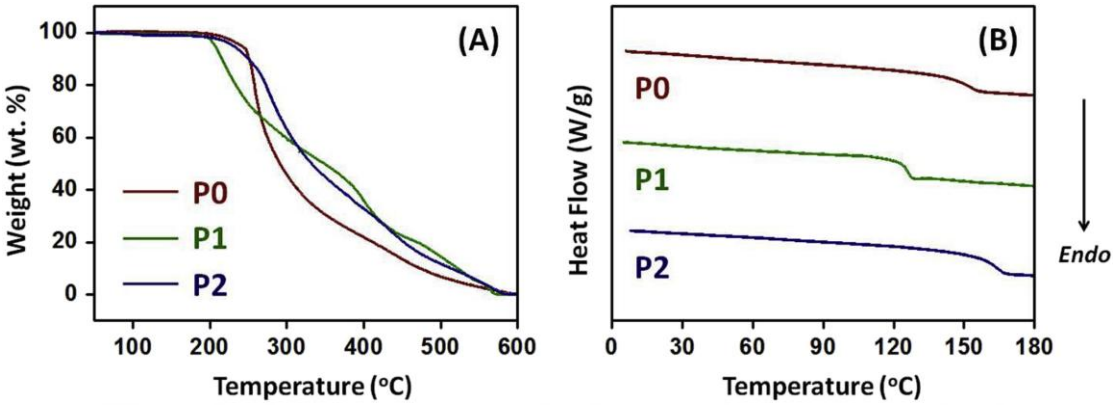

Figure 2.7 : a) TGA curves of P0–P2. b) Endothermic DSC thermograms of P0–P2.

As a result, dibromomaleimide-based postpolymerization modifications are an important tool in the development of functional polymers. Research in this area contributes to the design of next-generation polymeric materials, and these materials can show high performance in various applications [48].

2.3. Biomolecule Immobilization

In addition to their applications in polymer modification, DBM derivatives have emerged as powerful tools for the controlled immobilization and functionalization of biomolecules. Modifying proteins without affecting their structural integrity is one of the major problems. Disulfide bonds, in particular, play a critical role in maintaining three-dimensional structure and functionality of proteins [42,43,45,50]. Labor-intensive purification procedures are frequently needed for traditional techniques for reducing and rebridging these bonds. DBM derivatives simplify these processes, allowing for the efficient and controlled modification of biomolecules [42,45] (Figure 2.8). Consequently, they are versatile tools for protein engineering and site-specific immobilization of biomolecules. Recent research has also demonstrated the potential of DBM-based approaches in bioconjugation, specifically in promoting stable biomolecule attachment and disulfide bridge formation [45,50].

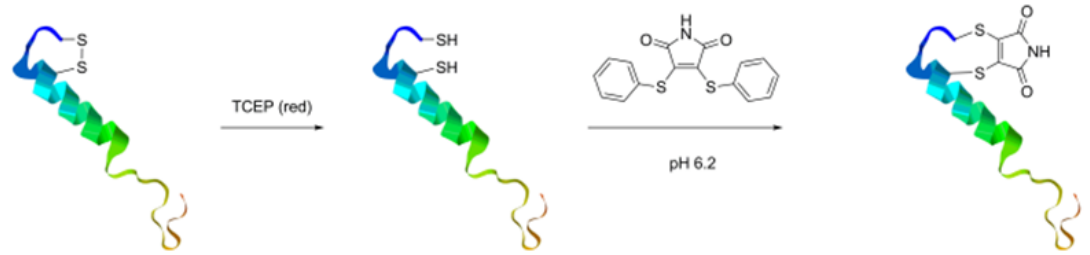

Figure 2.8 : Immobilization of biomolecules using DBM derivatives as disulfide bridging agents

For example, Haddleton and his team have conducted a comprehensive study on how dibromomaleimide (DBM) derivatives can be used in modifications directed at cysteine residues of proteins. Unlike classical maleimides, DBM stands out due to its ability to form reversible bonds in the chemical modification of proteins [45]. While traditional maleimides form irreversible bonds with cysteine rapidly and selectively, DBM allows biomolecules to be temporarily modified and returned to their original state when necessary [45]. This feature offers a significant advantage for the functional modification of biomolecules. In the study, it was observed that DBM showed high selectivity for protein modification, and that maleimide-based conjugates could be further functionalized by adding a second thiol group [45]. In this way, it became possible to reach three different attachment points on the protein surface. In addition, DBM derivatives were shown to be effective in the modification of disulfide bonds [45,50]. The somatostatin peptide, selected as the model biomolecule, was treated with DBM after TCEP reduction, thus forming a "maleimide bridge" between two cysteine residues while preserving the structural integrity (Figure 2.9) [45].

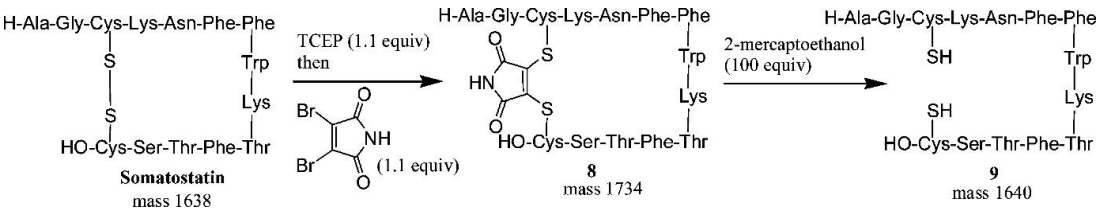

Figure 2.9 : Reversible modification of the disulfide bond of somatostatin by dibromomaleimide

This modification is important for the reversible regeneration of disulfide bonds and the traceability of biomolecules. Fluorescent labeling applications have been highlighted as an important method for labeling biomolecules with DBM and for tracking proteins immobilized in biological systems [45,50]. These results suggest that DBM-based reagents have several benefits, such as selective disulfide bond bridging,

bioconjugation with various functional groups, and reversible, transient modification of cysteine residues [45,50]. When combined, these traits make them effective instruments for the immobilization of biomolecules and the development of useful biomaterials (Figure 2.10) [45].

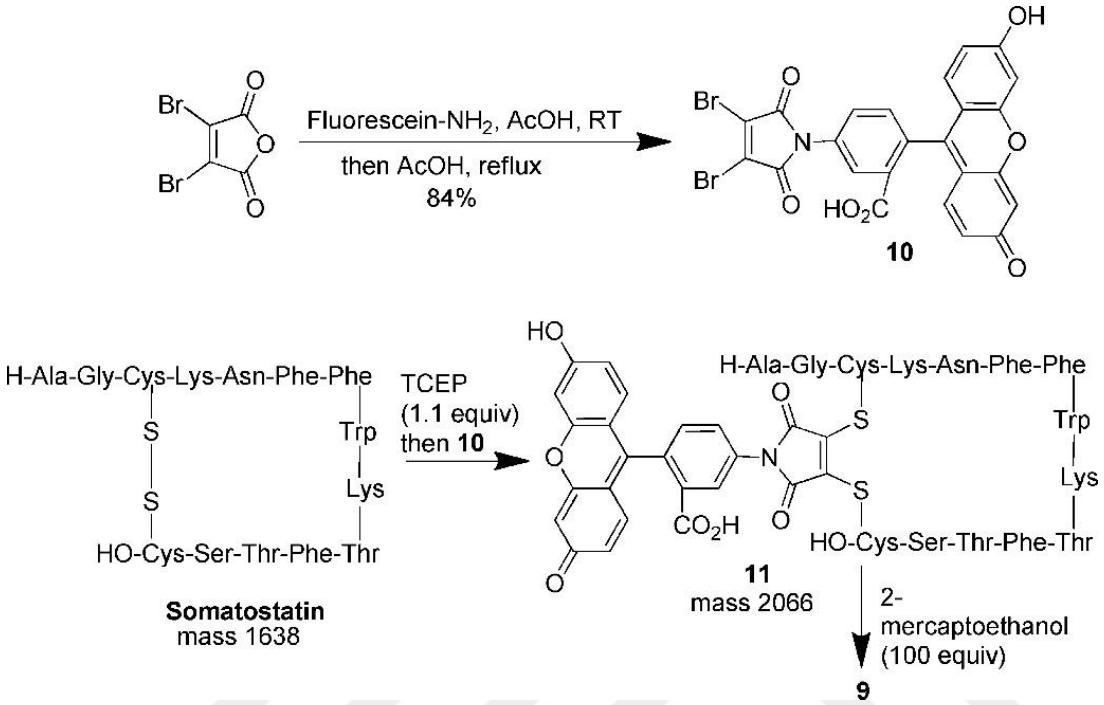

Figure 2.10 : Reversible modification of the disulfide bond of somatostatin by a fluorescent dibromomaleimide reagent.

In a similar line of research, Caddick, Baker and their team emphasized the importance of the modification of biomolecules while preserving their structural stability. Disulfide bridges play a critical role in maintaining the three-dimensional structure of proteins [42,43]. However, the reduction of these bonds can disrupt the structural stability of proteins, leading to instability, aggregation, or disulfide recombination [42,43]. Therefore, reduced disulfide bonds need to be rebridged quickly and efficiently to maintain biomolecular stability. In the study, it was shown that halogenated maleimide derivatives (e.g., dibromomaleimide, diiodomaleimide) and dithiomaleimides (e.g., dithiophenolmaleimide) replaced the disulfide bridges and preserved the original conformation of the protein structure [43,45]. In particular, after the reduction of the disulfide bridge of the somatostatin peptide using DBM, efficient re-bridging of the free cysteine residues was achieved, and it was confirmed that this modification preserved the biological activity of the peptide [45]. In addition, PEGylation of the somatostatin analog was performed using PEG-derived maleimides,

thus increasing the biological stability of the modified peptide [43,50]. In the biological activity tests performed after PEGylation, it was confirmed that the modified somatostatin analog maintained its biological activity by binding to G-protein-coupled receptors, similar to the original somatostatin [50]. This study revealed that DBM and similar maleimide-based reagents can be considered as promising compounds in biotechnological applications in terms of controlled modification while preserving the structural stability of biomolecules [50].

Further investigations by Haddleton and his team explored the effectiveness of DBM derivatives in re-bridging disulfide bonds. Disulfide bonds protect the structural integrity and function of proteins. However, the reduction of these bonds usually leads to a loss of protein function. DBM addresses this problem by allowing reduced disulfide bonds to be re-bridged via thiol groups, thus preserving the structural integrity of the biomolecule [45,50]. In the study, the salmon calcitonin (sCT) hormone was used as a model biomolecule. Reduced sCT reacted rapidly and selectively with DBM under slightly acidic conditions (pH 6.2), re-forming the disulfide bridge between the two thiol groups and forming a stable conjugate (Figure 2.11, Figure 2.12) [50].

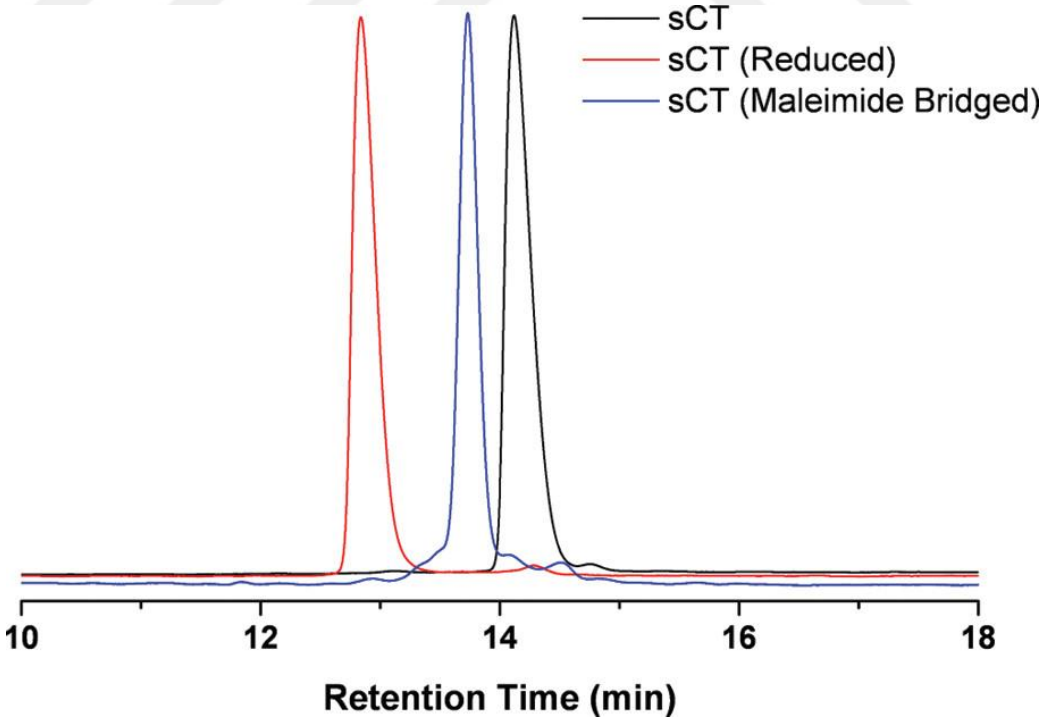

Figure 2.11 : RP-HPLC analysis of sCT disulfide-bridging with 2,3 dibromomaleimide following reduction of the disulfide bridge of sCT.

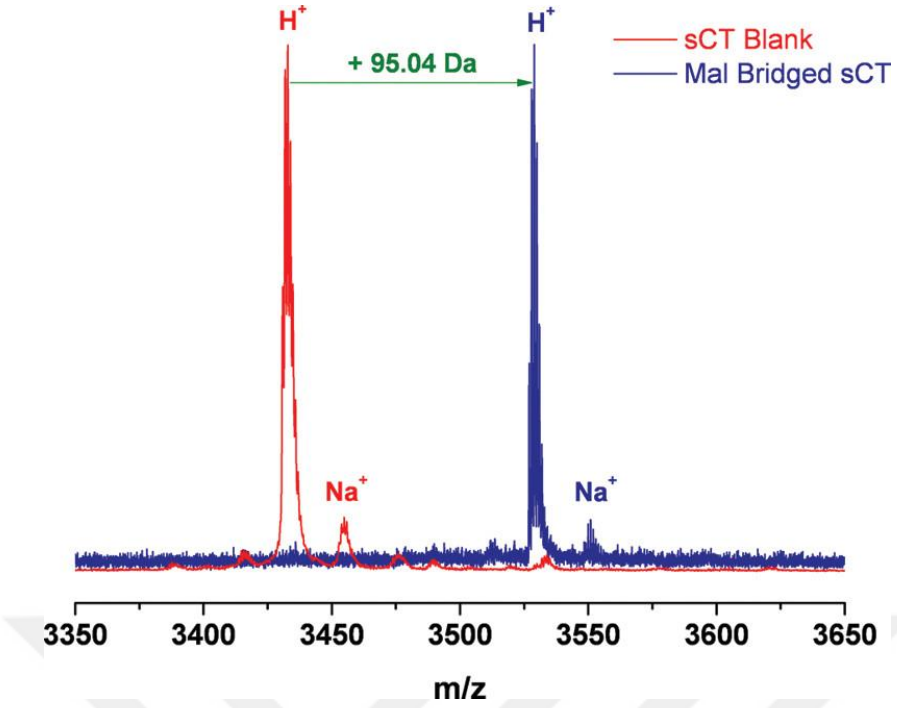

Figure 2.12 : MALDI-ToF-MS analysis of native sCT (red trace) and maleimide-bridged sCT following sampling after 10 min.

The completion of the reaction with high efficiency and without the formation of by-products was confirmed by RP-HPLC and MALDI-ToF-MS analyses [50]. In addition, PEGylation of sCT was performed using DBM-derived PEG polymers, and thanks to this modification, the protein structure was preserved and high-efficiency synthesis of functional polymer conjugates was achieved (Figure 2.13, Figure 2.14) [50].

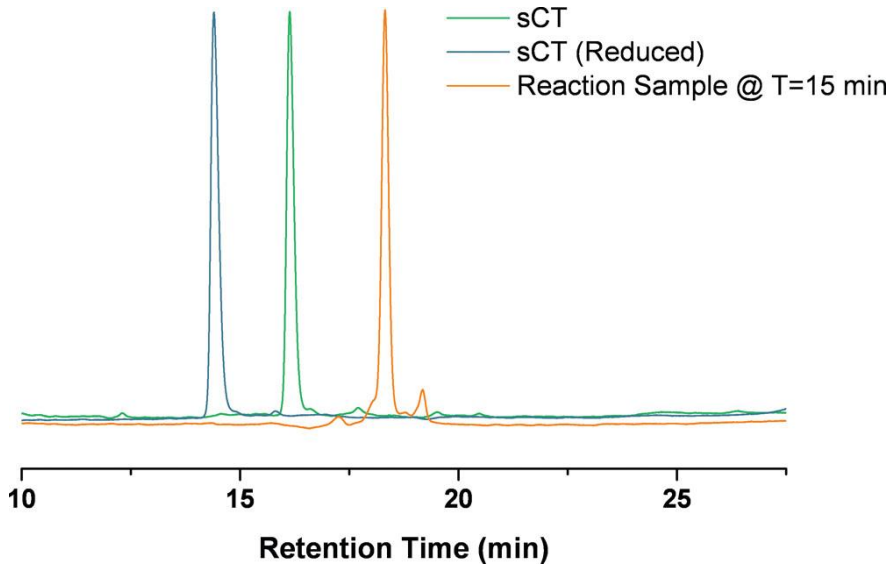

Figure 2.13 : RP- HPLC analysis of the disulfide-bridging of sCT using a dibromomaleimide-functional PEG chain following reduction with TCEP.

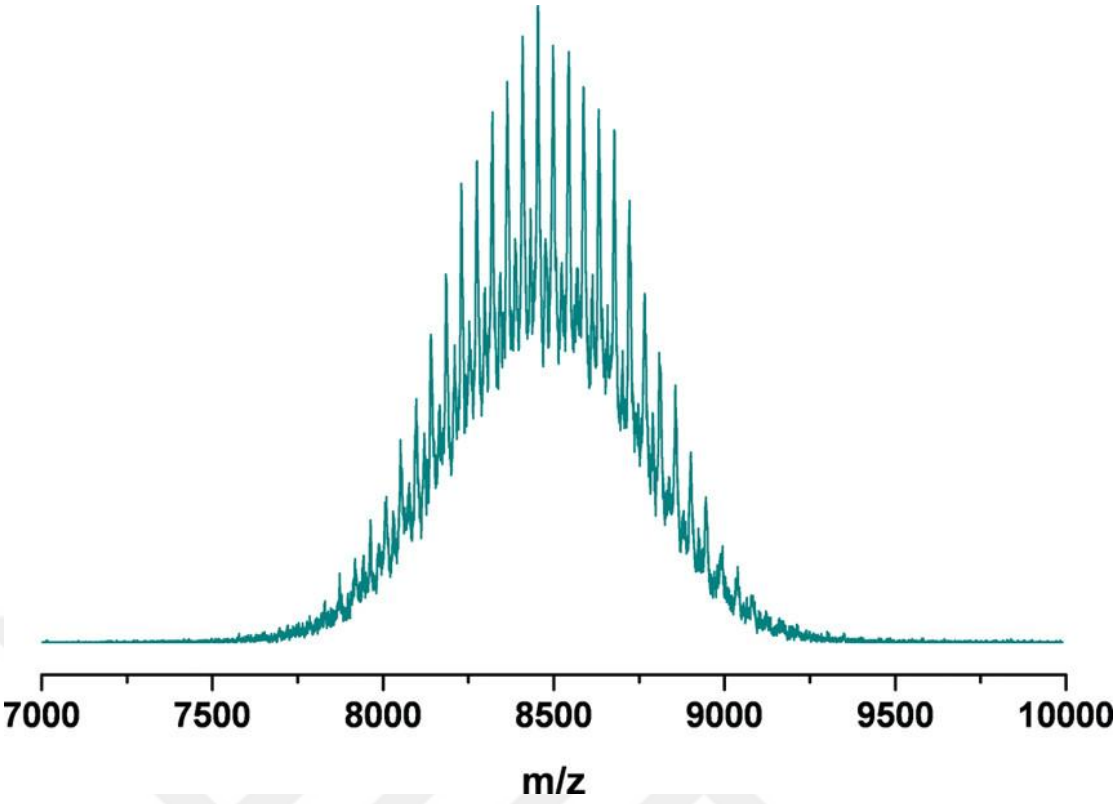

Figure 2.14 : After 15 minutes, the reaction mixture's MALDI-ToF-MS revealed the formation of the monoconjugated sCT-PEG$_{5000}$ species at about 8.5 kDa.

Additionally, functional polymers were synthesized in the study using the atom transfer radical polymerization (ATRP) technique (Figure 2.15) [50].

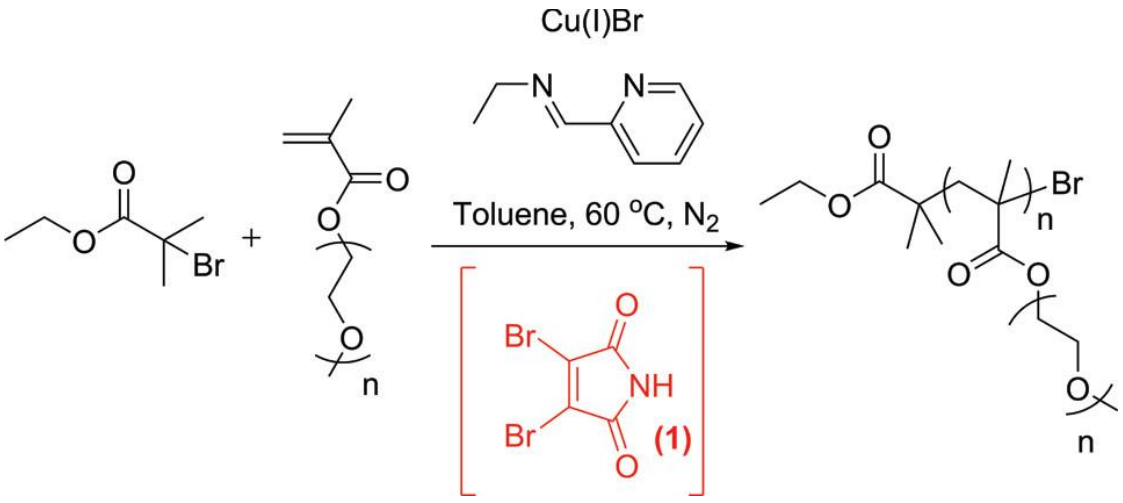

Figure 2.15 : ATRP polymerization of PEGMA in the presence and absence of the dibromomaleimide functionality.

DBM derivatives were successfully attached to the end groups of these polymers via click reactions (CuAAC) or condensation reactions (Figure 2.16) [50].

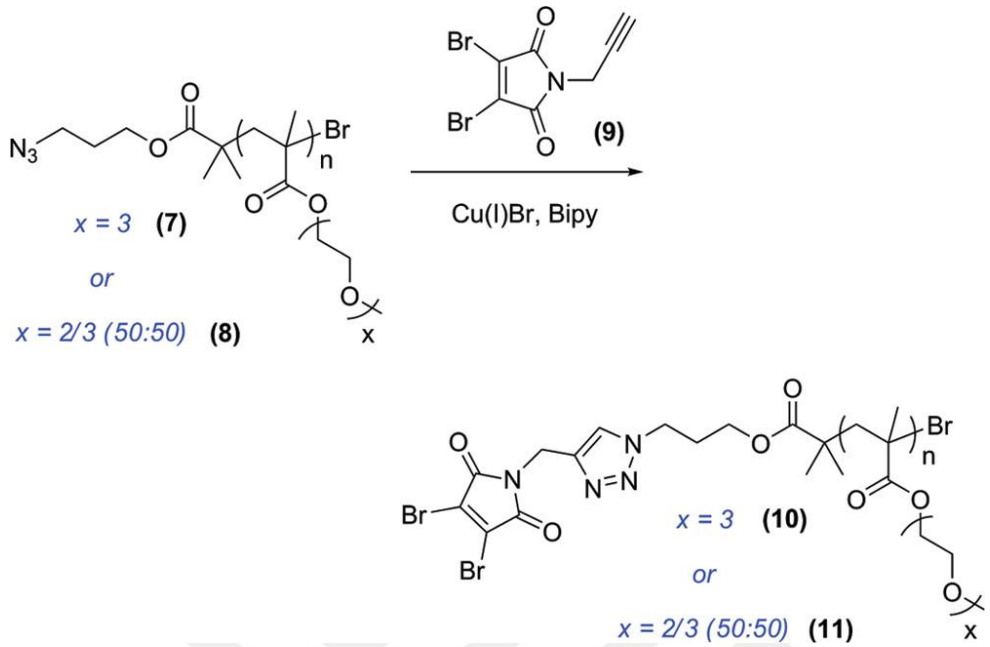

Figure 2.16 : Installation of dibromomaleimide functionality to α-azido functional polymers using CuAAC.

With these methods, controlled modification and immobilization of proteins via DBM-functional polymers with different structural properties were achieved [50]. This approach offers an effective method that simplifies protein modification and purification processes in biotechnological applications [50]. In addition, modification of disulfide bridges via DBM enables controlled and reversible degradation of the conjugate under intracellular conditions [50].

As a result, DBM derivatives stand out as an important tool for the modification of biomolecules. Providing high efficiency in both preserving the structural integrity of proteins and enabling functional modifications, DBM derivatives hold great potential for biotechnological applications [50]. These studies provide a strong foundation for the use of DBM in biomolecule immobilization, functional biomaterial design, and biotechnological drug delivery systems [45,50].

2.4. Polymer Conjugation & Polymer-Polymer Coupling

Similar to their role in biomolecule immobilization, dibromomaleimide (DBM) derivatives also offer highly efficient and versatile strategies for polymer conjugation and polymer–polymer coupling, particularly when utilized in combination with

advancements in controlled/living polymerization techniques and orthogonal "click" reactions such as thiol–maleimide or azide–alkyne cycloaddition chemistries [51,55]. These strategies enable the precise construction of well-defined macromolecular architectures with complex topologies and functionalities.

Among the DBM derivatives, N-(4-bromobutyl)-dibromomaleimide (dBMIB) has gained significant attention as a powerful and multifunctional coupling agent due to its bifunctional nature. In the study conducted by Wang et al., dBMIB was employed to dimerize thiol-terminated hydrophilic polymer chains, specifically poly(ethylene oxide) (PEO_{45}-SH), under mild aqueous conditions. The reaction proceeded in a stoichiometric 1:1 ratio, yielding the symmetric dimer structure $(PEO_{45})_2$MIB with a central maleimide unit (Figure 2.17). The efficiency and selectivity of this dimerization reaction highlight the strong reactivity of the thiol and dibromomaleimide functional groups even in water, a feature highly desirable for biocompatible or environmentally friendly polymer synthesis techniques.

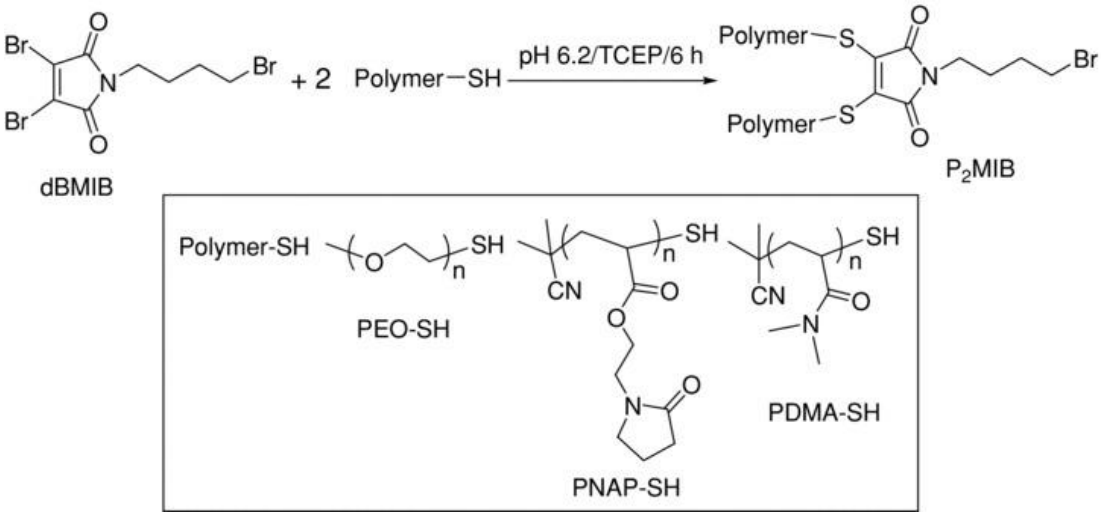

Figure 2.17 : dBMIB as a coupling agent to couple two thiol-terminated polymers into a polymer dimer.

More significantly, the study demonstrated that the remaining butylene bromide moiety within the central dBMIB core could be selectively transformed into an azide functional group [51]. This newly introduced azide group was then subjected to a Cu(I)-catalyzed azide–alkyne cycloaddition (CuAAC) reaction with an alkyne-terminated polymer chain, enabling the formation of an asymmetric A_2B-type miktoarm star polymer (Figure 2.18). This stepwise and modular synthetic approach

underscores the potential of dBMIB as a multifunctional platform for post-polymerization modification and topological polymer design [51].

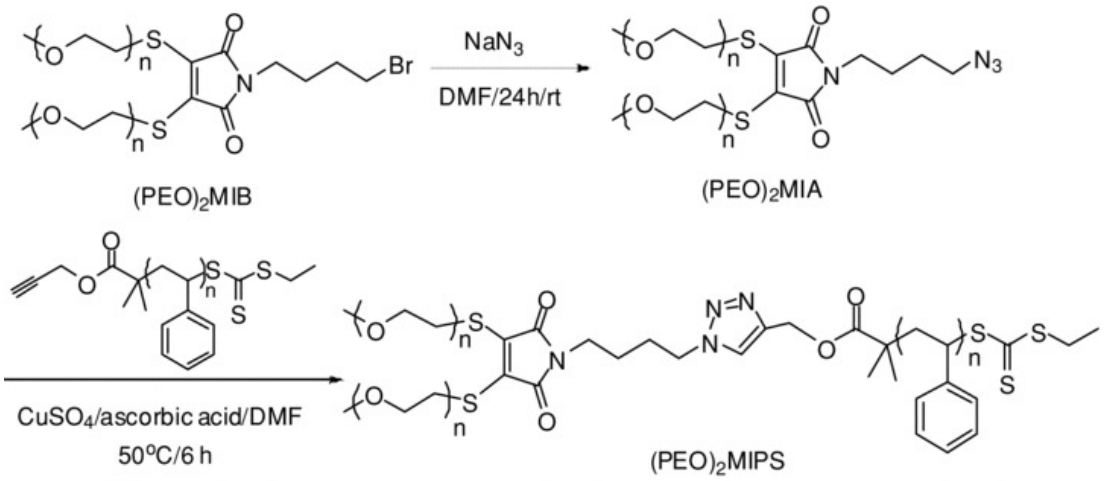

Figure 2.18 : Formation of A_2B star polymers by CuAAC click reaction.

Miktoarm star polymers, characterized by the presence of chemically distinct polymer arms radiating from a common junction point, are particularly attractive due to their ability to integrate disparate physical, chemical, or biological properties into a single macromolecular entity [2, 13-15]. The structural asymmetry and precise control over arm composition make them promising candidates for applications in nanomedicine, drug delivery, self-assembly, and advanced materials design [51].

This synthetic methodology, as developed by Wang and his team, thus offers a robust and adaptable tool for the creation of next-generation topological polymers, enabling both linear extension and branched growth through orthogonal and efficient chemical transformations [51]. In conclusion, the high reactivity, chemoselectivity, and structural adaptability of dBMIB in polymer conjugation and coupling reactions emphasize its broad potential not only in the field of biomolecular engineering but also in the development of sophisticated synthetic polymer systems with tailored architectures and functions [51].

3. EXPERIMENTAL PART

3.1. Materials

2,3-Dibromomaleimide (DBM, 97%), 1,6-hexanedithiol (HDT, 97%), 1,8-octanedithiol (97%), 1,5-pentanedithiol (96%), 1,4-butanedithiol (97%), 2,2′-(ethylenedioxy)diethanethiol (95%), 2,2′-thiodiethanethiol (90%, technical grade), benzene-1,4-dithiol (99%), 1,4-benzenedimethanethiol (98%), 4,4′-thiobisbenzenethiol (98%), trimethylolpropane tris(3-mercaptopropionate) (95%), triethylamine (TEA, 99.5%), *N*,*N*-diisopropylethylamine (DIPEA, 99%), 1,4-diazabicyclo[2.2.2]octane (DABCO, 98%), 1,8-diazabicyclo[5.4.0]undec-7-ene (DBU, 98%), 1,1,3,3-tetramethylguanidine (TMG, 99%), methyl propiolate (99%), ethyl propiolate (99%), *tert*-butyl propiolate (98%), 1-propanethiol (99%), tetrahydrofuran (THF, 99%), chloroform ($CHCl_3$, 99.8%, amylene stabilized) were all purchased from Aldrich and used as received. 1,10-Decanedithiol (95%), 6-(dibutylamino)-1,3,5-triazine-2,4-dithiol (98%) were purchased from Fisher Scientific and used as received. Dimethyl sulfoxide (DMSO, 99.9%, Aldrich), *N*,*N*-dimethylacetamide (DMAc, 99.8%, Aldrich), *N*,*N*-dimethylformamide (DMF, 99.8%, Aldrich), *N*-methyl-2-pyrrolidone (NMP, 99.5%, Aldrich) were anhydrous and used without further purification. Methanol was of reagent grade and used as received.

3.2. Instrumentation

^{1}H NMR (500 MHz) and ^{13}C NMR (125 MHz) spectra were recorded using an Agilent VNMRS 500 instrument in $CDCl_3$ and DMSO-d_6. Gel permeation chromatography (GPC) measurements were carried out with an Agilent instrument (model 1100) with a pump, refractive index and UV detectors, and four Waters Styragel columns (HR 5E, HR 4E, HR 3, HR 2) (4.6 mm internal diameter, 300 mm length, packed with 5 μm particles). The effective molecular weight ranges of the columns were 2000−4 000 000, 50−100 000, 500−30 000, and 500−20 000 g/mol, respectively. THF was used as an eluent at a flow rate of 0.3 mL/min at 30 °C, and 2,6-di-*tert*-butyl-4-methylphenol (BHT) was used as an internal standard. The weight-average molecular weights (M_w)

and dispersities (*Đ*) of the polymers were calculated based on linear polystyrene (PS) standards (Polymer Laboratories). Differential scanning calorimetry (DSC) measurements were performed under a nitrogen atmosphere using a TA Q1000 DSC apparatus. For the synthesized polymers, two different temperature procedures were applied based on their physical properties. P1-P6 polymer samples were first heated to 100 °C with a heating rate of 10 °C/min. The samples were kept at this temperature for 2 min, then cooled to -60 °C with a cooling rate of 10 °C/min and kept at this temperature for 2 min. Finally, they were reheated to 100 °C with a heating rate of 10 °C/min. P7-P11 polymer samples were first heated to 150 °C with a heating rate of 10 °C/min. The samples were kept at this temperature for 2 min, then cooled to -60 °C with a cooling rate of 10 °C/min and kept at this temperature for 2 min. Finally, they were reheated to 150 °C with a heating rate of 10 °C/min. In both cases, the data from the second heating cycle were reported. Fourier transform infrared (FTIR) spectra were recorded on a Shimadzu IRSpirit-T (Shimadzu, Japan) instrument in the 4000-650 cm^{-1} range.

3.3. Synthetic Procedures

3.3.1. General procedure for thiol-dibromomaleimide polymerization

To a 10 mL round-bottom flask equipped with a magnetic stir bar was added DBM (200 mg, 0.785 mmol, 1 equiv) and dissolved in NMP (785 μL). Dithiol monomer (0.785 mmol, 1 equiv) was then added, and upon complete dissolution, TEA (328.3 μL, 2.355 mmol, 3 equiv) was finally added to the flask. Upon the addition of TEA, an exothermic reaction occurred, accompanied by a color change and turbidity (salt formation). The reaction was allowed to stir at room temperature for 30 min. After the specified time, the reaction mixture was precipitated into acidified methanol and the supernatant was decanted, except for polymers P8 and P10, which were directly filtered. The dissolution–precipitation procedure (THF-acidified methanol) was repeated two times. The resultant polymers were dried *in vacuo*.

3.3.1.1. Synthesis of P1 (freshly prepared on a large scale)

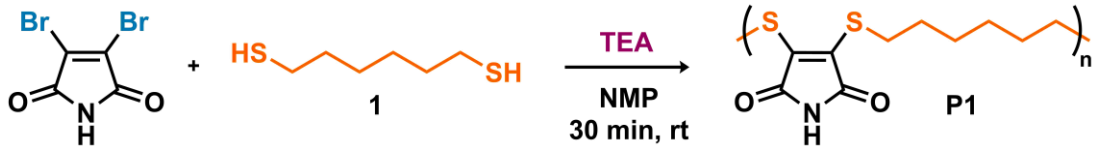

Figure 3.1 : Reaction scheme of P1.

Large-scale synthesis of P1 was conducted following the general procedure for thiol-DBM polymerization. DBM (600 mg, 2.355 mmol), HDT (360.0 µL, 2.355 mmol), TEA (984.8 µL, 7.065 mmol), and NMP (2.355 mL) were used. The polymer P1 was obtained as a yellow sticky material (yield: 492.6 mg, 86%). Figure 3.1 illustrates the reaction scheme of P1. ^{1}H NMR (DMSO-d_6, δ): 11.08 (s, 1H, NH), 3.19 (t, 4H, SCH2), 1.55 (m, 4H, SCH2CH2), 1.34 (m, 4H, SCH2CH2CH2). ^{13}C NMR (DMSO-d_6, δ): 167.84, 136.27, 31.29, 30.34, 27.77. FTIR (cm$_{-1}$): 3266, 2930, 2856, 1770, 1702, 1515, 1456, 1321, 1192, 1041, 735. GPC, DSC, and FTIR spectrums of P1 can be found in Figures A.1-A.3.

3.3.1.2. Synthesis of P2

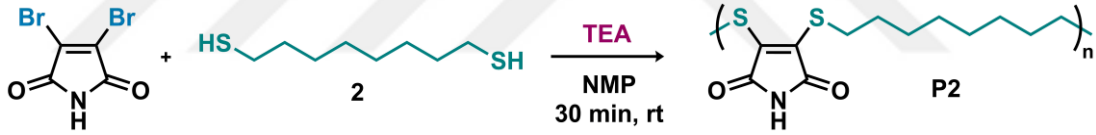

Figure 3.2 : Reaction scheme of P2.

General procedure for thiol-DBM polymerization was followed. DBM (200 mg, 0.785 mmol), 1,8-octanedithiol (144.4 µL, 0.785 mmol), TEA (328.3 µL, 2.355 mmol), and NMP (0.785 mL) were used. The polymer P2 was obtained as a yellow sticky material (yield: 185.3 mg, 87%). Figure 3.2 illustrates the reaction scheme of P2. ^{1}H NMR (DMSO-d_6, δ): 11.08 (s, 1H, NH), 3.19 (t, 4H, SCH2), 1.54 (m, 4H, SCH2CH2), 1.32 (m, 4H, SCH2CH2CH2), 1.23 (m, 4H, SCH2CH2CH2CH2). ^{13}C NMR (DMSO-d_6, δ): 167.85, 136.32, 31.37, 30.48, 28.88, 28.24. FTIR (cm$_{-1}$): 3275, 2924, 2856, 1770, 1699, 1515, 1463, 1322, 1190, 1039, 735. All characterization data (NMR, GPC, DSC and TGA spectrums) of P2 can be found in Figures A.4-A.8.

3.3.1.3. Synthesis of P3

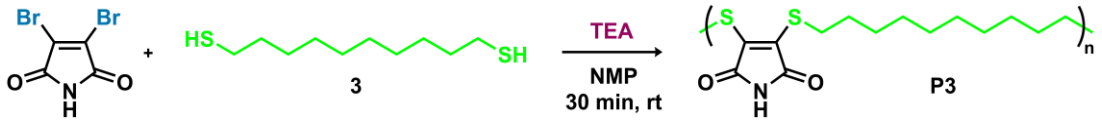

Figure 3.3 : Reaction scheme of P3.

General procedure for thiol-DBM polymerization was followed. DBM (200 mg, 0.785 mmol), 1,10-decanedithiol (170.6 µL, 0.785 mmol), TEA (328.4 µL, 2.355 mmol), and NMP (0.785 mL) were used. The polymer P3 was obtained as a yellow sticky material (yield: 169.2 mg, 72 %). Figure 3.3 illustrates the reaction scheme of P3. ^{1}H NMR (DMSO-d_6, δ): 11.09 (s, 1H, NH), 3.19 (t, 4H, SCH2), 1.54-1.21 (m, 16H, SCH2CH2 & SCH2CH2CH2 & SCH2CH2CH2CH2 & SCH2CH2CH2CH2CH2). ^{13}C NMR (DMSO-d_6, δ): 167.87, 136.37, 31.37, 30.52, 29.34, 29.00, 28.27. FTIR (cm$_{-1}$): 3275, 2924, 2856, 1770, 1710, 1515, 1459, 1321, 1189, 1046, 735. All characterization data (NMR, GPC, DSC and TGA spectrums) of P3 can be found in Figures A.9-A.13.

3.3.1.4. Synthesis of P4

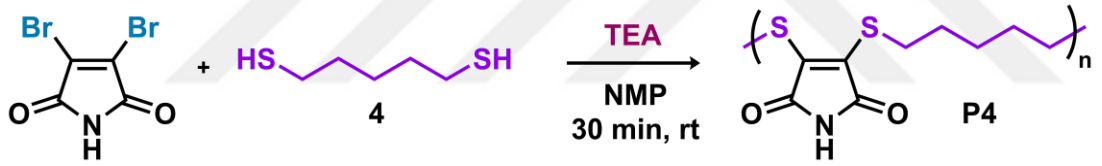

Figure 3.4 : Reaction scheme of P4.

General procedure for thiol-DBM polymerization was followed. DBM (200 mg, 0.785 mmol), 1,5-pentanedithiol (105.3 µL, 0.785 mmol), TEA (328.3 µL, 2.355 mmol), and NMP (0.785 mL) were used. The polymer P4 was obtained as a yellow sticky material (yield: 126.0 mg, 70%). Figure 3.4 illustrates the reaction scheme of P4. ^{1}H NMR (DMSO-d_6, δ): 11.07 (s, 1H, NH), 3.21 (t, 4H, SCH2), 1.58 (m, 4H, SCH2CH2), 1.44 (m, 4H, SCH2CH2CH2). ^{13}C NMR (DMSO-d_6, δ): 167.84, 136.26, 31.21, 29.90, 27.16. FTIR (cm^{-1}): 3269, 2930, 2858, 1770, 1699, 1518, 1454, 1321, 1189, 1035, 735. All characterization data (NMR, GPC, DSC and TGA spectrums) of P4 can be found in Figures A.14-A.18.

3.3.1.5. Synthesis of P5

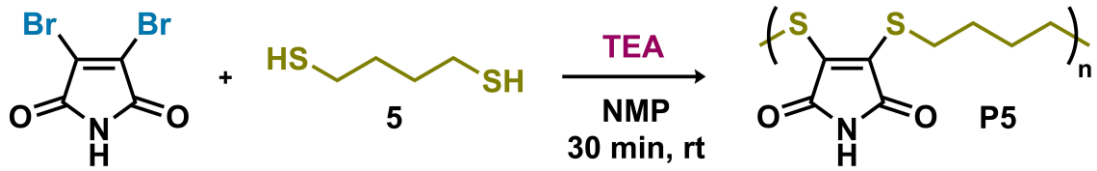

Figure 3.5 : Reaction scheme of P5.

General procedure for thiol-DBM polymerization was followed. DBM (200 mg, 0.785 mmol), 1,4-butanedithiol (92.1 µL, 0.785 mmol), TEA (328.3 µL, 2.355 mmol), and NMP (0.785 mL) were used. The polymer P5 was obtained as a yellow sticky material (yield: 84.5 mg, 50%). Figure 3.5 illustrates the reaction scheme of P5. ^{1}H NMR (DMSO-d_6, δ): 11.09 (s, 1H, NH), 3.23 (s, 4H, SCH2), 1.67 (s, 4H, SCH2CH2). ^{13}C NMR (DMSO-d_6, δ): 167.80, 136.29, 30.85, 29.25. FTIR (cm^{-1}): 3207, 2938, 1770, 1704, 1520, 1451, 1321, 1186, 1032, 735. All characterization data (NMR, GPC, DSC and TGA spectrums) of P5 can be found in Figures A.19-A.23.

3.3.1.6. Synthesis of P6

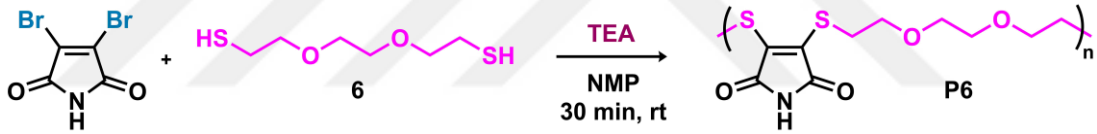

Figure 3.6 : Reaction scheme of P6.

General procedure for thiol-DBM polymerization was followed. DBM (200 mg, 0.785 mmol) 2,2′-(ethylenedioxy)diethanethiol (127.8 µL, 0.785 mmol), TEA (328.3 µL, 2.355 mmol), and NMP (0.785 mL) were used. The polymer P6 was obtained as a yellow sticky material (yield: 185.9 mg, 86%). Figure 3.6 illustrates the reaction scheme of P6. ^{1}H NMR (DMSO-d_6, δ): 11.09 (s, 1H, NH), 3.60 (t, 4H, SCH2CH2), 3.49 (t, 4H, SCH2), 3.39 (t, 4H, SCH2CH2OCH2). ^{13}C NMR (DMSO-d_6, δ): 167.86, 136.30, 70.34, 70.06, 31.12. FTIR (cm^{-1}): 3206, 2864, 1770, 1707, 1520, 1462, 1412, 1412, 1324, 1184, 1093, 1041, 735. ^{13}C NMR, GPC, DSC, and FTIR spectrum of P6 can be found in Figures A.24-A.27.

3.3.1.7. Synthesis of P7

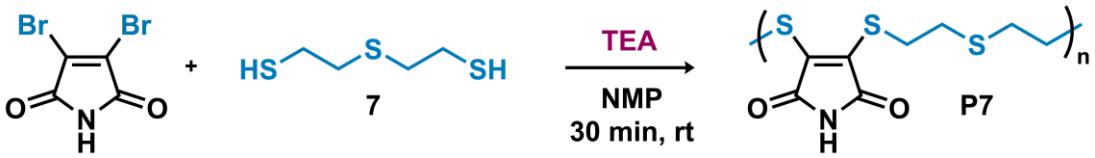

Figure 3.7 : Reaction scheme of P7.

General procedure for thiol-DBM polymerization was followed. DBM (200 mg, 0.785 mmol), 2,2′-thiodiethanethiol (102.4 µL, 0.785 mmol), TEA (328.3 µL, 2.355 mmol), and NMP (0.785 mL) were used. The polymer P7 was obtained as an orange powder (yield: 174.7 mg, 90%). Figure 3.7 illustrates the reaction scheme of P7. ^{1}H NMR (DMSO-d_6, δ): 11.12 (s, 1H, NH), 3.44 (t, 4H, SCH2), 2.82 (t, 4H, SCH2). ^{13}C NMR (DMSO-d_6, δ): 167.84, 135.80, 32.26, 31.42. FTIR (cm^{-1}): 3206, 2971, 2873, 1763, 1699, 1515, 1415, 1319, 1184, 1044, 735. All characterization data (NMR, GPC, DSC and TGA spectrums) of P7 can be found in Figures A.28-A.32.

3.3.1.8. Synthesis of P8

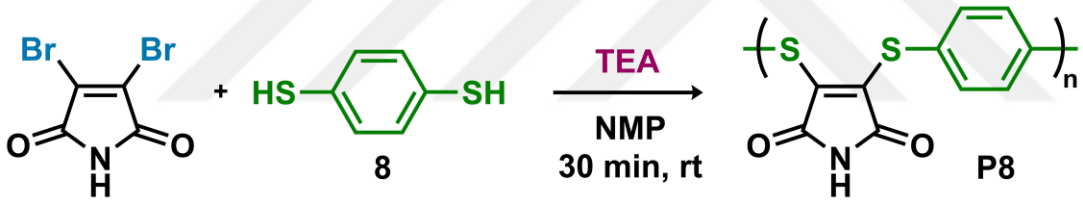

Figure 3.8 : Reaction scheme of P8.

General procedure for thiol-DBM polymerization was followed. DBM (200 mg, 0.785 mmol), benzene-1,4-dithiol (111.7 mg, 0.785 mmol), TEA (328.4 µL, 2.355 mmol), and NMP (0.785 mL) were used. The polymer P8 was obtained as an orange powder (yield: 157.0 mg, 85%). Figure 3.8 illustrates the reaction scheme of P8. ^{1}H NMR (DMSO-d_6, δ): 11.38 (s, 1H, NH), 7.12 (s, 4H, Ar-H). ^{13}C NMR (DMSO-d_6, δ): 167.78, 136.66, 131.46, 129.79. FTIR (cm^{-1}): 3270, 2981, 2863, 1776, 1719, 1518, 1473, 1327, 1186, 1041, 807, 735, 652. ^{13}C NMR, GPC, DSC, and FTIR spectrum of P8 can be found in Figures A.33-A.36.

3.3.1.9. Synthesis of P9

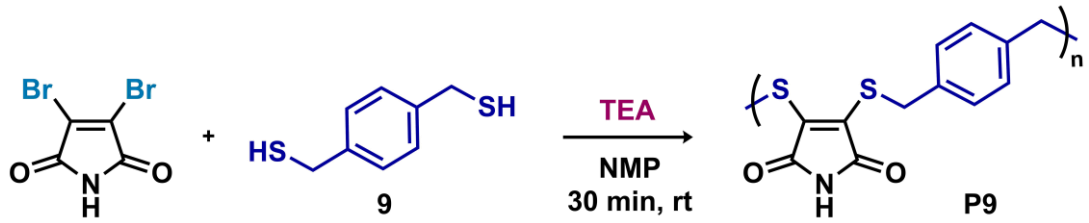

Figure 3.9 : Reaction scheme of P9.

General procedure for thiol-DBM polymerization was followed. DBM (200 mg, 0.785 mmol), 1,4-benzenedimethanethiol (133.7 mg, 0.785 mmol), TEA (328.3 µL, 2.355 mmol), and NMP (0.785 mL) were used. The polymer P9 was obtained as a yellow powder (yield: 155.0 mg, 75%). Figure 3.9 illustrates the reaction scheme of P9. ^{1}H NMR (DMSO-d_6, δ): 11.20 (s, 1H, NH), 7.18 (s, 4H, Ar-H), 4.38 (s, 4H, SCH2). ^{13}C NMR (DMSO-d_6, δ): 167.88, 136.78, 129.55, 35.29. FTIR (cm^{-1}): 3260, 2981, 2868, 1768, 1699, 1515, 1414, 1323, 1183, 1039, 735. ^{13}C NMR, GPC, DSC, and FTIR spectrum of P8 can be found in Figures A.37-A.40.

3.3.1.10. Synthesis of P10

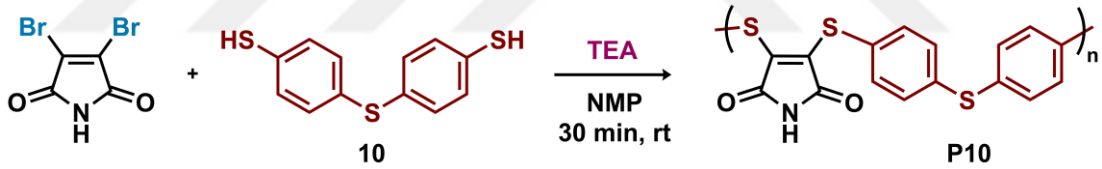

Figure 3.10 : Reaction scheme of P10.

General procedure for thiol-DBM polymerization was followed. DBM (200 mg, 0.785 mmol), 4,4′-thiobisbenzenethiol (196.6 mg, 0.785 mmol), TEA (328.3 µL, 2.355 mmol), and NMP (0.785 mL) were used. The polymer P10 was obtained as an orange powder (yield: 194.1 mg, 72%). Figure 3.10 illustrates the reaction scheme of P10. ^{1}H NMR (DMSO-d_6, δ): 11.40 (s, 1H, NH), 7.15 (m, 8H, Ar-H). ^{13}C NMR (DMSO-d_6, δ): 168.03, 136.19, 135.07, 134.70, 131.92, 131.36, 131.10, 130.47, 129.08. FTIR (cm^{-1}): 3255, 2959, 2873, 1773, 1714, 1569, 1523, 1471, 1318, 1179, 1041, 809, 735. All characterization data (NMR, GPC, DSC and TGA spectrums) of P10 can be found in Figures A.41-A.45.

3.3.1.11. Synthesis of P11

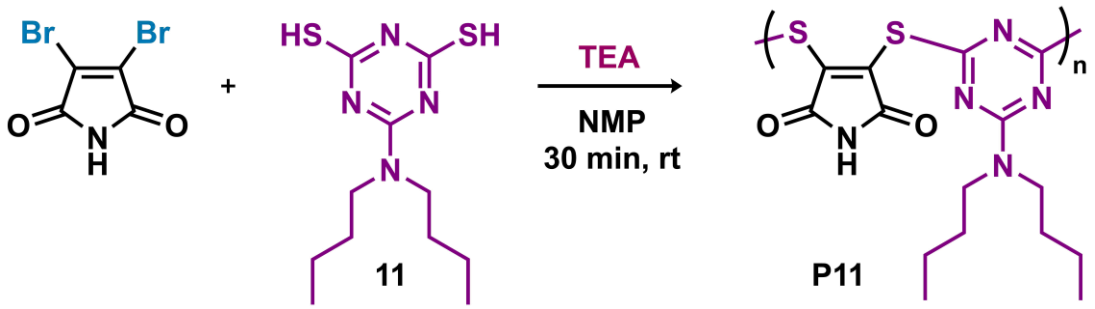

Figure 3.11 : Reaction scheme of P11.

General procedure for thiol-DBM polymerization was followed. DBM (200 mg, 0.785 mmol), 6-(dibutylamino)-1,3,5-triazine-2,4-dithiol (213.9 mg, 0.785 mmol), TEA (328.3 µL, 2.355 mmol), and NMP (0.785 mL) were used. The polymer P11 was obtained as an orange powder (yield: 252.5 mg, 88%). Figure 3.11 illustrates the reaction scheme of P11. ^{1}H NMR (DMSO-d_6, δ): 11.80 (s, 1H, NH), 3.39 (t, 4H, NCH2), 1.37 (br, 4H, NCH2CH2), 1.14 (br, 4H, NCH2CH2CH2), 0.79 (t, 6H, NCH2CH2CH2CH3). ^{13}C NMR (DMSO-d_6, δ): 175.74, 166.41, 160.75, 141.72, 47.53, 29.46, 19.97, 14.09. FTIR (cm^{-1}): 3264, 2958, 2870, 1782, 1729, 1564, 1530, 1459, 1302, 1236, 1195, 1154, 1041, 834, 735. ^{13}C NMR, GPC, DSC, and FTIR spectrum of P11 can be found in Figures A.46-A.50.

3.3.1.12. Polymerization reaction between DBM and 1,3-propanedithiol

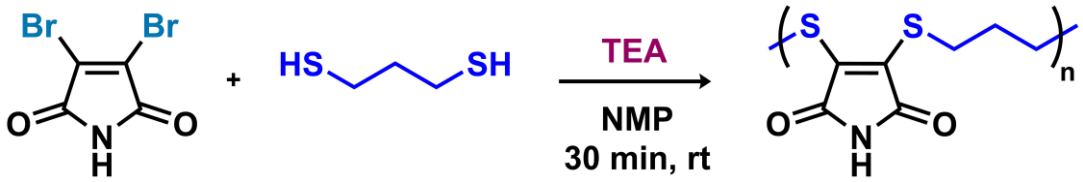

Figure 3.12 : Scheme of polymerization reaction between 1,3-propanedithiol and DBM.

Reaction of 1,3-propanedithiol with DBM was conducted following the general procedure for thiol-DBM polymerization. DBM (200 mg, 0.785 mmol), 1,3-propanedithiol (78.8 µL, 0.785 mmol), TEA (328.3 µL, 2.355 mmol) and NMP (785 µL) were used. Upon the addition of TEA, an exothermic reaction occurred, accompanied by a color change and turbidity (salt formation). The reaction was allowed to stir at room temperature for 30 min. After the specified time, the reaction mixture was precipitated into hexane and the resulting mixture was decanted. Then,

the mixture was diluted with DCM and extracted with distilled water. The organic phase was collected and dried over Na_2SO_4 to yield an orange solid compound (yield: 102.8 mg, 61%). Figure 3.12 illustrates the reaction scheme of polymerization reaction between 1,3-propanedithiol and DBM.

3.3.2. Postpolymerization modification of P1 via imide-yne click reaction

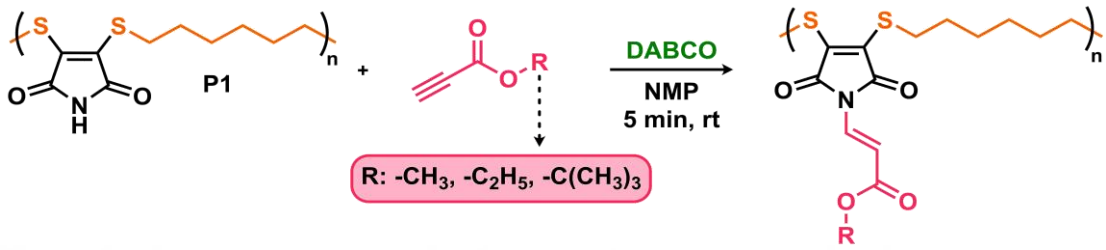

Figure 3.13 : Postpolymerization Modification of P1 with Propiolate Esters via an Imide-yne Click Reaction

To a 10 mL round-bottom flask equipped with a magnetic stir bar was added P1 (100 mg, 0.411 mmol, based on repeating unit, 1 equiv) and dissolved in 1 mL of NMP. Then, a propiolate ester compound (0.616 mmol, 1.5 equiv) and DABCO (4.59 mg, 0.0411 mmol, 0.1 equiv) were added to the reaction medium, respectively. Upon the addition of DABCO, the bright yellow solution instantly turned dark brown. The mixture was allowed to stir at room temperature for 5 min and then precipitated into acidified methanol, and the supernatant was decanted. The dissolution–precipitation procedure ($CHCl_3$-acidified methanol) was repeated two times. The resultant polymers were dried *in vacuo*. Figure 3.13 illustrates the postpolymerization modification of P1 with propiolate esters via an imide-yne click reaction.

3.3.2.1. Modification of P1 with ethyl propiolate

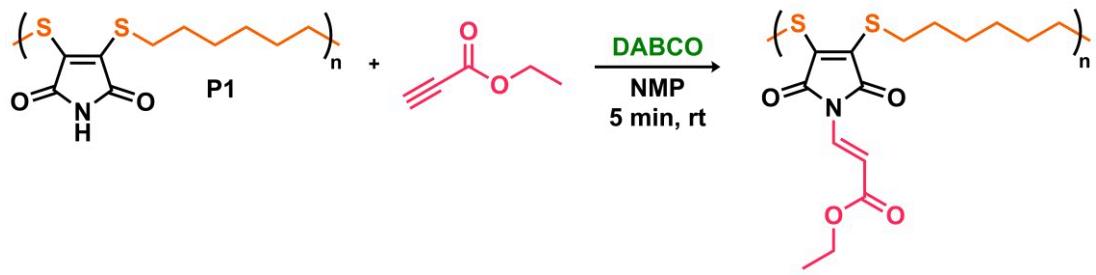

Figure 3.14 : Reaction scheme showing the modification of P1 with ethyl propiolate.

General procedure for postpolymerization modification was followed. P1 (100 mg, 0.411 mmol), ethyl propiolate (62.4 µL, 0.616 mmol), DABCO (4.59 mg, 0.041 mmol) and NMP (1 mL) were used. The modified polymer was obtained as a brown sticky material (yield: 116.5 mg, 83%). Figure 3.14 illustrates the reaction scheme for the modification of P1 with ethyl propiolate. ^{1}H NMR ($CDCl_3$, δ): 7.68 (d, 1H, NC*H*), 6.66 (d, 1H, NCH=C*H*), 4.21 (m, 2H, OCH_2), 3.34 (t, 4H, SCH_2), 1.69 (br, 4H, SCH_2CH_2), 1.47 (br, 4H, $SCH_2CH_2CH_2$), 1.30 (t, 3H, OCH_2CH_3). ^{13}C NMR ($CDCl_3$, δ): 167.09, 163.20, 136.67, 130.07, 107.00, 60.51, 31.60, 30.34, 27.93, 14.29. ^{13}C NMR and FTIR spectrum of ethyl propiolate modified P1 can be found in Figures B.1-B.2.

3.3.2.2. Modification of P1 with methyl propiolate

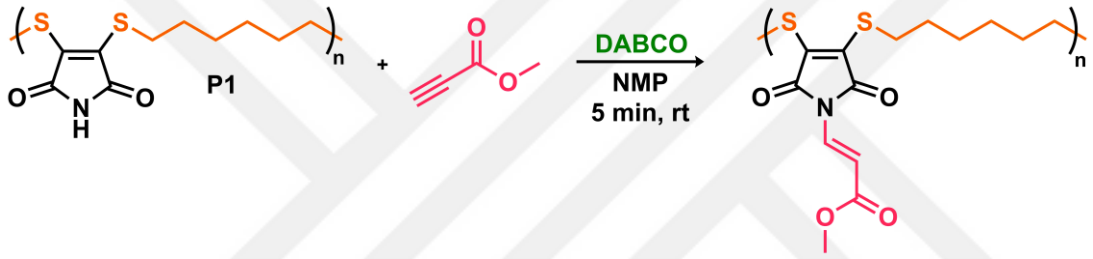

Figure 3.15 : Reaction scheme showing the modification of P1 with methyl propiolate.

General procedure for postpolymerization modification was followed. P1 (100 mg, 0.411 mmol), methyl propiolate (54.8 µL, 0.616 mmol), DABCO (4.59 mg, 0.041 mmol) and NMP (1 mL) were used. The modified polymer was obtained as a brown powder (yield: 109.4 mg, 81%). Figure 3.15 illustrates the reaction scheme for the modification of P1 with methyl propiolate. ^{1}H NMR ($CDCl_3$, δ): 7.70 (d, 1H, NC*H*), 6.71 (d, 1H, NCH=C*H*), 3.78 (s, 3H, OCH_3), 3.35 (m, 4H, SCH_2), 1.69-1.47 (br, 16H, SCH_2CH_2 & $SCH_2CH_2CH_2$). ^{13}C NMR ($CDCl_3$, δ): 167.74, 163.24, 136.77, 130.37, 106.46, 51.78, 31.62, 30.33, 27.86. ^{1}H NMR, ^{13}C NMR and FTIR spectrum of methyl propiolate modified P1 can be found in Figures B.3-B.5.

3.3.2.3. Modification of P1 with *tert*-butyl propiolate

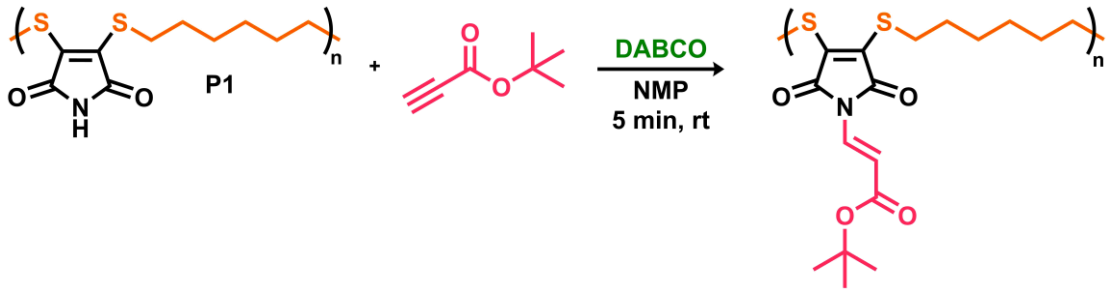

Figure 3.16 : Reaction scheme showing the modification of P1 with *tert*-butyl propiolate.

General procedure for postpolymerization modification was followed. P1 (100 mg, 0.411 mmol), *tert*-butyl propiolate (84.5 µL, 0.616 mmol), DABCO (4.59 mg, 0.041 mmol) and NMP (1 mL) were used. The modified polymer was obtained as an orange powder (yield: 113.9 mg, 75%). Figure 3.16 illustrates the reaction scheme showing the modification of P1 with *tert*-butyl propiolate. ^{1}H NMR ($CDCl_3$, δ): 7.57 (d, 1H, NC*H*), 6.63 (d, 1H, NCH=C*H*), 3.34 (m, 4H, SCH_2), 1.69-1.50 (br, 17H, SCH_2CH_2 & $SCH_2CH_2CH_2$ & $OC(CH_3)_3$). ^{13}C NMR ($CDCl_3$, δ): 166.38, 163.30, 136.62, 129.33, 108.96, 80.70, 31.61, 30.35, 28.20, 27.97. ^{1}H NMR, ^{13}C NMR and FTIR spectrum of *tert*-butyl propiolate modified P1 can be found in Figures B.6-B.8.

3.3.3. Degradation study of P1

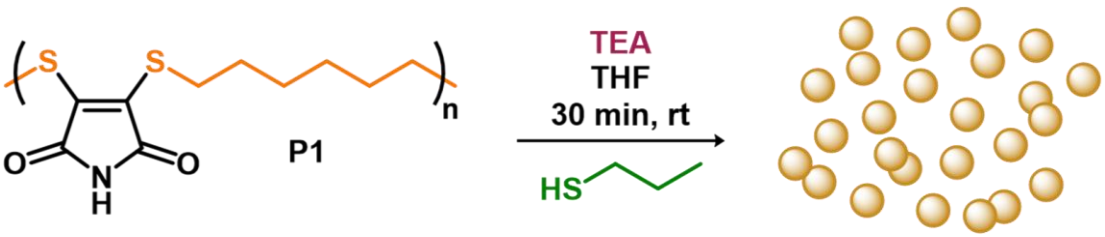

Figure 3.17 : Reaction scheme for degradation of P1.

To a 10 mL round-bottom flask equipped with a magnetic stir bar was added P1 (100 mg, 0.411 mmol, based on repeating unit, 1 equiv) and dissolved in 3 mL of THF. Then, 1-propanethiol (114.5 µL, 1.233 mmol, 3 equiv) and TEA (171.8 µL, 1.233 mmol, 3 equiv) were added to the reaction medium, respectively. Figure 3.17 illustrates the reaction scheme for degradation of P1.

Aliquots of 25 µL were withdrawn from the reaction medium at different time intervals and characterized by GPC. The GPC traces of degradation products with respect to reaction time are shown in Figure 3.18. Overlaid ^{1}H NMR spectra of degradation products of P1 can be found in Figure B.9. The FTIR spectrum of degraded P1 is shown in Figure B.10.

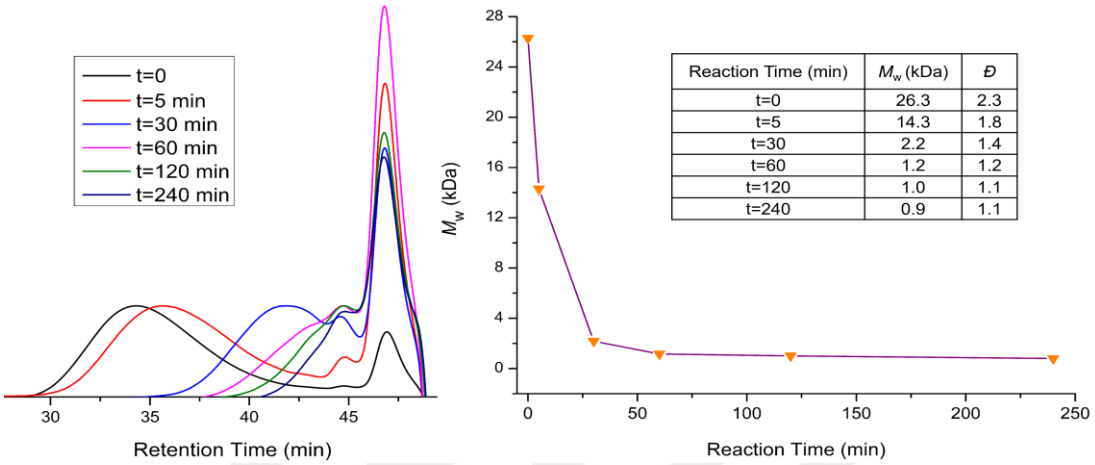

Reaction Time (min)	M_w (kDa)	$Đ$
t=0	26.3	2.3
t=5	14.3	1.8
t=30	2.2	1.4
t=60	1.2	1.2
t=120	1.0	1.1
t=240	0.9	1.1

Figure 3.18 : Overlaid GPC traces of P1 over time in the presence of TEA and 1-propanethiol.

3.3.4. Synthesis of cross-linked polymer

To a 10 mL round-bottom flask equipped with a magnetic stir bar was added DBM (200 mg, 0.785 mmol, 1.5 equiv) and dissolved in NMP (1.570 mL). Trimethylolpropane tris(3-mercaptopropionate) (172.3 µL, 0.523 mmol, 1 equiv) was then added, and upon complete dissolution, TEA (218.8 µL, 1.570 mmol, 3 equiv) was finally added to the flask. Upon the addition of TEA, an exothermic reaction and gel formation occurred simultaneously. Figure 3.19 illustrates the reaction scheme for the synthesis of cross-linked polymer. FTIR spectrum of cross-linked polymer is shown in Figure A.50.

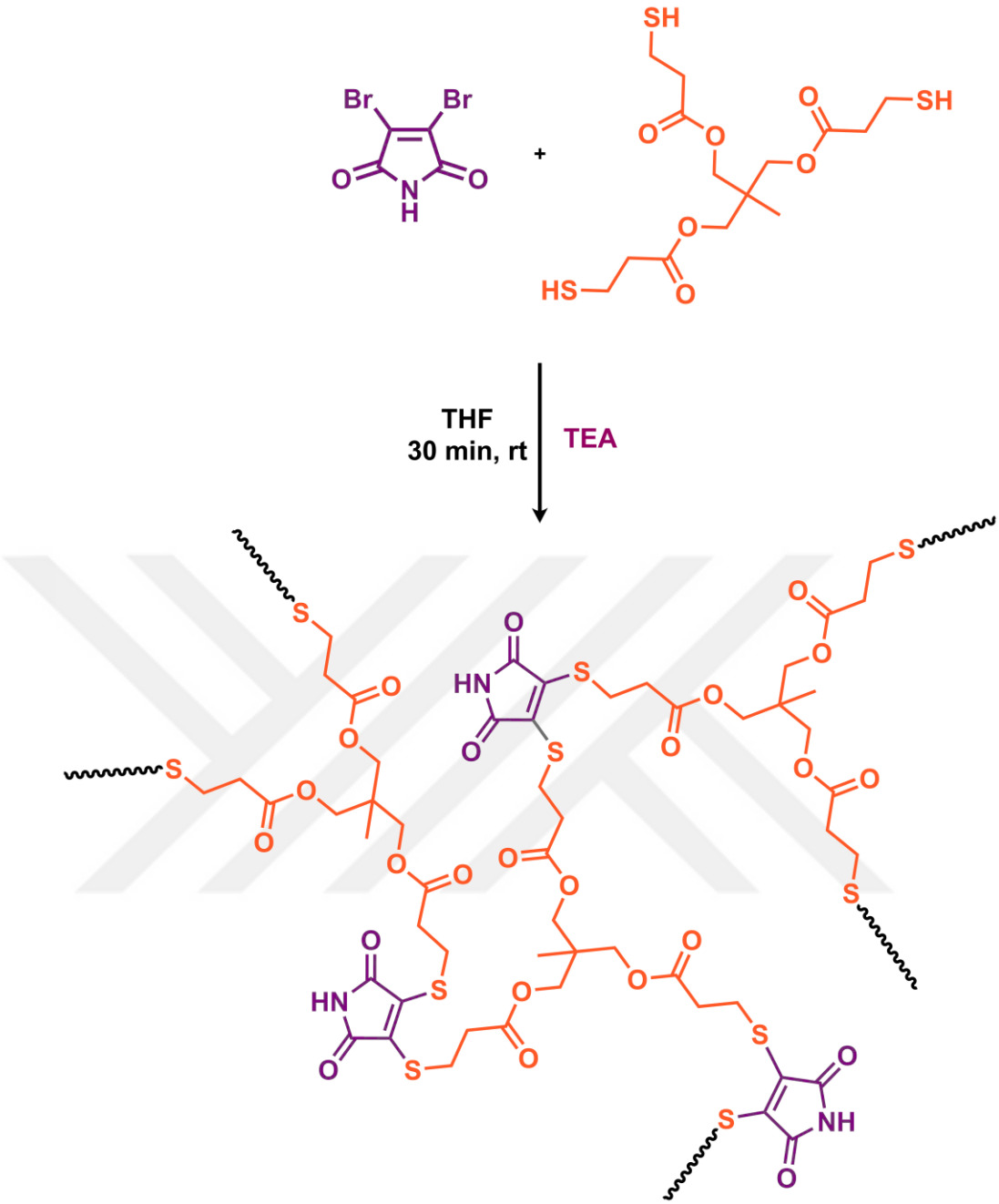

Figure 3.19 : Reaction scheme for the synthesis of cross-linked polymer.

3.3.5. Degradation of cross-linked polymer

To the same round-bottom flask with the cross-linked polymer, 3 mL of THF was added, followed by 1-propanethiol (145.8 µL, 1.570 mmol, 3 equiv relative to the used trimethylolpropane tris(3-mercaptopropionate)) and TEA (218.8 µL, 1.570 mmol, 3 equiv), respectively. Figure 3.20 illustrates the reaction scheme for degradation of cross-linked polymer. During degradation, the salts trapped within the gel were released and mixed with the solution. After 30 min, stirring was stopped, and the solid,

insoluble salts settled to the bottom. Then, the reaction solution was filtered to give a clear solution. Figure 4.4 illustrates the degradation process of cross-linked polymer through visual representations. FTIR spectrum of degraded cross-linked polymer is shown in Figure B.11.

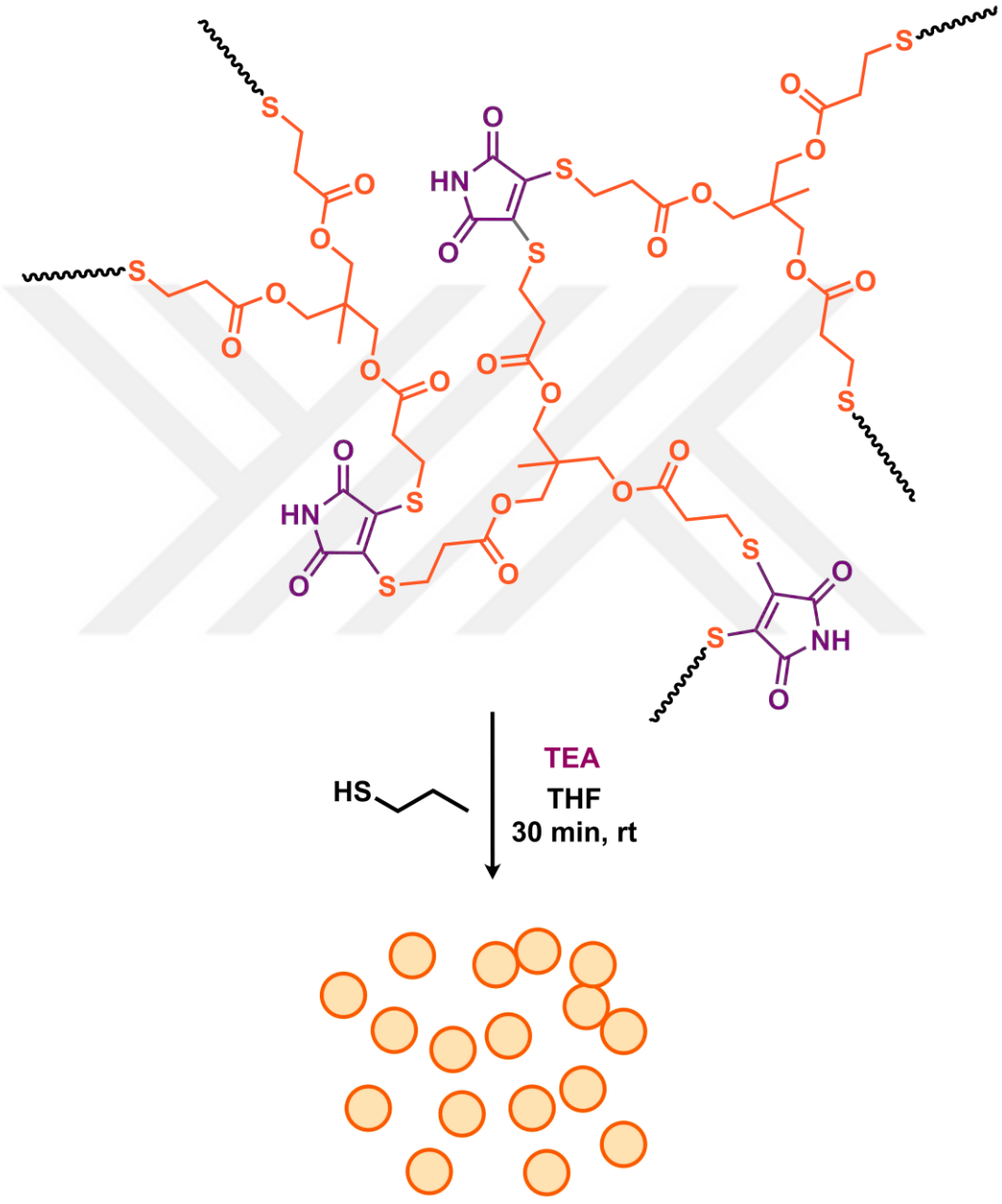

Figure 3.20 : Reaction scheme for degradation of cross-linked polymer.

4. RESULTS AND DISCUSSION

4.1. General Aspects of Thiol-Dibromomaleimide Polymerization

Firstly, HDT was selected as the model dithiol and reacted with DBM in an equimolar ratio. Both monomers and the obtained polymer P1 were dissolved in different polar solvents at a concentration of 0.5 M to ensure complete solubility (Table 4.1). Since the substitution reaction produces HBr, TEA was initially used in a 3-fold molar excess to maintain the basic environment during the polymerization process. In addition, an exothermal reaction occurred when TEA was added to the reaction medium, and excess salt (triethylammonium bromide) was formed, which increased the viscosity of the medium. Polymerization reactions were monitored by GPC for up to 8 hours. Among the tested solvents, NMP produced higher molecular weight polymers compared to DMSO, DMAc, and DMF, making NMP the most suitable solvent for polymerization (Table 4.1, entries 1-4). An increase in molecular weights was observed when the monomer concentration was increased to 0.75 and 1 M (Table 4.1, entries 5 and 6). However, a further increase in monomer concentration made it difficult to mix the reaction medium properly. The increase in viscosity of the reaction mixture prevented the provision of a homogeneous solution. Therefore, the base species and its equivalent were systematically tested at 0.5 M concentration.

Table 4.1 : Solvent Optimization for Thiol-DBM Polymerization[a].

entry	solvent	M_w (kDa)[b] / $Đ$[b]						
		5 min	30 min	1h	2h	4h	6h	8h
1	NMP	14.6 / 2.0	15.7 / 2.1	15.8 / 2.2	16.2 / 2.2	16.3 / 2.1	16.7 / 2.1	17.6 / 2.0
2	DMSO	13.5 / 1.7	14.6 /2.2	15.4 / 2.1	15.1 / 2.1	15.1 / 2.1	15.3 / 2.2	15.4 / 2.3
3	DMAc	9.6 / 1.9	10.4 / 1.9	10.5 / 2.1	10.4 / 2.0	10.5 / 1.9	11.7 / 2.2	11.8 / 2.1
4	DMF	13.1 / 2.1	13.1 / 2.1	13.3 / 2.0	13.6 / 2.1	14.2 / 2.1	14.7 / 2.2	14.9 / 2.2
5[c]	NMP	19.1 / 2.2	22.3 / 2.0	22.3 / 2.4	22.9 / 2.3	23.4 / 2.0	24.3 / 2.4	24.3 / 2.0
6[d]	NMP	21.6 / 2.0	25.2 / 2.0	25.5 / 1.9	25.8 / 2.3	25.9 / 2.2	26.1 / 2.4	26.7 / 2.3

[a]Reaction conditions: 0.785 mmol of DBM, 0.785 mmol of HDT, and 2.355 mmol of TEA in 1.57 mL of solvent at room temperature. [b] Determined by GPC calibrated based on linear PS standards in THF. [c]Reaction was carried out using monomer concentrations of 0.75 M. [d]Reaction was carried out using monomer concentrations of 1 M.

Following the initial results obtained with TEA, various organobases were evaluated to identify the most effective organobase. Among these, DBU demonstrated

outstanding performance, producing relatively high molecular weight polymers in just 5 min (Table 4.2, entry 2). However, longer reaction times with DBU led to depolymerization. Another point to note here is that DBU is the most basic and nucleophilic compound among the organobases tested in this study [56−59]. Therefore, it is thought that the combination of these two properties might have accelerated depolymerization over time. In contrast, both DIPEA and TMG produced lower molecular weight polymers compared to TEA over a period of 8 h (Table 4.2, entries 3 and 4). Therefore, TEA was selected as the most suitable base for polymerization and was used in the rest of the study.

Table 4.2 : Determination of suitable base for Thiol-DBM polymerization[a].

entry	base	M_w (kDa)[b] / $Đ$[b]						
		5 min	30 min	1h	2h	4h	6h	8h
1	TEA	14.6 / 2.0	15.7 / 2.1	15.8 / 2.2	16.2 / 2.2	16.3 / 2.1	16.7 / 2.1	17.6 / 2.0
2	DBU	16.6 / 2.3	15.9 / 2.5	13.6 / 2.3	11.5 / 2.2	9.4 / 2.0	8.6 / 2.1	8.0 / 2.0
3	DIPEA	9.1 / 1.8	10.5 / 1.9	10.5 / 1.9	10.7 / 1.9	10.9 / 1.9	10.7 / 1.9	11.0 / 1.9
4	TMG	12.7 / 2.2	13.0 / 2.4	13.3 / 2.1	13.7 / 2.2	13.6 / 2.3	14.2 / 2.4	14.4 / 2.4

[a]Reaction conditions: 0.785 mmol of DBM, 0.785 mmol of HDT, and 2.355 mmol of base in 1.57 mL of NMP at room temperature. [b] Determined by GPC calibrated based on linear PS standards in THF.

Finally, we investigated the effect of the TEA equivalents on the polymerization. As mentioned before, 3 equivalents of TEA were initially used to provide a basic medium for the polymerizations. When the TEA was reduced to 2 equivalents, lower molecular weight polymers were obtained (Table 4.3, entry 1). When the TEA concentration was increased to 4 equivalents, the molecular weight of the polymers slightly increased (Table 4.3, entry 3). Lower molecular weight polymers were obtained when the polymerization was carried out at 0 °C, indicating that an exothermal reaction was required to promote the polymerization (Table 4.3, entry 4).

Table 4.3 : Optimization of TEA equivalent for Thiol-DBM polymerization[a].

entry	equiv	M_w (kDa)[b] / $Đ$[b]						
		5 min	30 min	1h	2h	4h	6h	8h
1	2	15.4 / 1.6	17.8 / 1.6	17.8 / 1.6	17.7 / 1.7	19.1 / 2.2	18.9 / 2.1	19.0 / 2.0
2	3	21.6 / 2.0	25.2 / 2.0	25.5 / 1.9	25.8 / 2.3	25.9 / 2.2	26.1 / 2.4	26.7 / 2.3
3	4	22.5 / 2.1	26.3 / 2.3	27.1 / 2.0	27.2 / 2.0	27.9 / 2.1	28.1 / 2.2	28.7 / 2.3
4[c]	3	11.0 / 1.5	11.6 / 1.6	11.7 / 1.6	11.9 / 1.7	12.0 / 1.7	12.4 / 1.8	12.5 / 1.9

[a]Reaction conditions: 0.785 mmol of DBM and 0.785 mmol of HDT in 0.785 mL of NMP at room temperature. [b] Determined by GPC calibrated based on linear PS standards in THF. [c]Reaction was carried out at 0 °C.

Based on the findings of the optimization studies, it was determined that NMP was the optimal solvent and TEA was the most appropriate base. To produce high molecular weight polymers, dithiol:DBM:TEA molar ratios were established to 1:1:3, and a monomer concentration of 1 M was employed throughout the diversification tests. It is also worth mentioning that optimization tests demonstrated that a reaction period of 30 minutes was adequate for the proposed polymerization; no discernible difference was seen beyond this time, suggesting a time-saving polymerization procedure (Table 4.1, entry 6).

4.2. Characterization of Poly(maleimide thioether)s

Prior to the diversification experiments, the model polymer, P1, was analyzed using NMR spectroscopy. The ^{1}H NMR spectrum revealed four distinct peaks that corresponded to the polymer structure (Figure 4.1a). The imide NH proton was found at δ 11.08 ppm, while S-CH_2 protons appeared at δ 3.19 ppm. The remaining linear alkyl main chain protons, SCH_2CH_2 and $SCH_2CH_2CH_2$, were observed at 1.55 and 1.34 ppm, respectively. The structure of P1 was further confirmed by ^{13}C NMR analysis (Figure 4.1b). The imide carbonyl carbons and double bond carbons were detected at δ 167.84 and 136.27 ppm, respectively. Peaks corresponding to HDT main chain carbons were observed at δ 31.29, 30.34, and 27.77 ppm. The FTIR spectrum of P1 (Figure A.3) showed peaks corresponding to C═O (symmetric and asymmetric), C─N, and C─S stretching vibrations at 1770, 1702, 1321, 1192, and 735 cm^{-1}, respectively. All of these results confirm the successful synthesis of the expected product, P1, and indicate that the thiol-DBM polymerization proceeded smoothly. It is important to note that, under the same reaction conditions, the polymerization of DBM with 1,3-propanedithiol did not yield a polymeric product. Instead, a complex mixture with unidentified structures was obtained, suggesting the occurrence of significant side reactions beyond simple cyclization (Figure B.9).

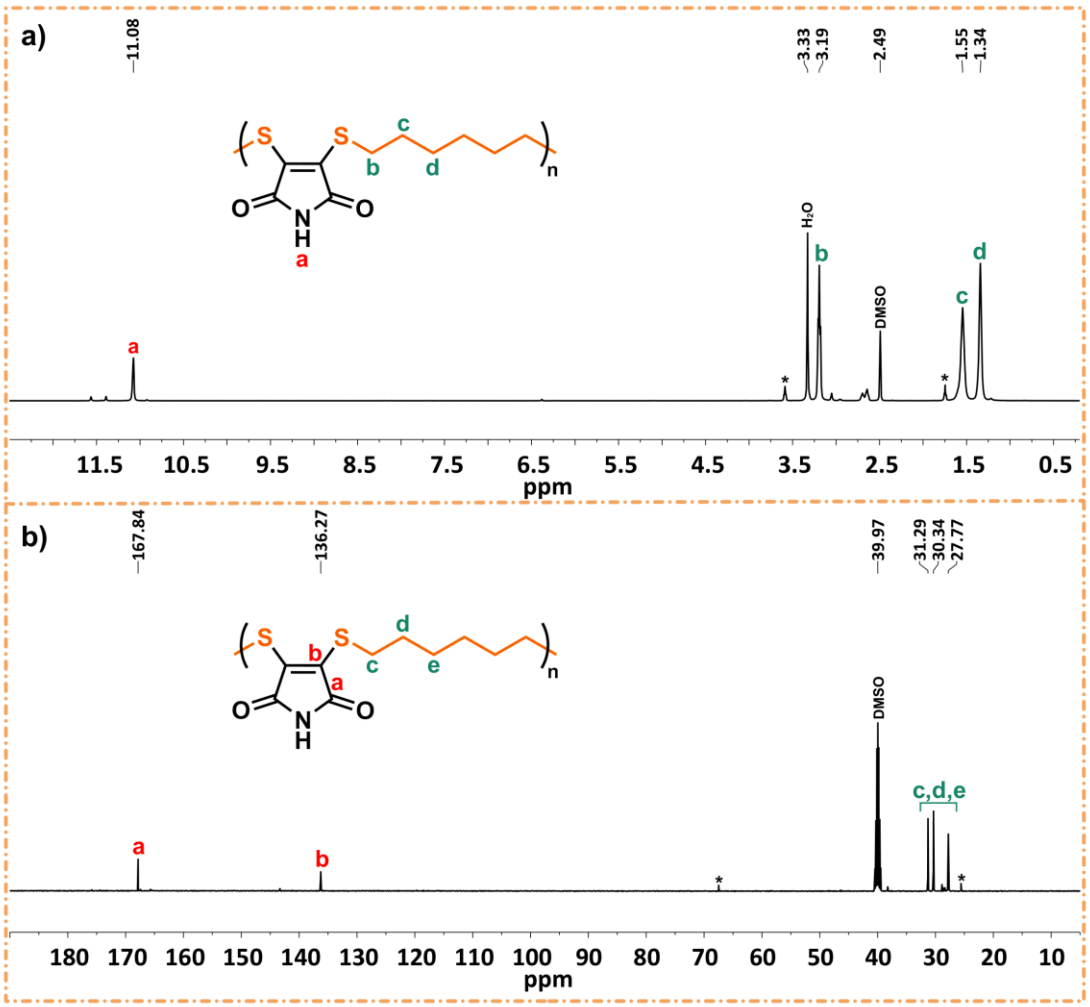

Figure 4.1 : ^{1}H NMR spectrum a) and ^{13}C NMR spectrum b) of P1 in DMSO-d_6 (500 MHz). Residual THF peaks are marked with an asterisk (*).

Various dithiols, ranging from aliphatic to aromatic, were treated with DBM under optimized conditions, and the corresponding results are summarized in Table 4.4. Aliphatic dithiols (P1–P5), including hexane-1,6-dithiol (HDT), led to the formation of polymers with modest molecular weights, ranging from 7.3 to 26.3 kDa. Among these; polymer P5, synthesized from 1,4-butanedithiol, exhibited the lowest molecular weight (Mw = 7.3 kDa). This result may be attributed to potential side reactions, such as intramolecular cyclization occurring during the polymerization process, which can limit effective chain growth. In contrast, heteroatom-containing dithiols, specifically 2,2′-(ethylenedioxy)diethanethiol (P6) and 2,2′-thiodiethanethiol (P7), afforded polymers with moderate molecular weights and were obtained in good isolated yields.

These findings indicate that both the chain length and the presence of heteroatoms in the dithiol structure can significantly affect the polymerization outcome. Aromatic dithiols were then examined to assess their influence on polymer formation. Specifically, benzene-1,4-dithiol (P8), 4,4′-thiobisbenzenethiol (P10), and 1,4-benzenedimethanethiol (P9) were subjected to polymerization reactions under identical conditions. Although P8 and P10 are considered to be more sterically congested than P9 due to their rigid aromatic structures and shorter linker lengths, the resulting polymers from P8 and P10 exhibited moderate molecular weights. In contrast, polymerization with P9 afforded a polymer with significantly lower molecular weight.

These results demonstrate a clear variation in polymerization behavior depending on the dithiol structure. These findings show that in a highly basic medium, thiophenol structures can easily lose their acidic protons and transform into thiophenolates, which are highly nucleophilic when reacting with DBM. However, 1,4-benzenedimethanethiol, which has a methylene spacer between the SH group and the benzene ring, becomes less nucleophilic under the same conditions, resulting in a lower molecular weight polymer. Surprisingly, the largest molecular weight polymer (P11, Mw = 68.2 kDa) in this study was produced by the reaction of 6-(dibutylamino)-1,3,5-triazine-2,4-dithiol with DBM. Given the sterically hindered structure of 6-(dibutylamino)-1,3,5-triazine-2,4-dithiol, this result is indeed unexpected. However, because P11 has a stiff backbone, improper folding may result in a large hydrodynamic volume, thus leading to a high molecular weight polymer.

Figure 4.2 depicts superimposed ^{1}H NMR spectra of typical polymers. As shown in the figure, the expected primary backbone signals are clearly visible in all cases, confirming smooth polymerization.

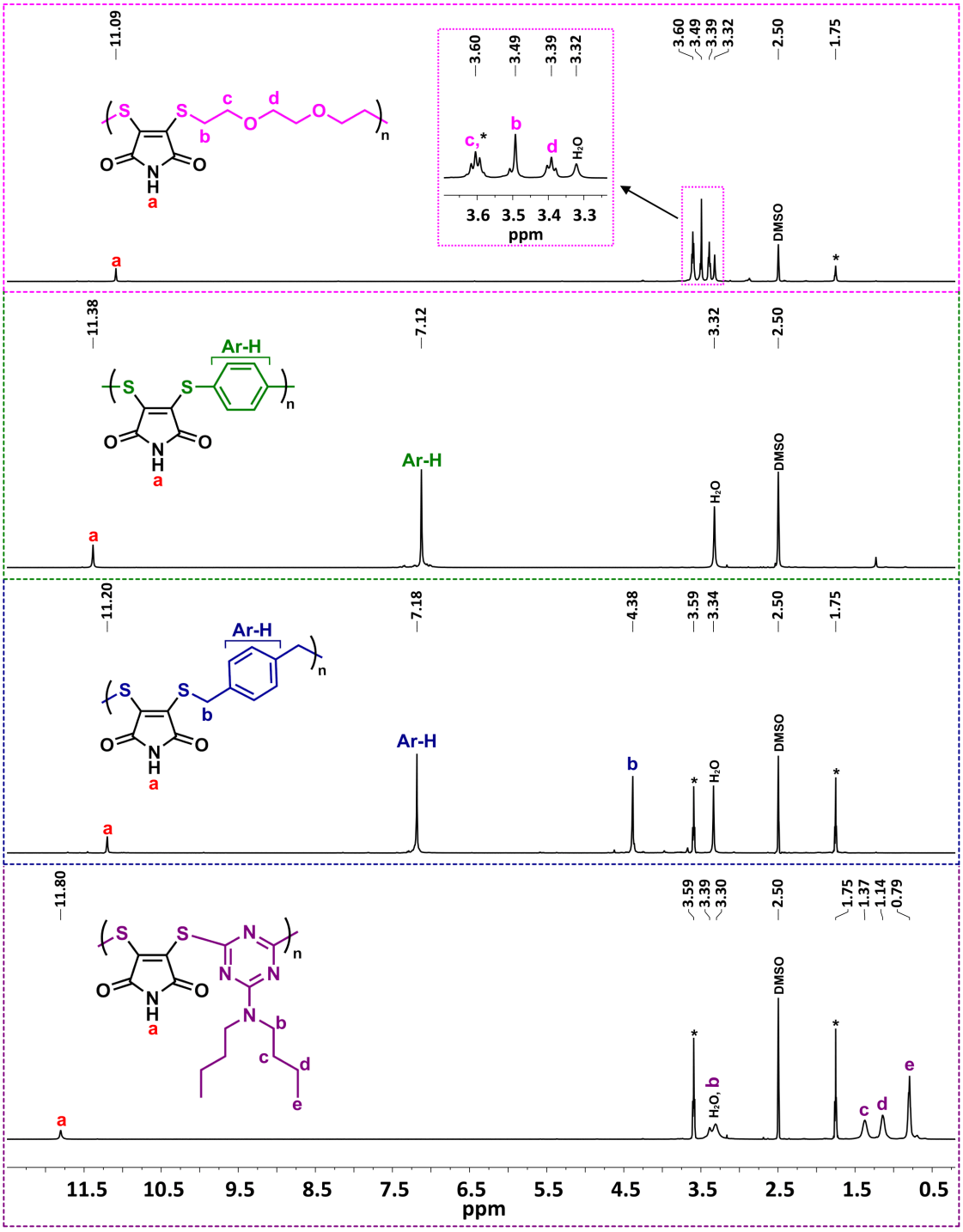

Figure 4.2 : ^{1}H NMR spectra of P6, P8, P9, and P11 (from top to bottom) in DMSO-d_6 (500 MHz). Residual THF peaks are marked with an asterisk (*).

4.3. Thermal Properties of the Polythioethers

The synthesized polymers had T_gs ranging from -45.9 to 104.4 °C, as shown in Table 4.4. Dithiols with linear alkyl chain lengths ranging from 4 to 10 carbons were added to polymers P1–P5 in the following order: P5 (shortest chain) < P4 < P1 < P2 < P3

(longest chain). The T_g values showed a clear decreasing trend as the chain length increased, demonstrating that chain flexibility improved with the number of main chain methylene units. P10 has the highest T_g among the polymers synthesized from aromatic dithiols, which can be attributed to its very stiff aromatic backbone. P11, synthesized from 6-(dibutylamino)-1,3,5-triazine-2,4-dithiol, exhibited a moderate T_g of 57.8 °C. P8, with thiol groups directly linked to the benzene ring, has a T_g of 43.1 °C. In contrast, P9 has a somewhat lower T_g of 41.3 °C than P8, most likely due to the enhanced flexibility provided by the extra methylene groups. Furthermore, P6 and P2 are derived from dithiol compounds with the same number of atoms and identical chain lengths. P2 is formed from 1,8-octanedithiol, whereas P6, derived from 2,2′-(ethylenedioxy)diethanethiol, has a similar dithiol structure, with two carbon atoms replaced by oxygen atoms. Both P6 and P2 produced identical molecular weights; however, P6's T_g was 19.3 degrees higher than that of P2. This was attributed to higher intermolecular forces, or dipole-dipole interactions (polarity), in P6 due to the presence of oxygen atoms. P7 has a greater T_g than its structural equivalent, P4, which might be attributed to its larger molecular weight. Furthermore, it is hypothesized that the flexible 2,2′-thiodiethanethiol-containing chains in P7 aided in the ordering and molecular packing of the poly(thioether) chains rather than increasing free volume.

Table 4.4 : Results of synthesized polymers[a]

polymer	dithiol	M_w[b] (kDa)	$Đ$[b]	T_g (°C)[c]	isolated yield (%)[d]
P1[e]	1,6-hexanedithiol	26.3	2.3	-19.9	86
P2	1,8-octanedithiol	23.4	2.0	-26.2	87
P3	1,10-decanedithiol	16.7	1.7	-45.9	72
P4	1,5-pentanedithiol	12.7	1.6	-18.6	70
P5	1,4-butanedithiol	7.3	1.3	-2.3	50
P6	2,2′-(ethylenedioxy)diethanethiol	24.0	1.8	-6.9	86
P7	2,2′-thiodiethanethiol	26.0	2.0	36.3	90
P8	benzene-1,4-dithiol	18.9	1.9	43.1	85
P9	1,4-benzenedimethanethiol	7.4	1.5	41.3	75
P10	4,4′-thiobisbenzenethiol	14.7	1.8	104.4	72
P11	6-(dibutylamino)-1,3,5-triazine-2,4-dithiol	68.2	2.7	57.8	88

[a]Reaction conditions: 0.785 mmol of DBM, 0.785 mmol of dithiol monomer, and 2.355 mmol of TEA in 0.785 mL of NMP at room temperature for 30 min. [b]Determined by GPC calibrated based on linear PS standards in THF. [c]Determined by DSC from the second heating cycle. [d]Gravimetric yield obtained after first precipitation. [e]Freshly prepared on a large scale.

4.4. Postpolymerization Modification of Polythioether P1 via Imide-Yne Click Reaction

One of the most noteworthy findings of this work is the creation of pendant imide N-H groups, which can be used for post polymerization modification (PPM). Recently, our research revealed that imide N-H groups can easily attack reactive triple bonds via the imide-yne reaction, resulting in linear polymer architectures (55). After successfully synthesizing maleimide main-chain polymers, an attempt was made to further functionalize this group via the imide-yne click reaction. Three distinct propiolate esters were used in PPM reactions with the P1 polymer (Table 4.4) (Figure 3.15).

The imide-yne reactions occurred quickly at room temperature using the nucleophilic organocatalyst DABCO. All processes yielded quantitative modification efficiencies, and the products were solely E-isomers, as confirmed by ^{1}H NMR. The ^{1}H NMR spectrum of the polymer formed by the reaction of P1 with ethyl propiolate was analyzed in detail; NMR and FTIR spectra of all modified polymers are shown in the Appendix B (Figures B.1-B.8). The ^{1}H NMR spectra revealed that the imide NH peak at δ 11.08 ppm was completely absent, whereas N-vinyl proton signals appeared at δ 7.68 and 6.66 ppm. Additionally, the ethyl group's methylene protons (OCH_2CH_3) were detected at δ 4.21 ppm and δ 1.30 ppm, respectively (Figure 4.3). The ^{13}C NMR study revealed the carbonyl carbons of the imide and ester groups at δ 167.09 and 163.20 ppm, respectively. Figure B.1 shows that the vinyl carbon of maleimide adjacent to S is at δ 136.67, while the carbons of the pendant vinyl units originating from the imide-yne reaction appear at δ 130.07 and 107.00 ppm. Both the ^{1}H and ^{13}C analyses confirm the successful PPM.

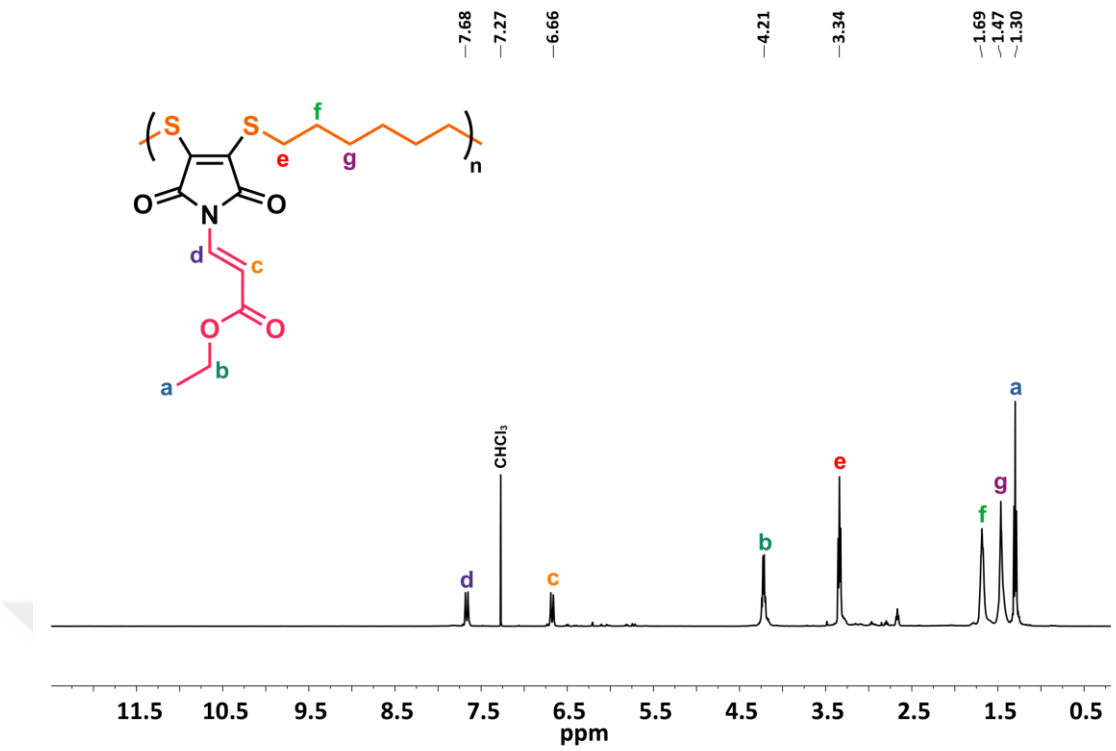

Figure 4.3 : ^{1}H NMR spectrum of ethyl propiolate modified P1 in $CDCl_3$ (500 MHz).

4.5. Degradation of Polythioether P1 and Cross-Linked Polymer

It is well understood that the Csp^2-S bond in thiol-DBM products can easily undergo a thiol exchange reaction in the presence of excess thiol or be rapidly broken by a reducing agent [42]. It is hypothesized that using one of these techniques on the resultant poly(maleimide thioether) polymers may cause chain scission and, consequently, polymer breakdown. To investigate this phenomenon, we reacted P1 (Table 4.4) with a 3-fold excess (with respect to the polymer repeating unit) of 1-propanethiol and TEA at room temperature (Figure 4.4a). GPC monitored the progress of the reaction by sampling the reaction medium at various time intervals. As shown in Figure 3.17, the polymer began to disintegrate after 5 minutes, and its molecular weight dropped to 14.3 kDa. This decrease continued for an hour and then stabilized. This finding suggests that the polymer main chain undergoes a thiol exchange reaction with the monothiol, resulting in the cleavage of the polymer chain into low molecular weight oligomeric fractions.

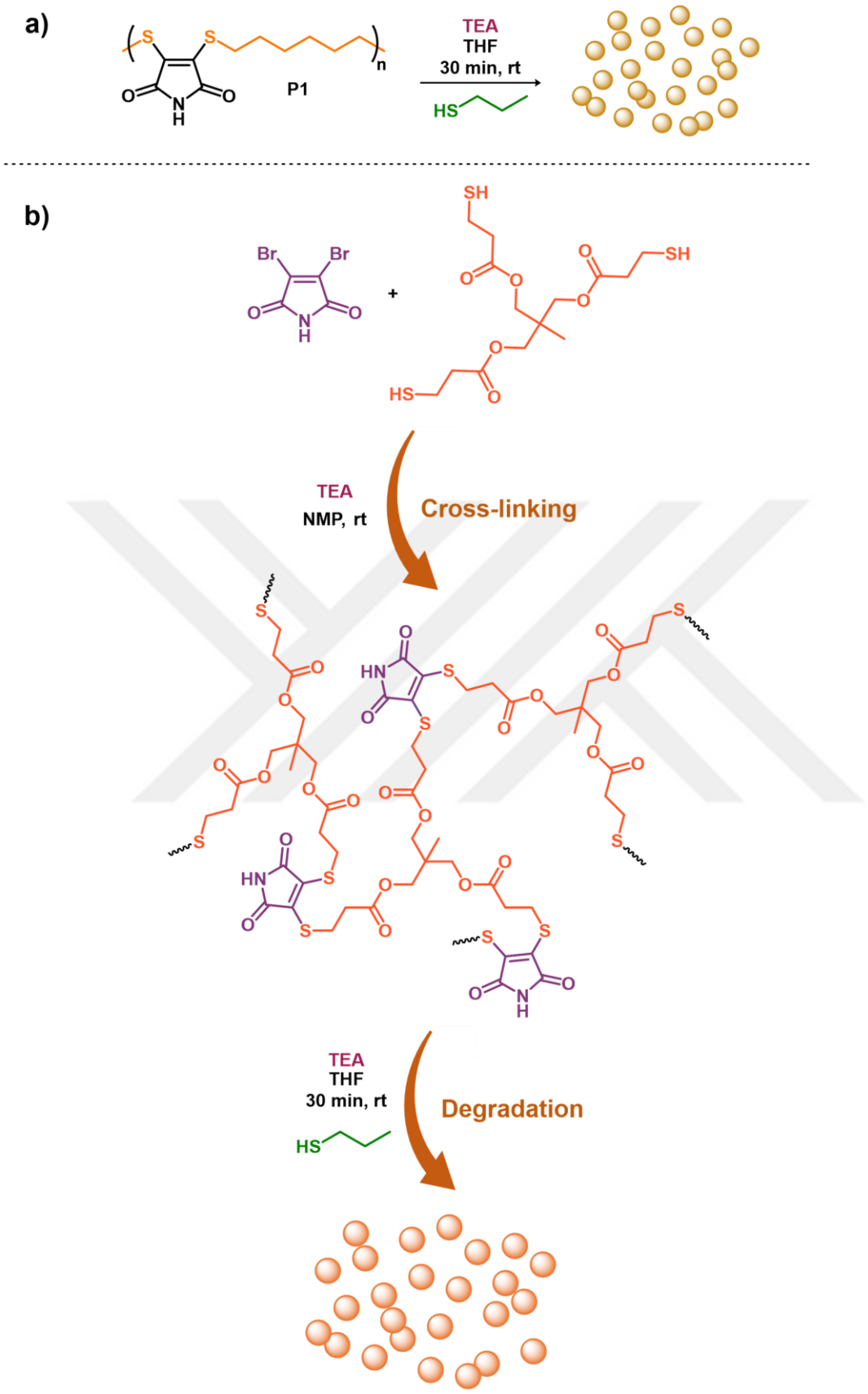

Figure 4.4 : a) Degradation of the linear polymer P1, b) synthesis and following degradation of the cross-linked material.

Nowadays, one of the most significant challenges in chemistry is the degradation of cross-linked materials using simple reactions under moderate conditions. To achieve this, we used the thiol-DBM process to create a cross-linked material, which we then degraded via the aforementioned thiol-exchange reaction. A cross-linked polymer was synthesized using DBM and a trifunctional thiol (trimethylolpropane tris(3-mercaptopropionate)) (Figure 4.4b).

We successfully broke down the cross-linked network using the same degradation method. In our case, salts produced during gelation became confined within the gel matrix. These salts could be removed by repeated swelling and deswelling cycles; however, in our experiment, the gel was used as is. Within 30 minutes, the previously insoluble gel had converted into a soluble mixture containing insoluble ions, demonstrating the effectiveness of the degradation process (Figure 4.5). Degradation studies in both linear and cross-linked polymers highlight the high potential of the proposed chemical for future applications.

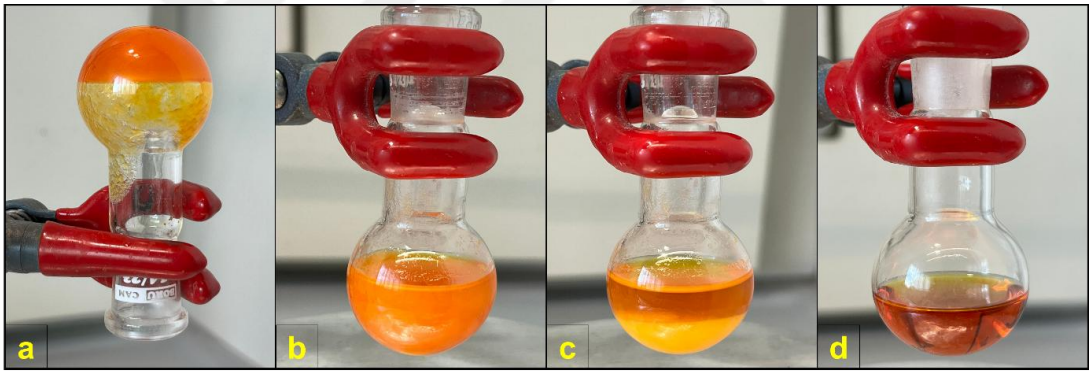

Figure 4.5 : Images of a) cross-linked polymer, b) liberation of entrapped salts from the gel during degradation, c) phase separation of salt and solution after stirring was stopped, and d) clear reaction solution after filtration.

5. CONCLUSIONS

In summary, thiol-DBM chemistry has been demonstrated as a practical method for preparing linear polymers with a maleimide backbone. Optimization studies showed that NMP and TEA are ideal solvents and bases for polymerization. The polymerization reactions proceeded at room temperature, and 30 min reaction time was found to be sufficient to reach high molecular weights. Various poly(maleimide thioether)s with different chemical backbones and varying molecular weights were found to be accessible in good to high yields using the optimum conditions. The resulting polymers exhibited a wide range of glass transition temperatures parallel to the thiol type used. The resulting polymers could also be readily functionalized via imide-yne click reaction between the N–H bonds in the polymers and the propiolate esters, highlighting another useful feature of the proposed chemistry. Due to the easily cleavable nature of the Csp^2-S bond in the resulting polymeric structure, P1, as a model polymer, was subjected to degradation via a thiol-exchange mechanism using an excess of 1-propanethiol; the kinetic experiment indicated that the polymer was rapidly degraded within a short time. The versatility of the proposed thiol-DBM chemistry was also utilized to create a network structure, and its degradation was subsequently demonstrated by employing the same thiol-exchange reactions.

The presented polymer synthesis strategy is believed to offer several advantages, such as mild conditions, metal-free, and readily available starting materials. Additionally, the obtained polymers can be easily functionalized and degraded, meeting many demands of today's polymer science. As such, we believe the findings of this study will draw considerable attention from the literature and will be a strong tool in the hands of polymer and material chemists.

REFERENCES

[1] Kirkpatrick, B.E., Anseth, K.S. & Hebner, T.S. (2025). Diverse reactivity of maleimides in polymer science and beyond. *Polymer International*, 74 (4), 296-306.

[2] Ravasco, J.M.J.M., Faustino, H., Trindade, A., Gois, P.M.P. (2019). Bioconjugation with Maleimides: A Useful Tool for Chemical Biology. *Chemical European Journal*, 25(1), 43.

[3] Dolci, E., Froidevaux, V., Joly-Duhamel, C., Auvergne, R., Boutevin, B. & Caillol, S. (2016). Maleimides as a building block for the synthesis of high-performance polymers. *Polymer Reviews*, 56(3), 512–556.

[4] Barker, J., Tibbetts, J., Ferguson, C., Xie, Y. & O'Reilly, R.K. (2024). Substituted maleimides: Self-reportable linkers and tags in bioconjugation, material science, and nanotechnology. *Angewandte Chemie International Edition*, 63(43), 1–12.

[5] Gok, O., Durmaz, H., Ozdes, E.S., Hizal, G., Tunca, U. & Sanyal, A. (2010). Maleimide-based thiol reactive multiarm star polymers via Diels-Alder/retro Diels-Alder strategy. *Journal of Polymer Science, Part A: Polymer Chemistry*, 48(12), 2546–2556.

[6] Abel, B.A. & McCormick, C.L. (2016). "One-pot" aminolysis/thiol–maleimide end-group functionalization of RAFT polymers: Identifying and preventing Michael addition side reactions. *Macromolecules*, 49(17), 6193–6202.

[7] Guo, X., Gao, F., Chen, F., Huang, J., Gao, X. & Shen, L. (2024). Novel maleimide-amine dynamic polymers with excellent mechanical strength, recyclability, and engineered shape memory features. *Reactive and Functional Polymers*, 196, 105831.

[8] Mather, B.D., Viswanathan, K., Miller, K.M. & Long, T.E. (2006). Michael addition reactions in macromolecular design for emerging technologies. *Progress in Polymer Science*, 31(5), 487–531.

[9] White, J.E., Snider, D.A. & Scaia, M.D. (1984). Synthesis and properties of some new polyimidosulfides with highly mobile backbones. *Journal of Polymer Science: Polymer Chemistry Edition*, 22(3), 589–596.

[10] Crivello, J.V. (1976). Polyimidothioethers. *Journal of Polymer Science: Polymer Chemistry Edition*, 14(1), 159–182.

[11] Dix, L.R., Ebdon, J.R. & Hodge, P. (1995). Chain extension and crosslinking of telechelic oligomers—II. Michael additions of bisthiols to bismaleimides, bismaleates and bis(acetylene ketone)s to give linear and crosslinked polymers. *European Polymer Journal*, 31(7), 653–658

[12] Liu, Y., Tsai, S., Wu, C. & Jeng, R. (2004). Preparation and characterization of hyperbranched polyaspartimides from bismaleimides and triamines. *Journal of Polymer Science, Part A: Polymer Chemistry*, 42(23), 5921–5928.

[13] Northrop, B.H., Frayne, S.H. & Choudhary, U. (2015). Thiol–maleimide "click" chemistry: Evaluating the influence of solvent, initiator, and thiol on the reaction mechanism, kinetics, and selectivity. *Polymer Chemistry*, 6(18), 3415–3430.

[14] Nair, D.P., Podgórski, M., Chatani, S., Gong, T., Xi, W., Fenoli, C.R. & Bowman, C.N. (2013). The thiol-Michael addition click reaction: A powerful and widely used tool in materials chemistry. *Chemistry of Materials*, 26(1), 724–744.

[15] Baldwin, A.D. and Kiick, K.L. (2013). Reversible maleimide–thiol adducts yield glutathione-sensitive poly(ethylene glycol)–heparin hydrogels. *Polymer Chemistry*, 4(1), 133–143.

[16] Stolz, R.M. and Northrop, B.H. (2013). Experimental and theoretical studies of selective thiol–ene and thiol–yne click reactions involving N-substituted maleimides. *The Journal of Organic Chemistry*, 78(16), 8105–8116.

[17] Goussé, C. and Gandini, A. (1999). Diels–Alder polymerization of difurans with bismaleimides. *Polymer International*, 48(8), 723–731.

[18] Gacal, B., Durmaz, H., Tasdelen, M. A., Hizal, G., Tunca, U., Yagci, Y. & Demirel, A. L. (2006). Anthracene−Maleimide-Based Diels−Alder "Click Chemistry" as a Novel Route to Graft Copolymers. *Macromolecules*, 39(15), 5330–5336.

[19] Durmaz, **H.**, **Dag**, **A.**, **Altintas**, **O.**, **Erdogan**, **T.**, **Hizal**, **G.**, **Tunca**, **U.** (2007). One-Pot Synthesis of ABC Type Triblock Copolymers via in Situ Click [3 + 2] and Diels−Alder [4 + 2] Reactions. *Macromolecules*, 40(2), 191–198.

[20] Sanyal, **A.** (2010). Diels–Alder Cycloaddition-Cycloreversion: A Powerful Combo in Materials Design. *Macromolecular Chemistry and Physics*, 211(12), 1417–1425.

[21] Hizal, **G.**, **Tunca**, **U. & Sanyal**, **A.** (2011). Discrete Macromolecular Constructs via the Diels–Alder "Click" Reaction. *Journal of Polymer Science: Part A: Polymer Chemistry*, 49(19), 4103–4120.

[22] Tasdelen, **M. A.** (2011). Diels–Alder "Click" Reactions: Recent Applications in Polymer and Material Science. *Polymer Chemistry*, 2(10), 2133.

[23] Hall, **D. J.**, **Van Den Berghe**, **H. M. & Dove**, **A. P.** (2011). Synthesis and Post-polymerization Modification of Maleimide-containing Polymers by 'Thiol-ene' Click and Diels–Alder Chemistries. *Polymer International*, 60(8), 1149–1157.

[24] Chen, **X.**, **Wudl**, **F.**, **Mal**, **A. K. & Shen**, **H.** (2003). New Thermally Remendable Highly Cross-Linked Polymeric Materials. *Macromolecules*, 36(6), 1802–1807.

[25] Mcelhanon, **J. R.**, **Russick**, **E. M.**, **Wheeler**, **D. R.**, **Loy**, **D. A. & Aubert**, **J. H.** (2002). Removable Foams Based on an Epoxy Resin Incorporating Reversible Diels–Alder Adducts. *J. Appl. Polym. Sci.*, 85(7), 1496–1502.

[26] Durmaz, **H.**, **Colakoglu**, **B.**, **Tunca**, **U. & Hizal**, **G.** (2006). Preparation of block copolymers via Diels–Alder reaction of maleimide– and anthracene–end functionalized polymers. *J. Polym. Sci., Part A: Polym. Chem.*, 44, 1667–1675.

[26] Durmaz, **H.**, **Colakoglu**, **B.**, **Tunca**, **U. & Hizal**, **G.** (2006). Preparation of block copolymers via Diels–Alder reaction of maleimide– and anthracene–end functionalized polymers. *J. Polym. Sci., Part A: Polym. Chem.*, 44(5), 1667–1675.

[27] Dispinar, **T.**, **Sanyal**, **R. & Sanyal**, **A.** (2007). A Diels–Alder/Retro Diels–Alder Strategy to Synthesize Polymers Bearing Maleimide Side Chains. *Journal of Polymer Science, Part A: Polymer Chemistry*, 45(20), 4545–4551.

[28] Polaske, **N. W.**, **McGrath**, **D. V. & McElhanon**, **J. R.** (2011). Thermally Reversible Dendronized Linear AB Step-Polymers via "Click" Chemistry. *Macromolecules*, 44(9), 3203–3210.

[29] Liu, **Y.-L.**, **Hsieh**, **C.-Y. & Chen**, **Y.-W.** (2006). Thermally Reversible Cross-Linked Polyamides and Thermo-Responsive Gels by Means of Diels–Alder Reaction. *Polymer*, 47(8), 2581–2586.

[30] Vilela, **C.**, **Cruciani**, **L.**, **Silvestre**, **A. J. D. & Gandini**, **A.** (2011). A Double Click Strategy Applied to the Reversible Polymerization of Furan/Vegetable Oil Monomers. *Macromolecular Rapid Communications*, 32(17), 1319–1323.

[31] Tawney, **P. O.**, **Snyder**, **R. H.**, **Conger**, **R. P.**, **Leibbrand**, **K. A.**, **Stiteler**, **C. H. & Williams**, **A. R.** (1961). The Chemistry of Maleimide and Its Derivatives. II. Maleimide and N-Methylolmaleimide. *Journal of Organic Chemistry*, 26(1), 15–21.

[32] Haas, **H. C.** (1973). Maleimide Polymers. II. Radical Polymerization Kinetics. *Journal of Polymer Science: Polymer Chemistry Edition*, 11(1), 315–318.

[33] Ji, X., Tian, W., Jin, K., Diao, H., Huang, X., Song, G., & Zhang, J. (2022). Anionic polymerization of nonaromatic maleimide to achieve full-color nonconventional luminescence. *Nature Communications*, 13.

[34] Agarwal, P., Yu, Q., Harant, A., & Berglund, K. A. (2003). Synthesis and characterization of polymaleimide. *Industrial & Engineering Chemistry Research*, 42, 2881–2884.

[35] Kojima, K., Yoda, N., & Marvel, C. S. (1966). Base-catalyzed polymerization of maleimide and some derivatives and related unsaturated carbonamides. *Journal of Polymer Science, A-1 Polym. Chem.*, 4(5), 1121–1134.

[36] Xie, Y., Liu, D., Zhang, H., Wang, D., Zhao, Z., & Tang, B. Z. (2022). Clusteroluminescence in maleimide: From well-known phenomenon to unknown mechanism. *ChemRxiv*.

[37] Azechi, M., Toyota, N., Yamabuki, K., Onimura, K., & Oishi, T. (2010). Anionic polymerization of N-substituted maleimide with achiral and chiral amines as an initiator. *Polymer Bulletin*, 67, 631–640.

[38] Rzaev, Z. M. O. (2000). Complex-radical alternating copolymerization. *Progress in Polymer Science*, 25(2), 163–217.

[39] Kuroda, S., & Hagiwara, T. (2011). Synthesis and polymerization of maleimide-type new macromonomer with polystyrene having controlled chain length. *Polymer*, 52(9), 1869–1873.

[40] Aktas Eken, G., & Ober, C. K. (2022). Strong polyelectrolyte brushes via alternating copolymers of styrene and maleimides: Synthesis, properties, and stability. *Macromolecules*, 55(13), 5291–5300.

[41] Tedaldi, L. M., Smith, M. E. B., Nathani, R. I., & Baker, J. R. (2009). Bromomaleimides: New reagents for the selective and reversible modification of cysteine. *Chem. Commun.*, 6583–6585.

[42] Smith, M. E. B., Schumacher, F. F., Ryan, C. P., Tedaldi, L. M., Papaioannou, D., Waksman, G., Caddick, S., & Baker, J. R. (2010). Protein modification, bioconjugation, and disulfide bridging using bromomaleimides. *Journal of the American Chemical Society*, 132(6), 1960–1965

[43] Schumacher, F. F., Nobles, M., Ryan, C. P., Smith, M. E. B., Tinker, A., Caddick, S., & Baker, J. R. (2011). In situ maleimide bridging of disulfides and a new approach to protein PEGylation. *Bioconjugate Chemistry*, 22(2), 132–136.

[44] Robin, M. P., Jones, M. W., Haddleton, D. M., & O'Reilly, R. K. (2011). Dibromomaleimide end functional polymers by RAFT polymerization without the need of protecting groups. *ACS Macro Letters*, 1(1), 222–226.

[45] Jones, M. W., Strickland, R. A., Schumacher, F. F., Caddick, S., Baker, James. R., Gibson, M. I. & Haddleton, D. M. (2012). Polymeric dibromomaleimides as extremely efficient disulfide bridging bioconjugation and pegylation agents. *Journal of the American Chemical Society*, *134*(3), 1847–1852.

[46] Tan, M., Wang, X., Xie, T., Zhang, Z., Shi, Y., Li, Y. & Chen, Y. (2022). Fluorogenic mechanophore based on dithiomaleimide with dual responsiveness. *Macromolecules*, *55*(15), 6860–6865.

[47] Robin, M. P. & O'Reilly, R. K. (2014). Fluorescent and chemico-fluorescent responsive polymers from dithiomaleimide and dibromomaleimide functional monomers. *Chemical Science*, *5*(7), 2717–2723.

[48] Li, Z.-L., Sun, L., Ma, J., Zeng, Z. & Jiang, H. (2016). Synthesis and post-polymerization modification of polynorbornene bearing dibromomaleimide side groups. *Polymer*, *84*(3), 336–342.

[49] Ross, A., Durmaz, H., Cheng, K., Deng, X., Liu, Y., Oh, J., Chen, Z. & Lahann, J. (2015). Selective and reversible binding of thiol-functionalized biomolecules on polymers prepared via chemical vapor deposition polymerization. *Langmuir*, *31*(18), 5123–5129.

[50] Jones, M. W., Strickland, R. A., Schumacher, F. F., Caddick, S., Baker, James. R., Gibson, M. I. & Haddleton, D. M. (2012). Highly efficient disulfide bridging polymers for bioconjugates from radical-compatible dithiophenol maleimides. *Chemical Communications*, *48*(34), 4064–4066.

[51] Cui, Y., Yan, Y., Chen, Y. & Wang, Z. (2012). Dibromomaleimide derivative as an efficient polymer coupling agent for building topological polymers. *Macromolecular Chemistry and Physics*, *214*(4), 470–477.

[52] Bahou, C., Szijj, P. A., Spears, R. J., Wall, A., Javaid, F., Sattikar, A., Love, E. A., Baker, J. R. & Chudasama, V. (2021). A plug-and-play platform for the formation of trifunctional cysteine bioconjugates that also offers control over thiol cleavability. *Bioconjugate Chemistry*, *32*(4), 672–679.

[53] Bishop, A., Balmaceda, E., Iacono, S. T. & Jennings, A. R. (2024). Synthesis and characterization of perfluorocyclopentene-thioether polymers. *Polymer International*, *73*(8), 631–638.

[54] Yan, J. J., Wang, D., Wu, D. C. & You, Y. Z. (2013). Synthesis of sequence-ordered polymers via sequential addition of monomers in one pot. *Chemical Communications*, *49*(54), 6057–6059.

[55] Aslanturk, O., Sagdic, G., Cakmakci, E., Durmaz, H. & Gunay, U. S. (2024). Imide-yne click polymerization: a new and versatile tool for the toolbox of X-yne click polymerization. *Polymer Chemistry*, *15*(39), 3991–4004.

[56] Lepore, S. D., Khoram, A., Bromfield, D. C., Cohn, P., Jairaj, V. & Silvestri, M. A. (2005). Studies on the manganese-mediated isomerization of alkynyl carbonyls to allenyl carbonyls. *The Journal of Organic Chemistry*, *70*(18), 7443–7446.

[57] Glasovac, Z., Eckert-Maksić, M. & Maksić, Z. B. (2009). Basicity of organic bases and superbases in acetonitrile by the polarized continuum model and DFT calculations. *New Journal of Chemistry*, *33*(3), 588–597.

[58] Ammer, J., Baidya, M., Kobayashi, S. & Mayr, H. (2010). Nucleophilic reactivities of tertiary alkylamines. *Journal of Physical Organic Chemistry*, *23*(11), 1029–1035.

[59] Gholamipour-Shirazi, A. & Rolando, C. (2012). Kinetics screening of the N-alkylation of organic superbases using a continuous flow microfluidic device: basicity versus nucleophilicity. *Organic & Biomolecular Chemistry*, *10*(40), 8059–8063.

[60] Zhang, J., Zhang, Q., Zhou, S., Liu, Y. & Huang, W. (2018). Synthesis and characterization of amphiphilic miktoarm star polymers based on sydnone-maleimide double cycloaddition. *Polymer Chemistry*, *9*(2), 203–212.

[61] Mabire, A. B., Robin, M. P., Quan, W.-D., Willcock, H., Stavros, V. G. & O'Reilly, R. K. (2015). Aminomaleimide fluorophores: a simple functional group with bright, solvent dependent emission. *Chemical Communications*, *51*(47), 9733–9736.

APPENDICES

APPENDIX A: Characterization Data of Linear and Cross-linked Poly(maleimide thioether)s Obtained by Thiol-Dibromomaleimide Polymerization

APPENDIX B: Characterization Data of Postpolymerization Modification via Imide-yne Click Reaction and Degradation of Poly(maleimide thioether)s

APPENDIX A

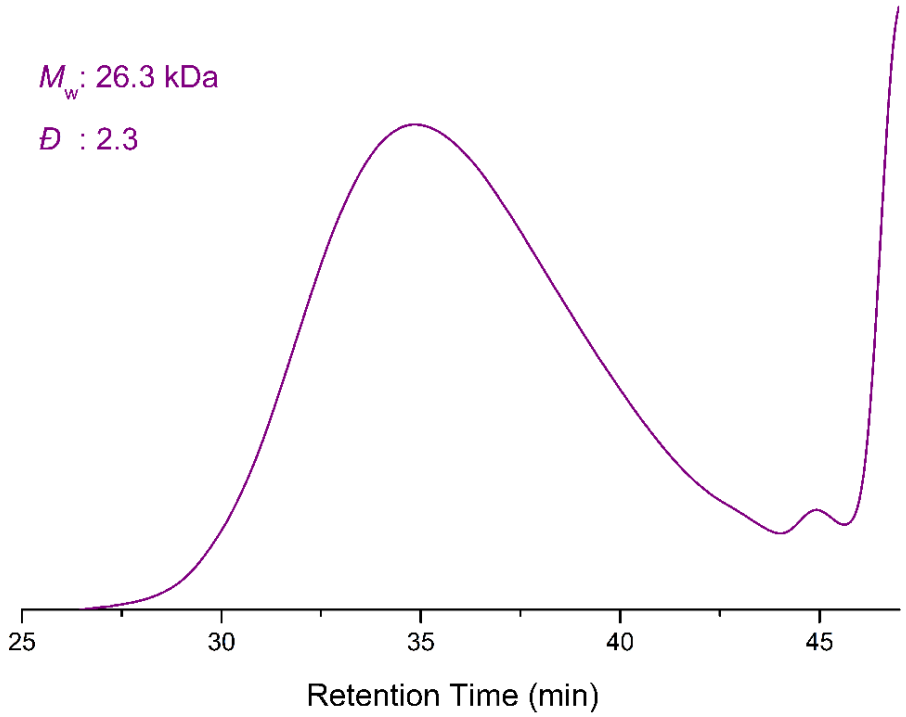

Figure A.1 : GPC trace of P1.

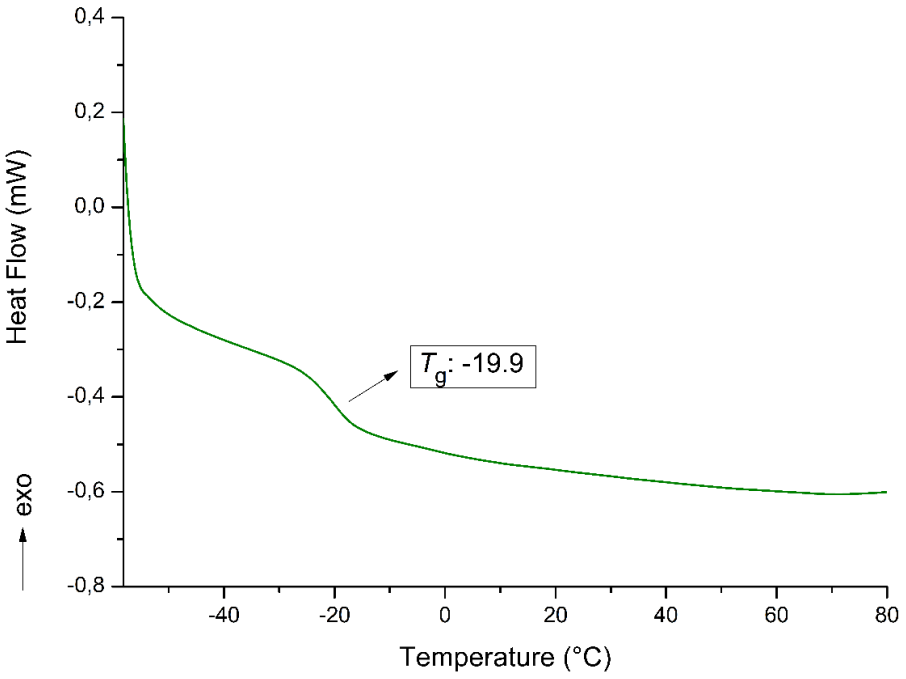

Figure A.2 : DSC spectrum of P1.

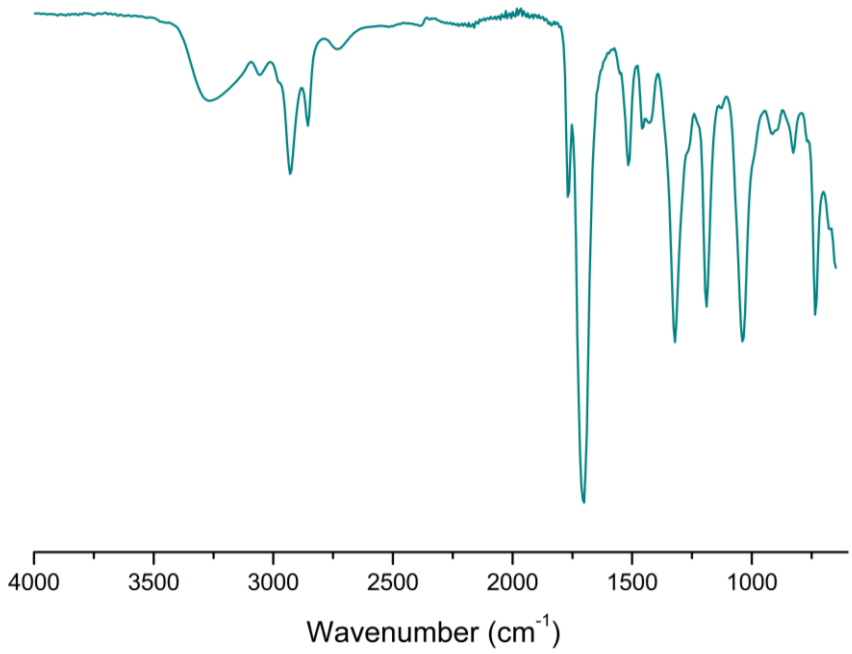

Figure A.3 : FTIR spectrum of P1.

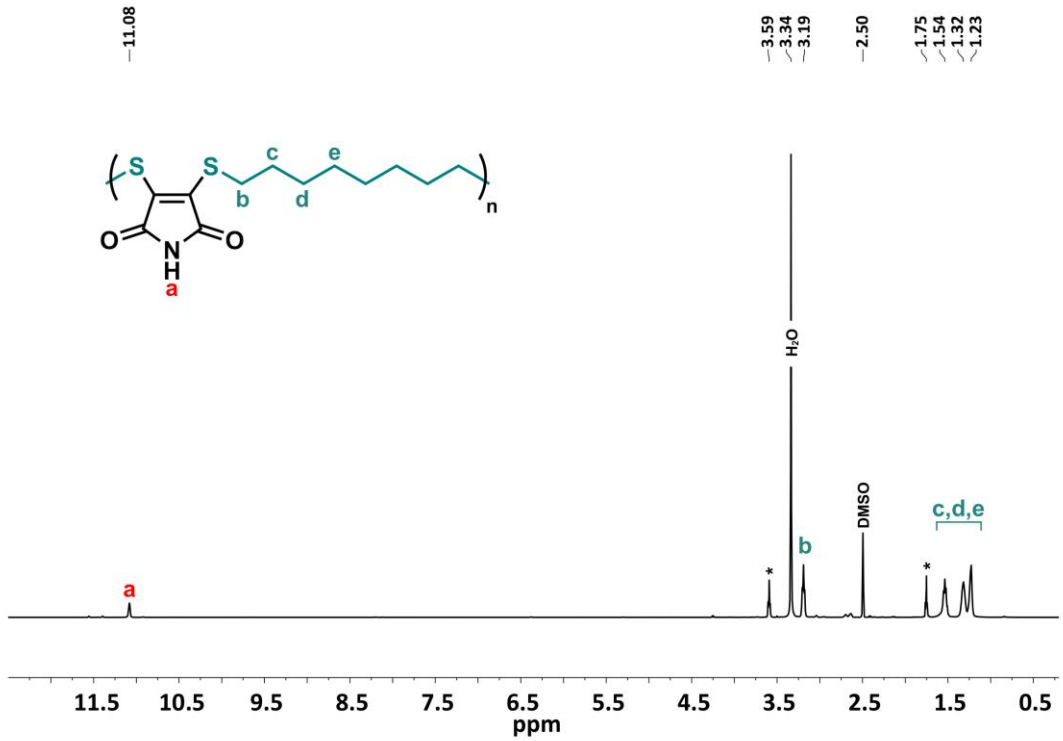

Figure A.4 : ^{1}H NMR spectrum of P2 in DMSO-d_6 (500 MHz). Residual THF peaks are marked with an asterisk (*).

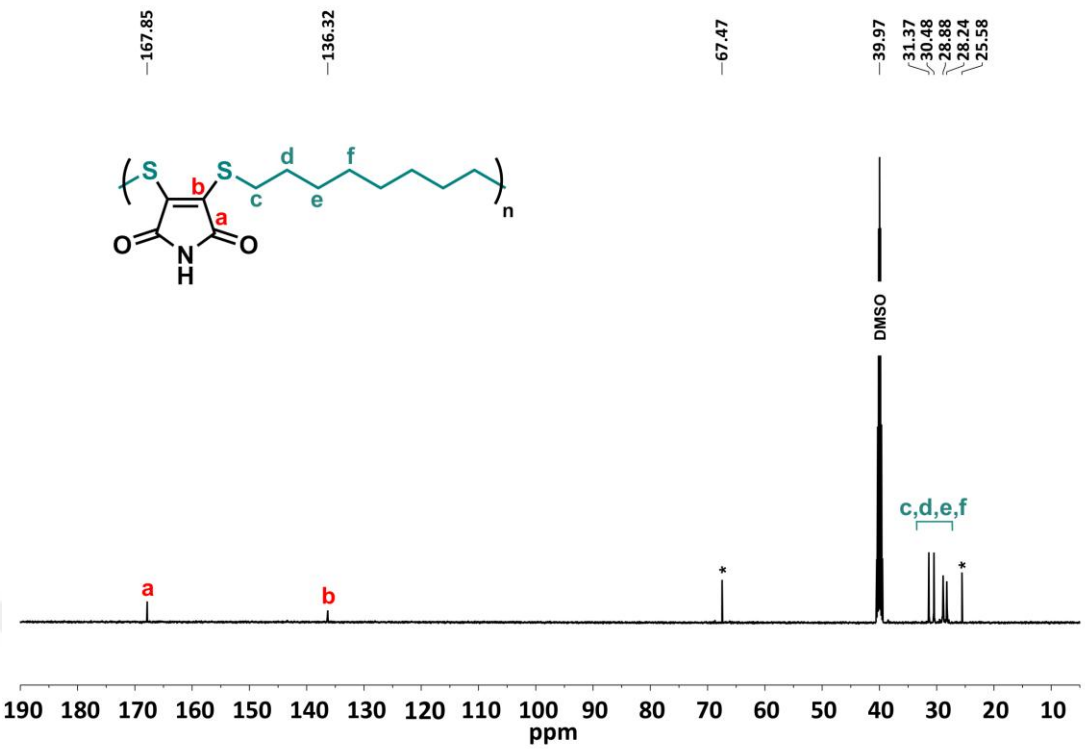

Figure A.5 : ^{13}C NMR spectrum of P2 in DMSO-d_6 (125 MHz). Residual THF peaks are marked with an asterisk (*).

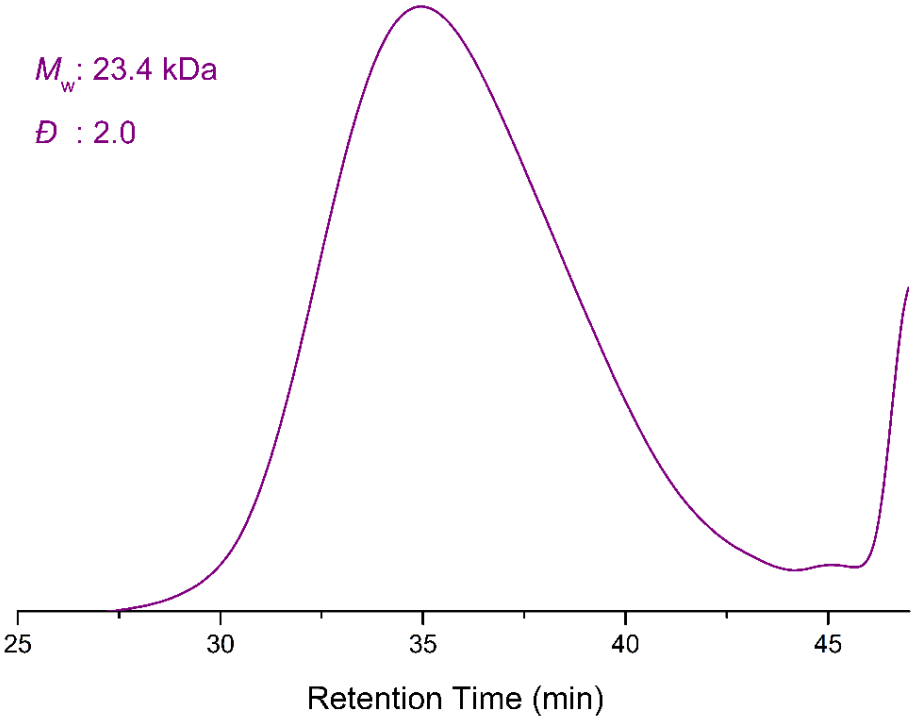

Figure A.6 : GPC trace of P2.

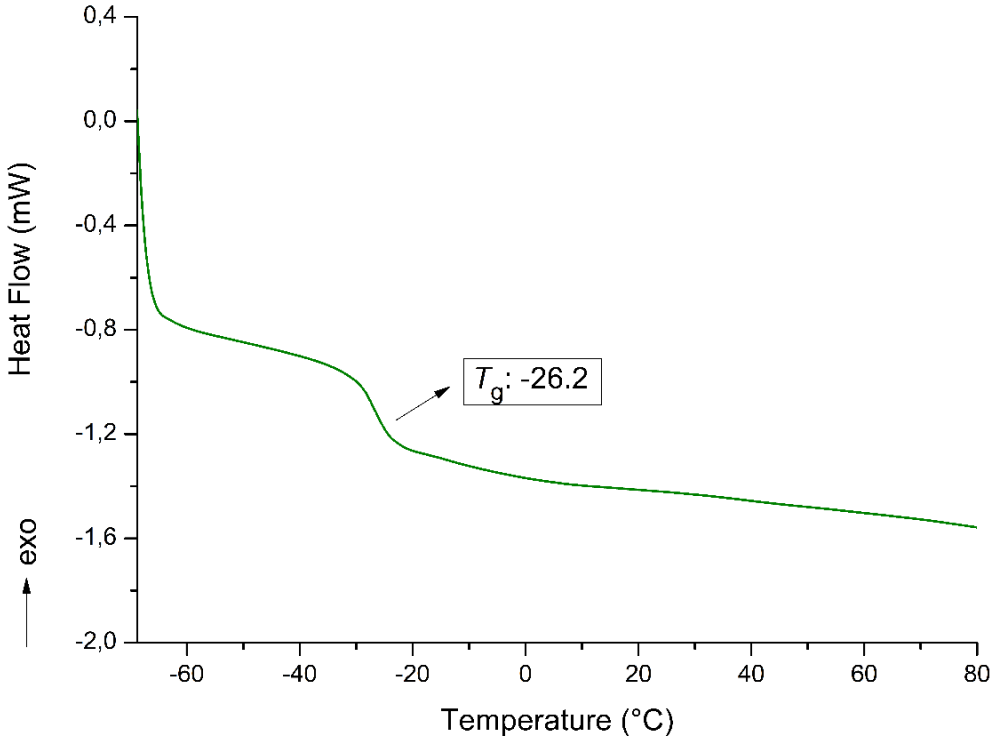

Figure A.7 : DSC spectrum of P2.

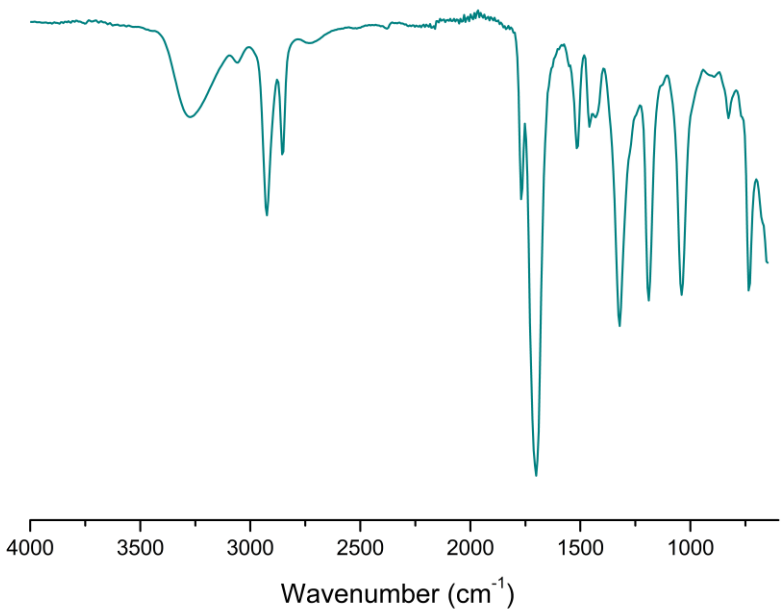

Figure A.8 : FTIR spectrum of P2.

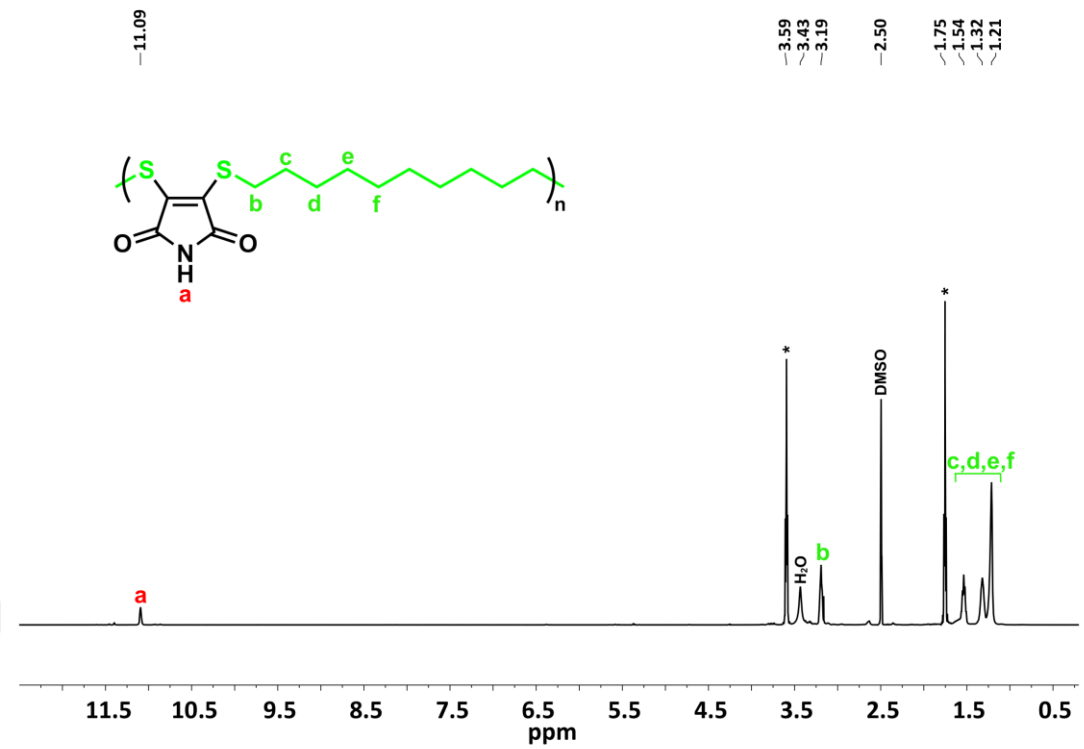

Figure A.9 : ^{1}H NMR spectrum of P3 in DMSO-d_6 (500 MHz). Residual THF peaks are marked with an asterisk (*).

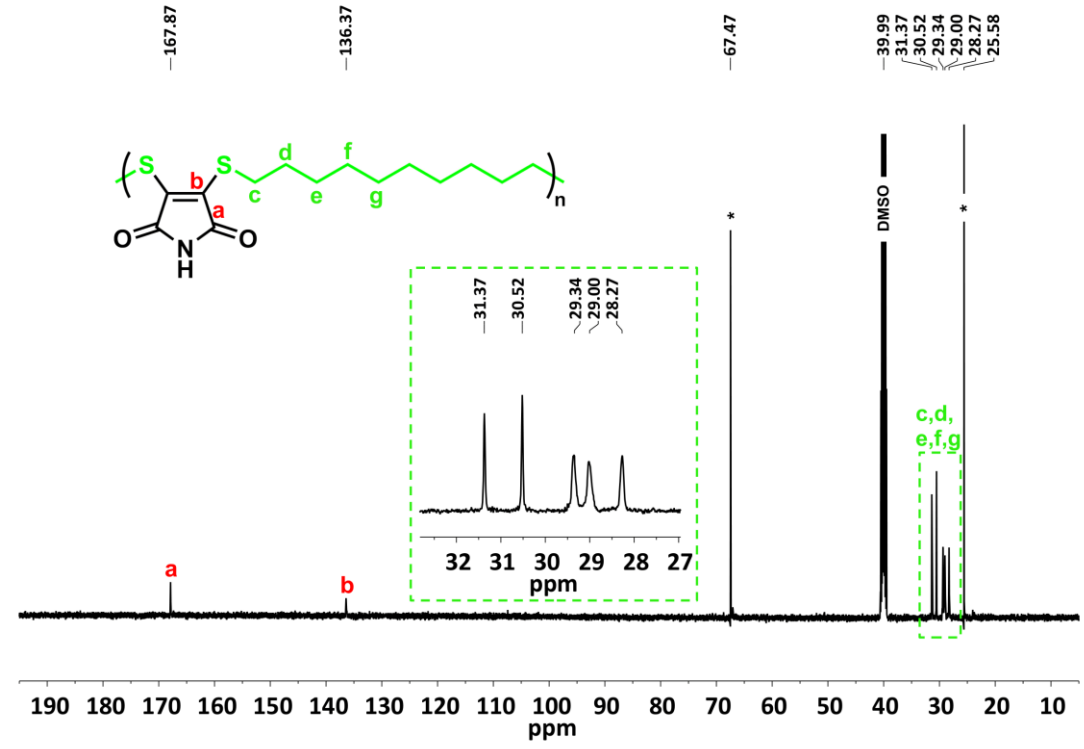

Figure A.10 : ^{13}C NMR spectrum of P3 in DMSO-d_6 (125 MHz). Residual THF peaks are marked with an asterisk (*).

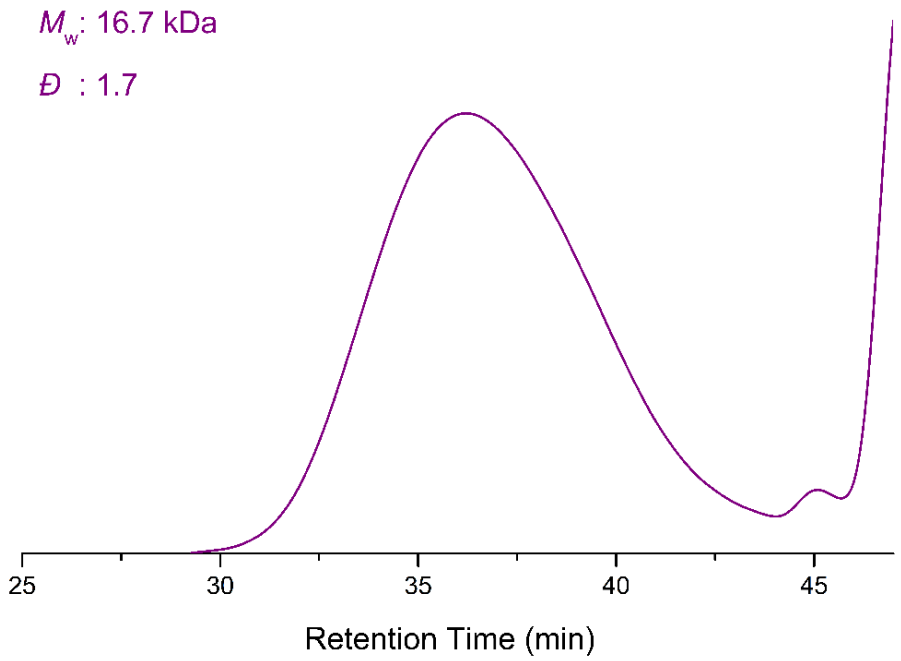

Figure A.11 : GPC trace of P3.

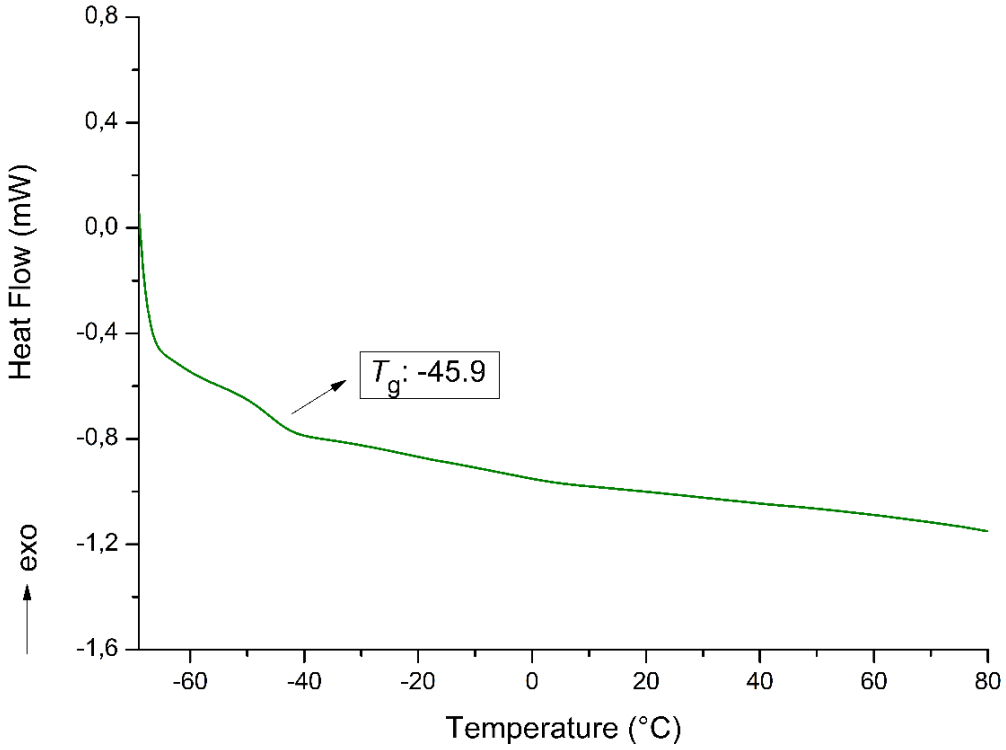

Figure A.12 : DSC spectrum of P3.

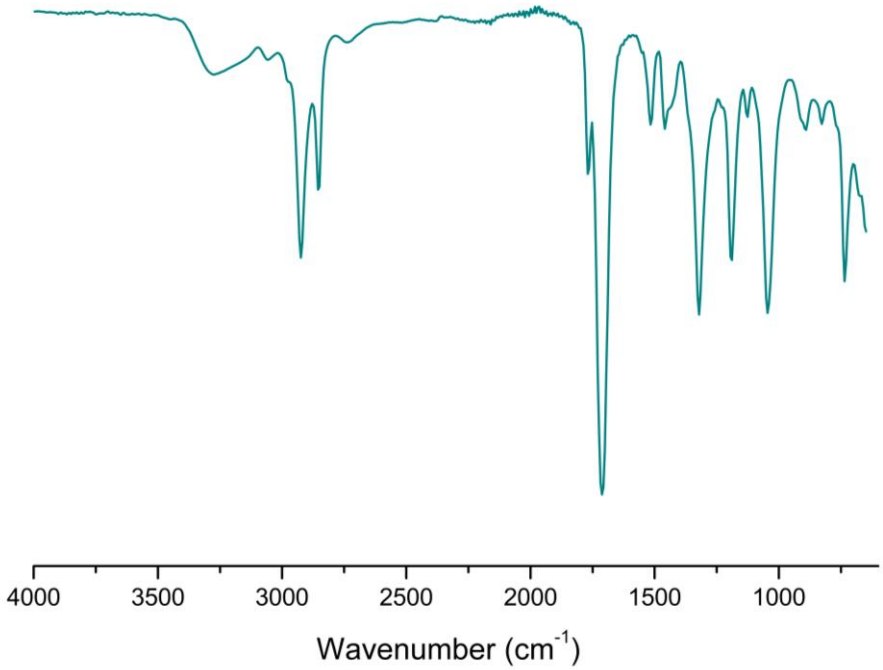

Figure A.13 : FTIR spectrum of P3.

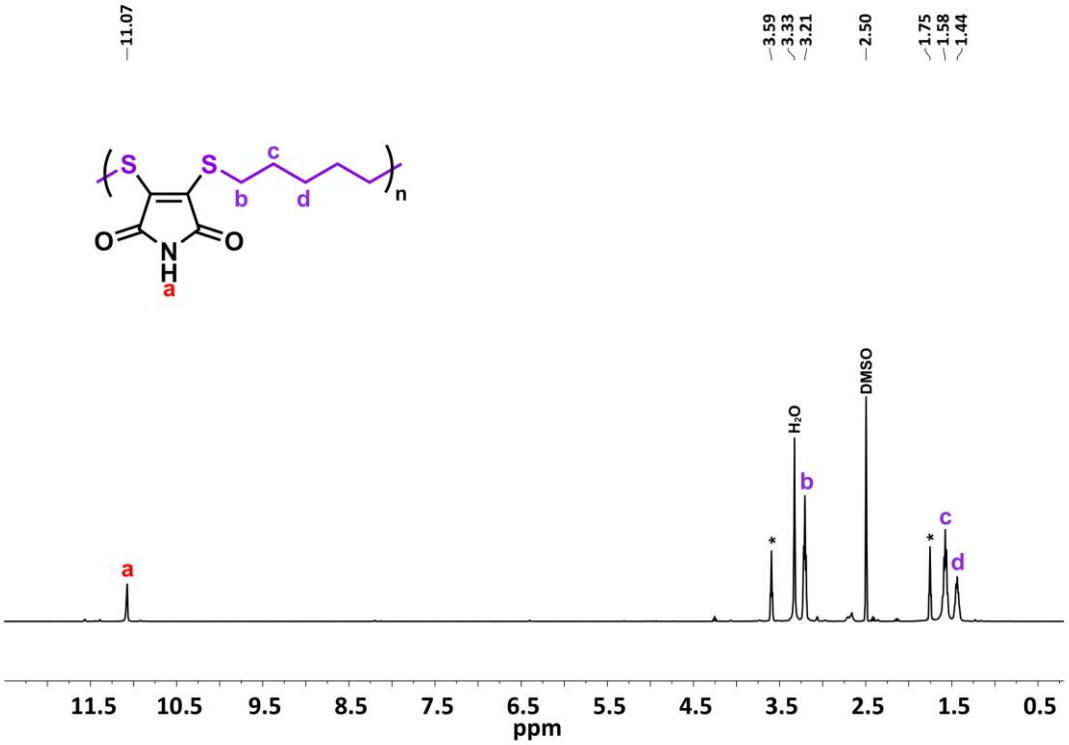

Figure A.14 : ^{1}H NMR spectrum of P4 in DMSO-d_6 (500 MHz). Residual THF peaks are marked with an asterisk (*).

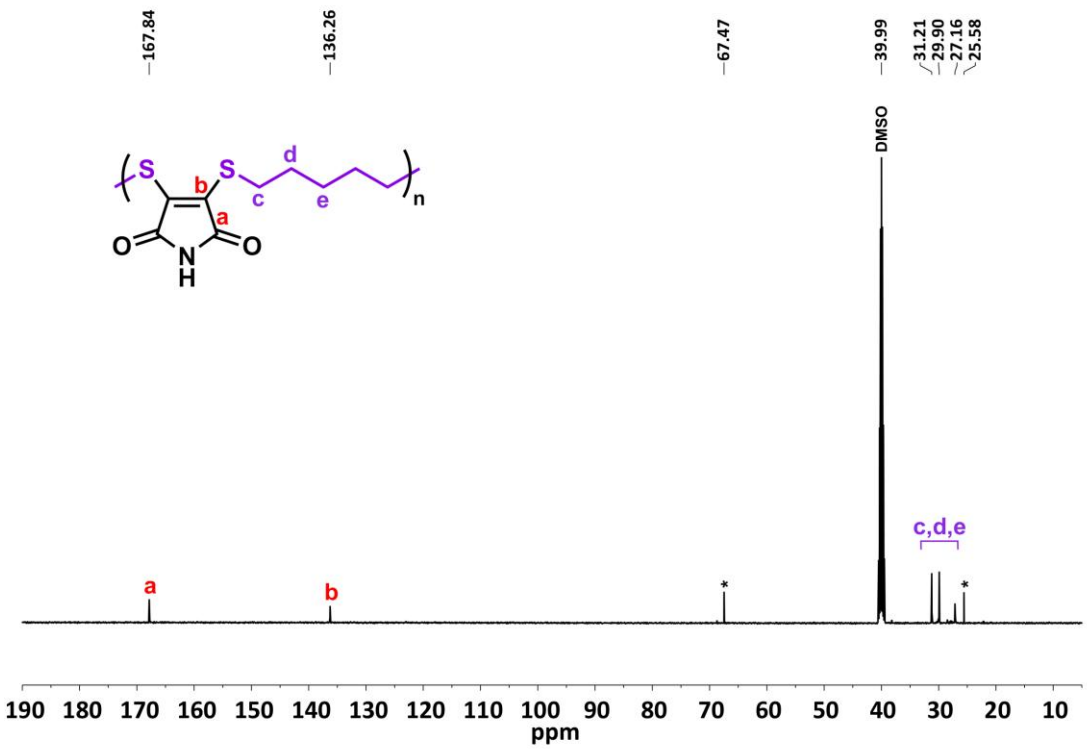

Figure A.15 : ^{13}C NMR spectrum of P4 in DMSO-d_6 (125 MHz). Residual THF peaks are marked with an asterisk (*).

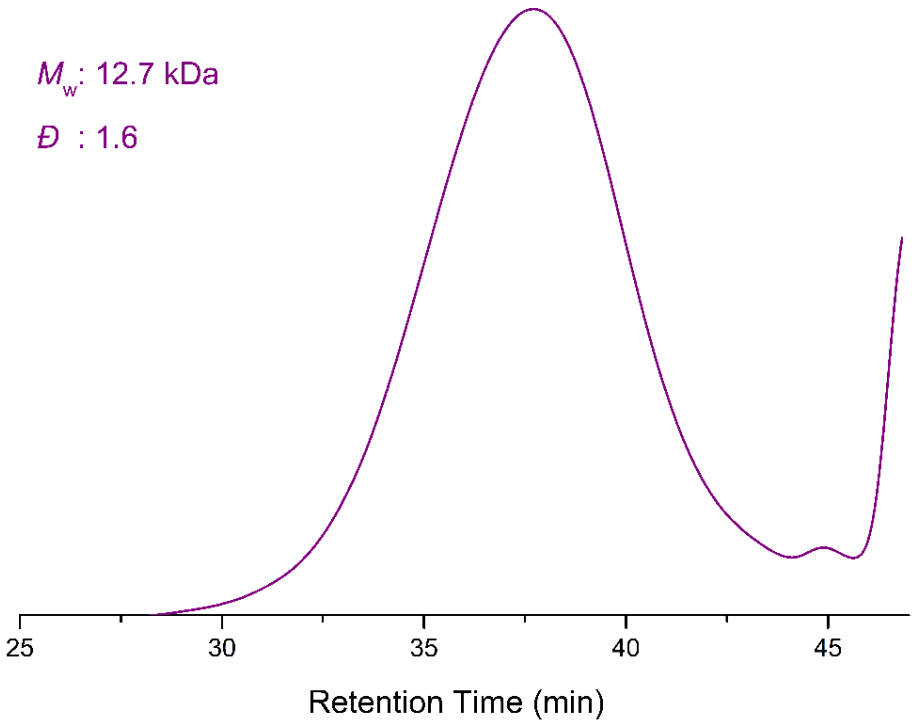

Figure A.16 : GPC trace of P4.

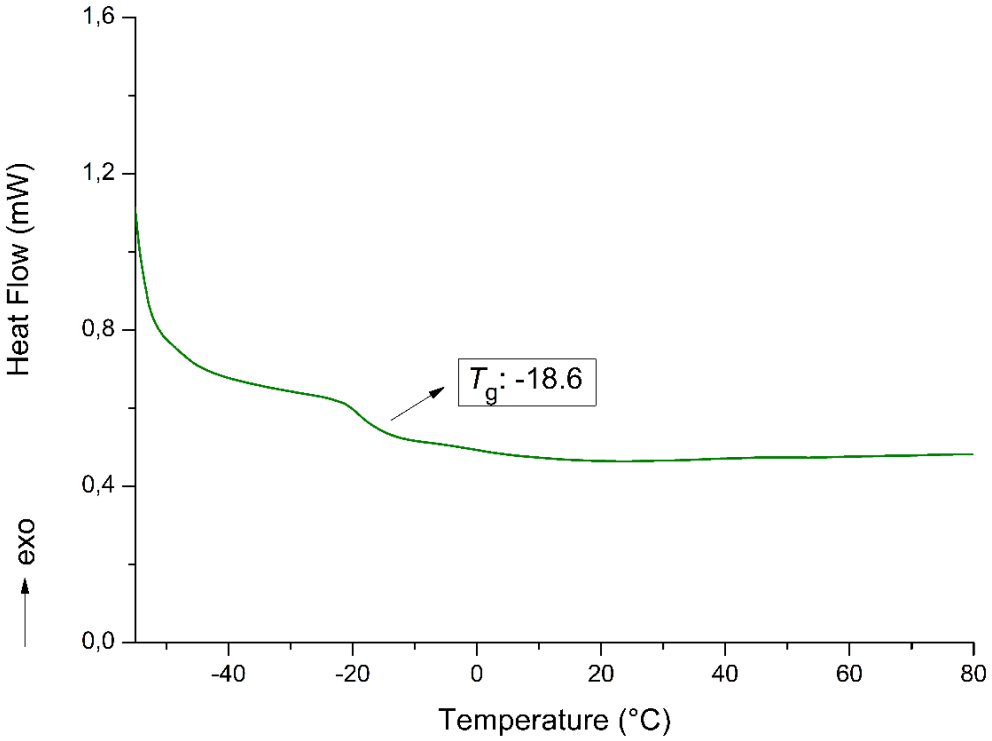

Figure A.17 : DSC spectrum of P4.

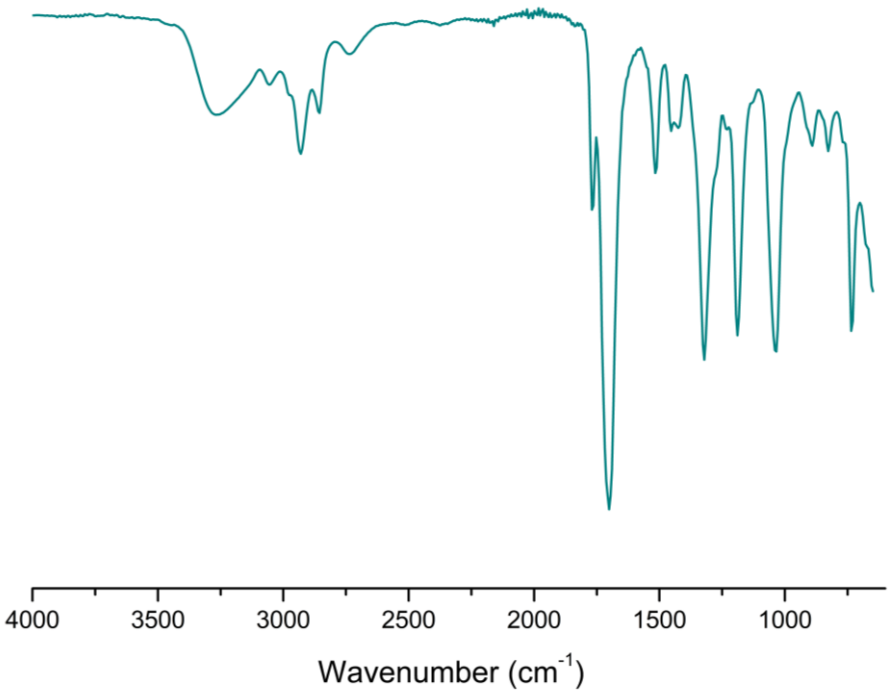

Figure A.18 : FTIR spectrum of P4.

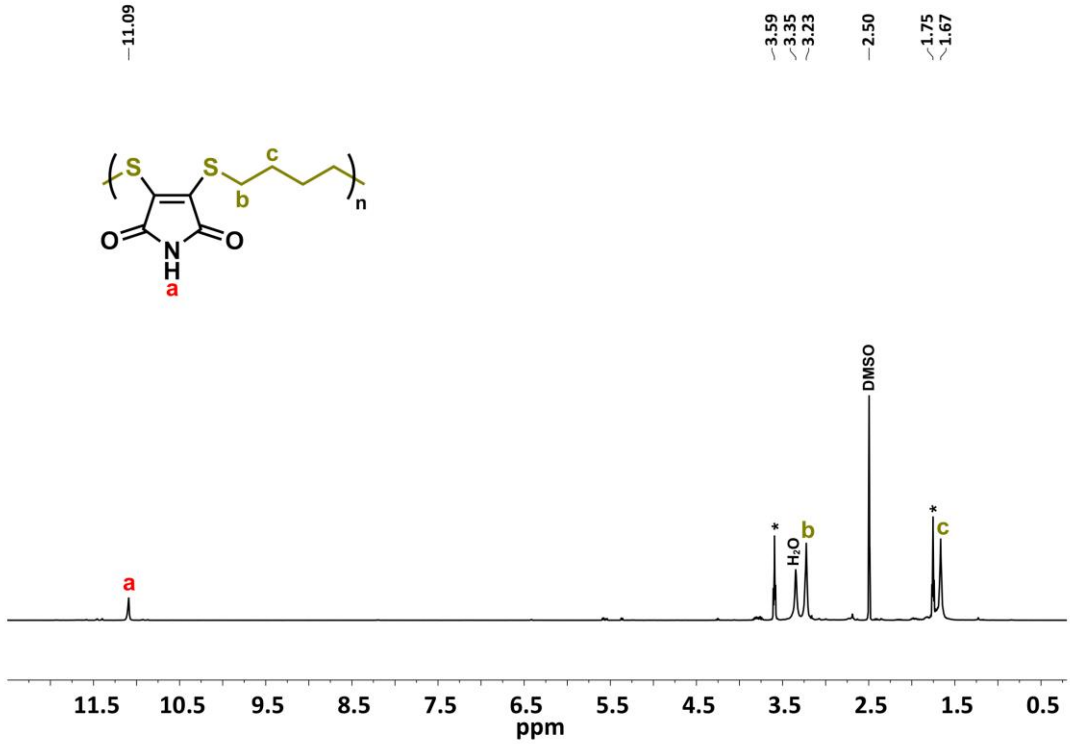

Figure A.19 : ^{1}H NMR spectrum of P5 in DMSO-d_6 (500 MHz). Residual THF peaks are marked with an asterisk (*).

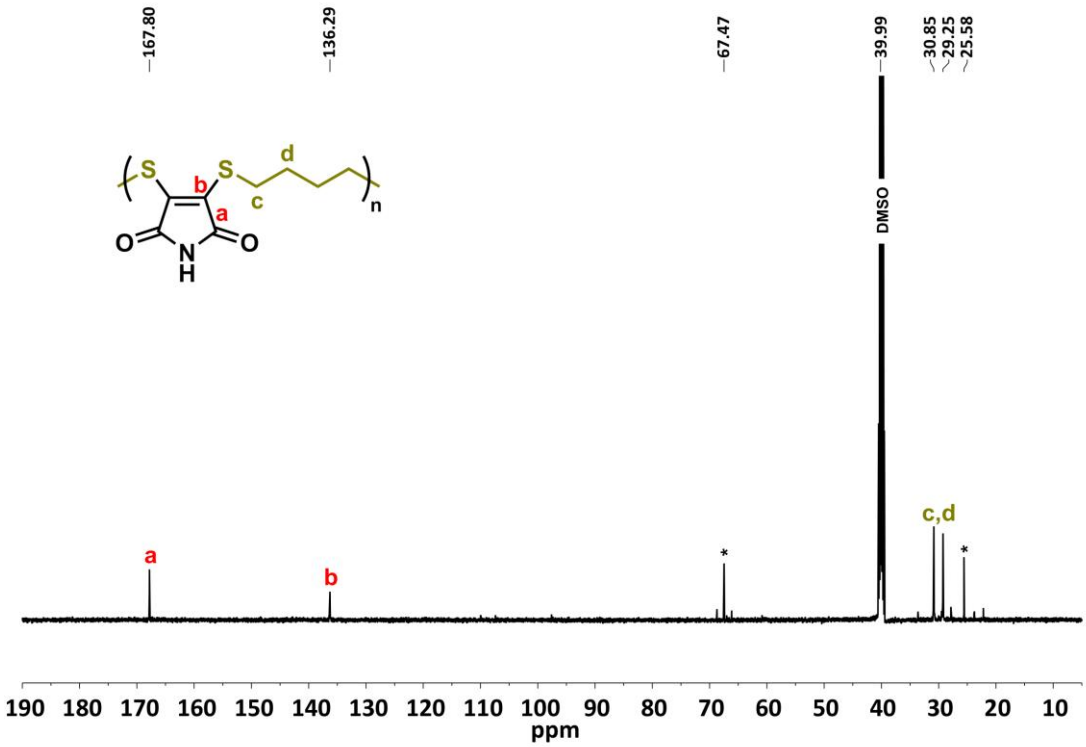

Figure A.20 : ^{13}C NMR spectrum of P5 in DMSO-d_6 (125 MHz). Residual THF peaks are marked with an asterisk (*).

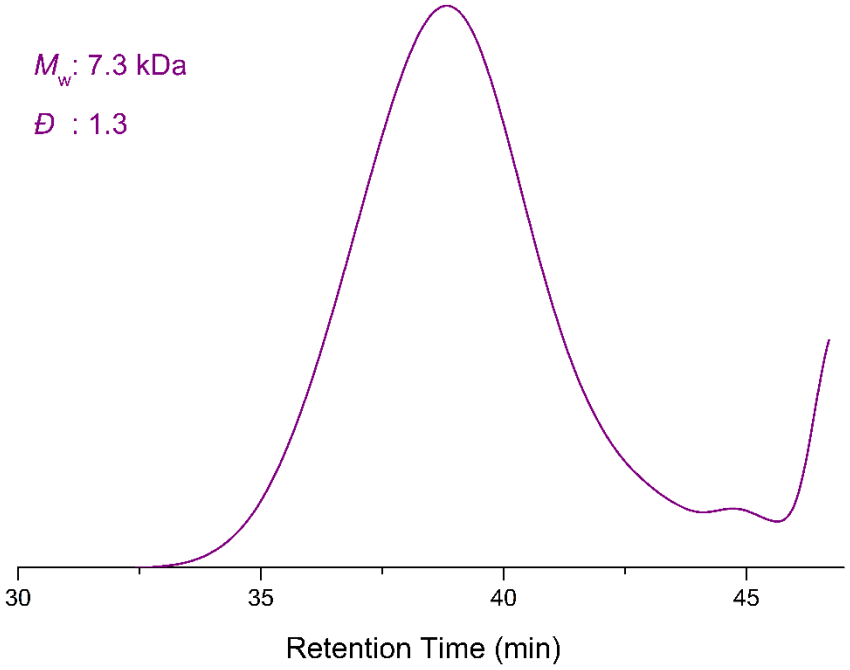

Figure A.21 : GPC trace of P5.

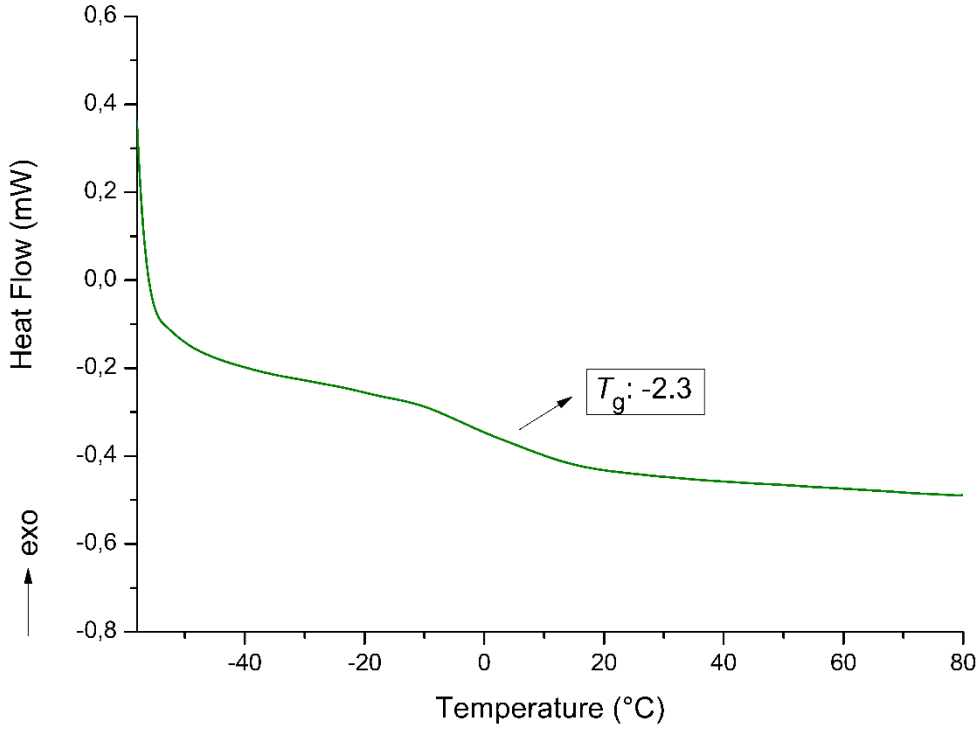

Figure A.22 : DSC spectrum of P5.

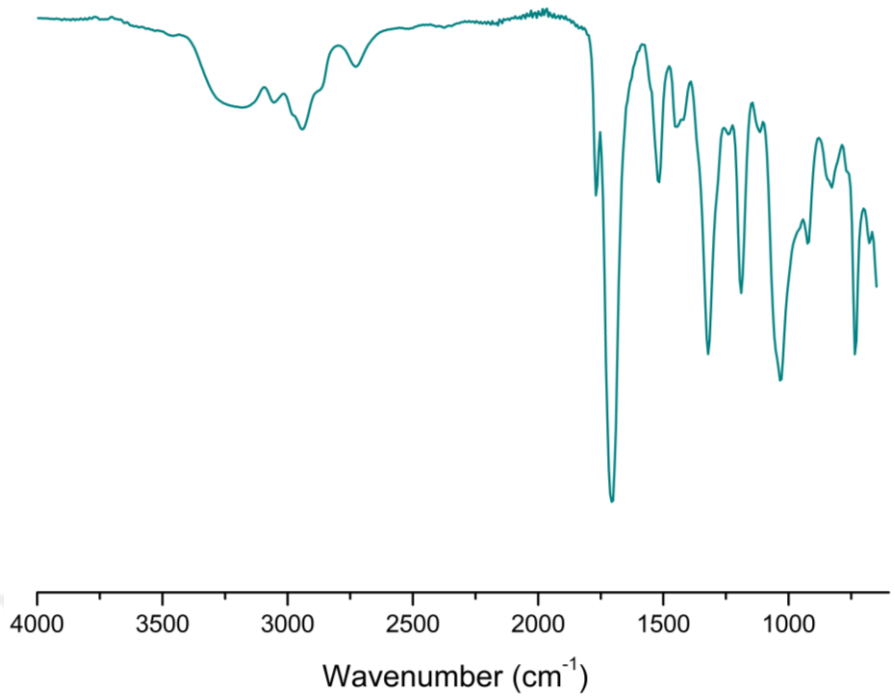

Figure A.23 : FTIR spectrum of P5.

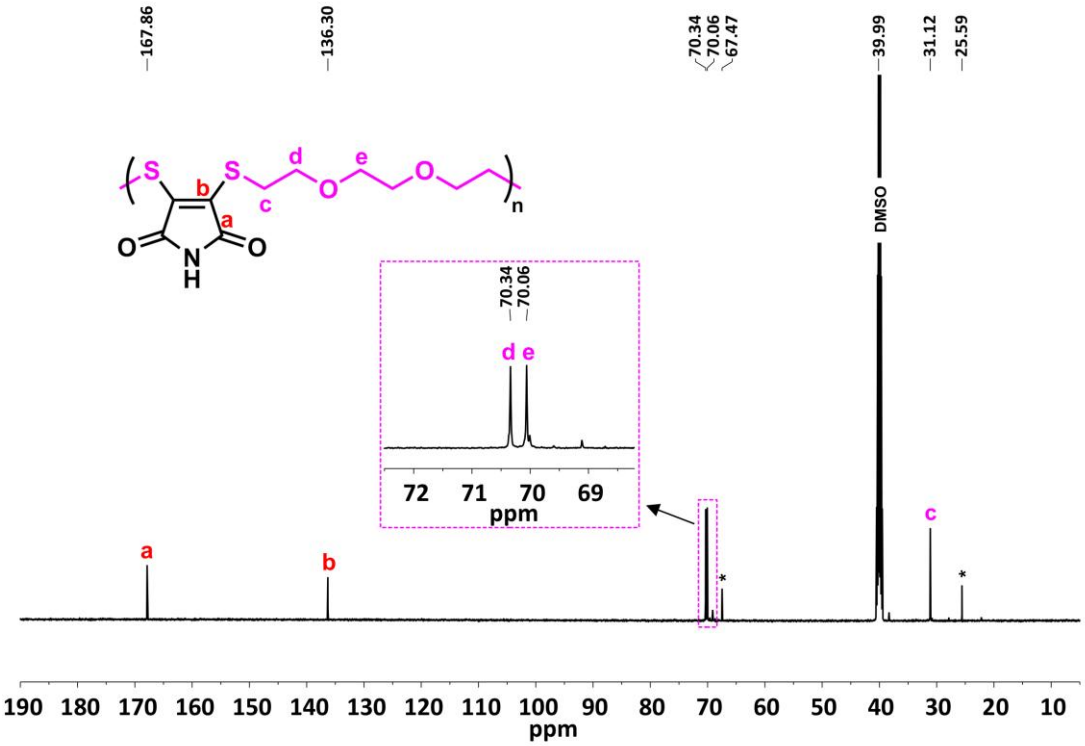

Figure A.24 : ^{13}C NMR spectrum of P6 in DMSO-d_6 (125 MHz). Residual THF peaks are marked with an asterisk (*).

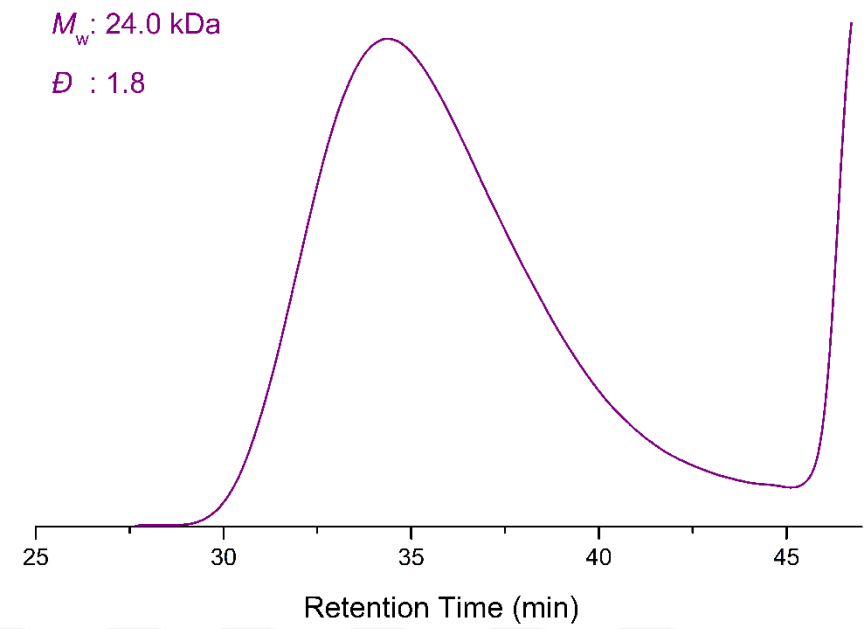

Figure A.25 : GPC trace of P6.

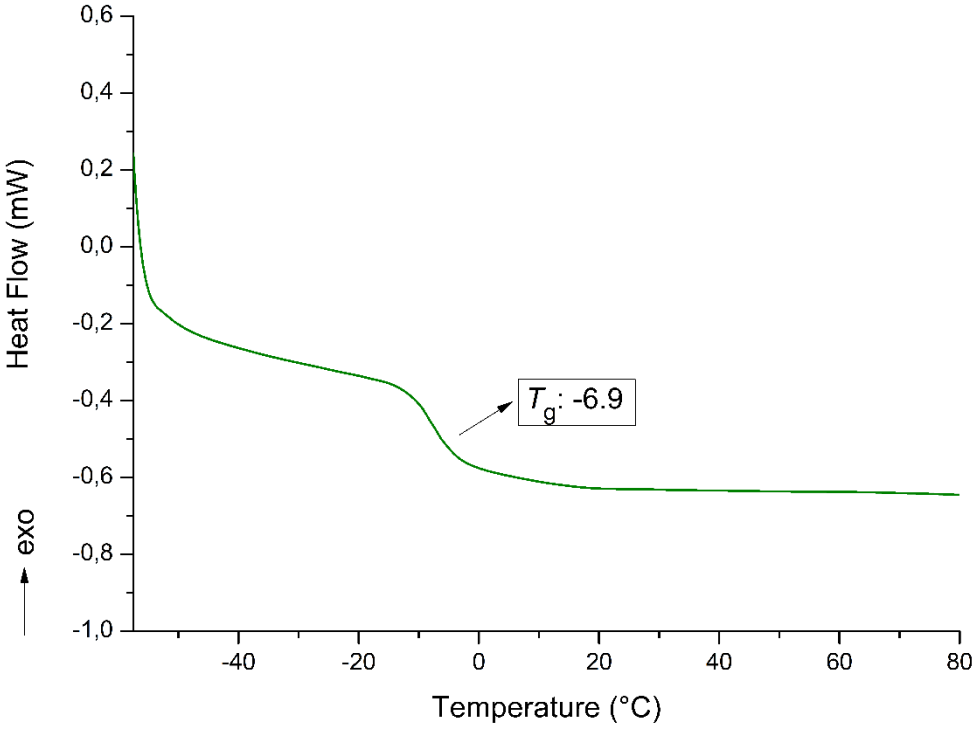

Figure A.26 : DSC spectrum of P6.

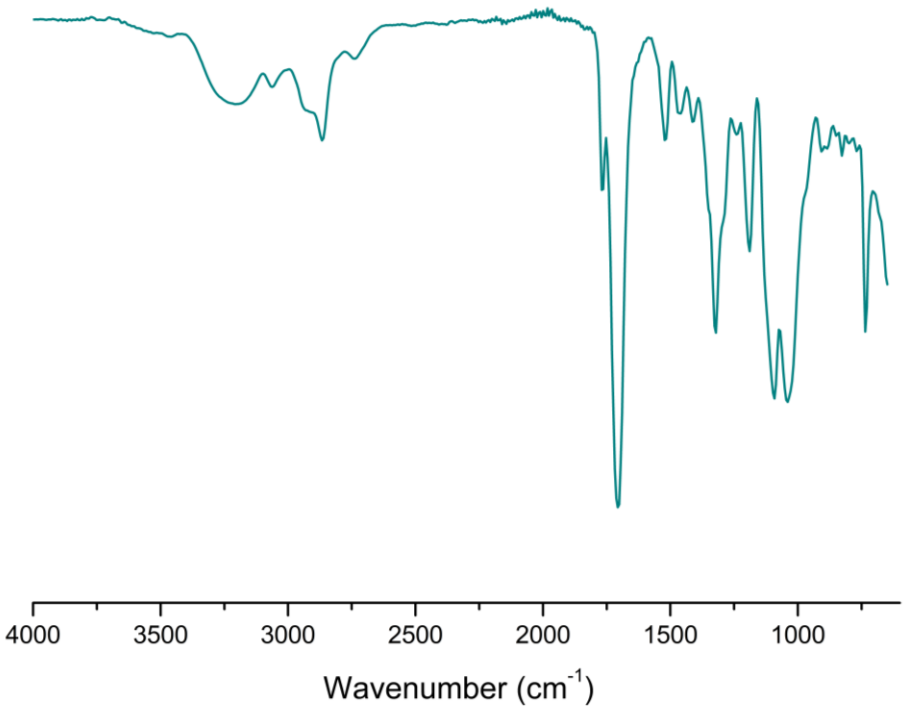

Figure A.27 : FTIR spectrum of P6.

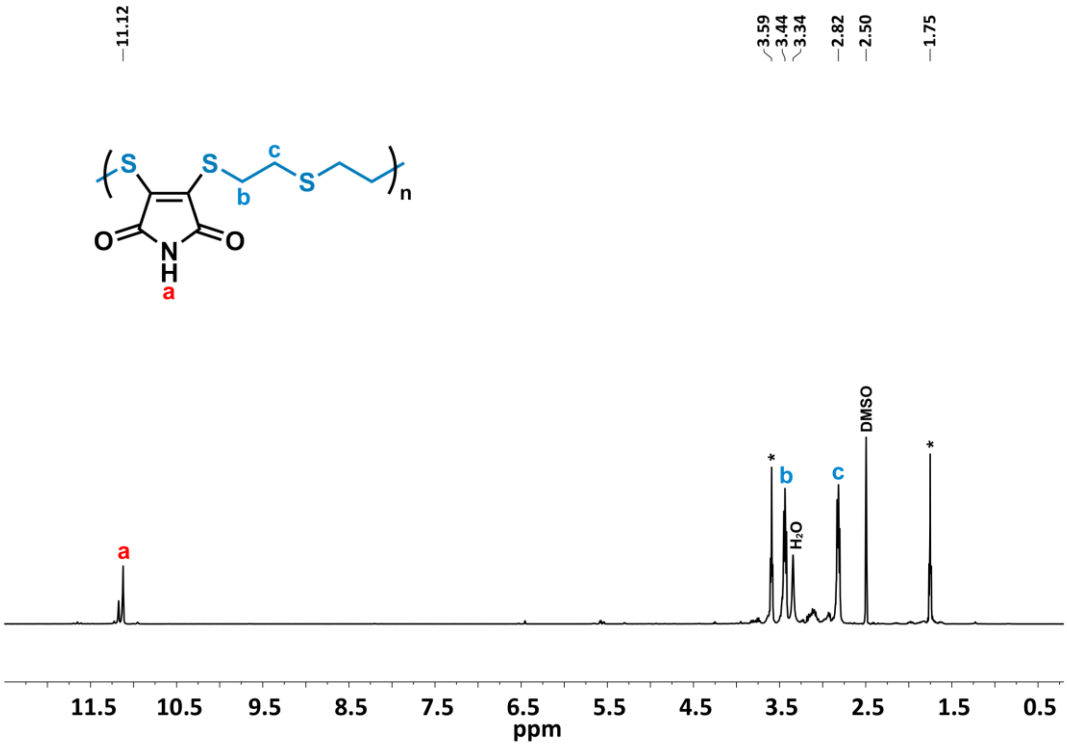

Figure A.28 : ^{1}H NMR spectrum of P7 in DMSO-d_6 (500 MHz). Residual THF peaks are marked with an asterisk (*).

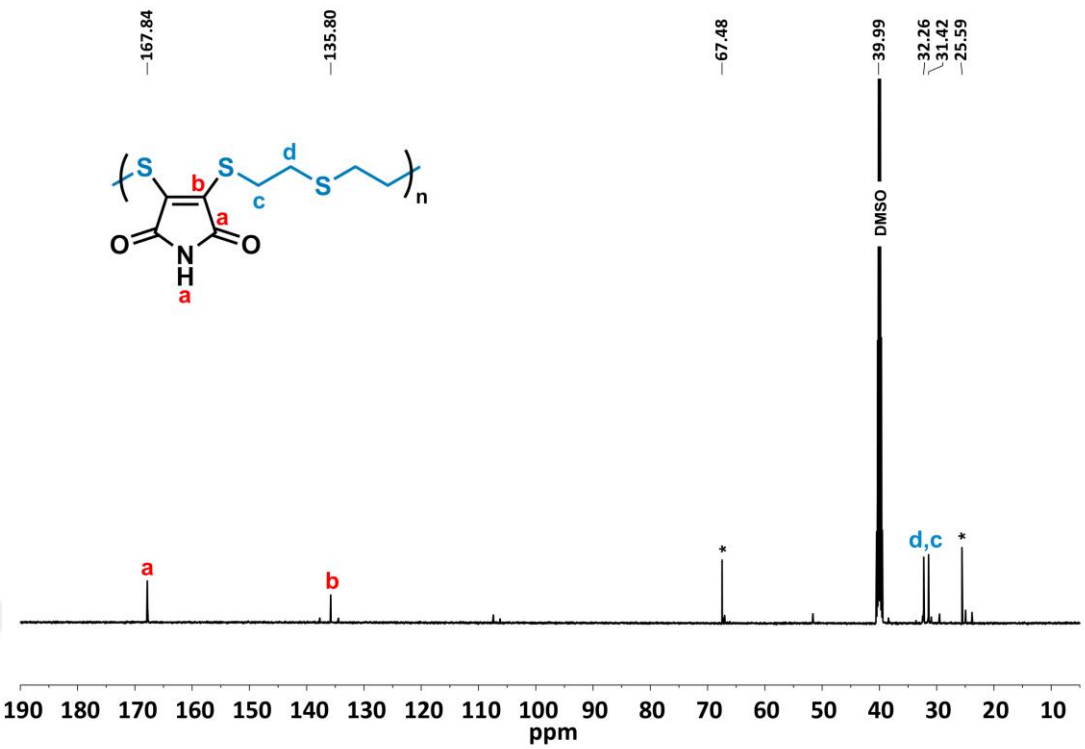

Figure A.29 : ^{13}C NMR spectrum of P7 in DMSO-d_6 (125 MHz). Residual THF peaks are marked with an asterisk (*).

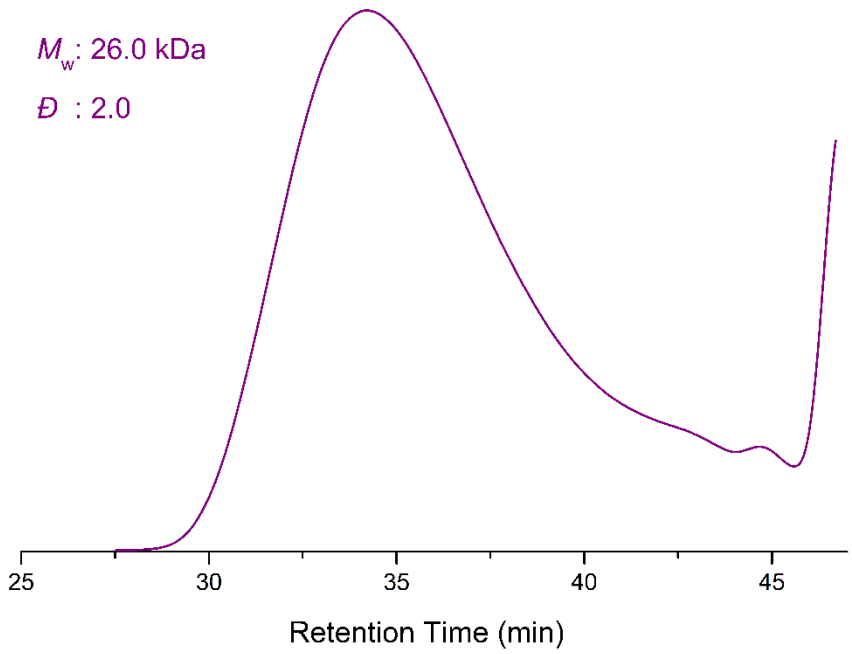

Figure A.30 : GPC trace of P7.

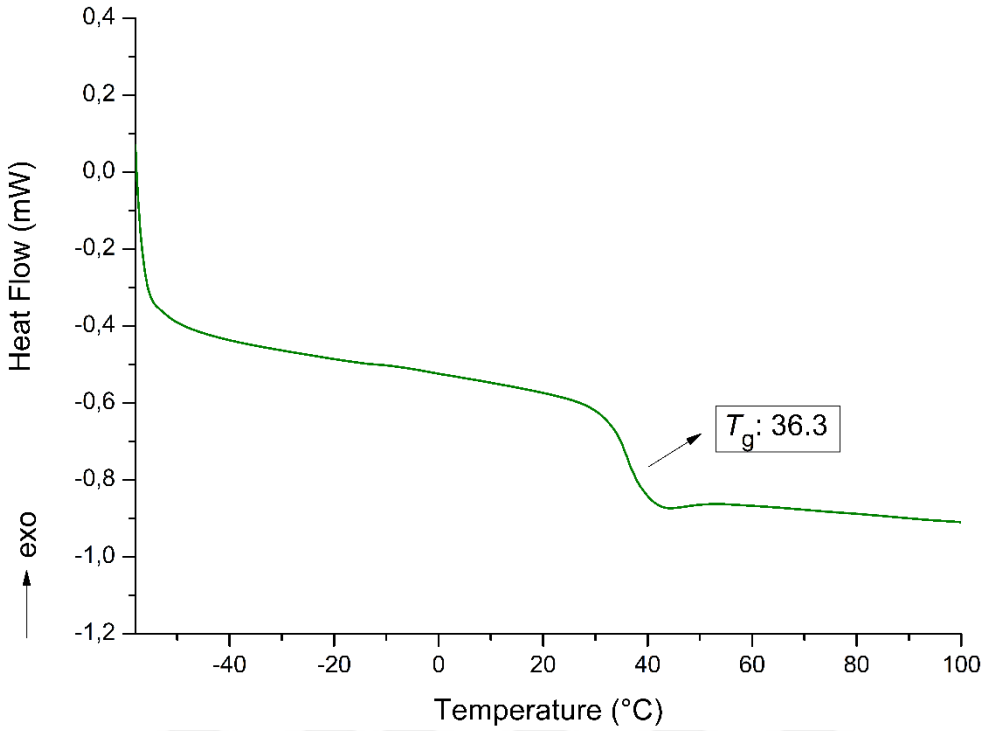

Figure A.31 : DSC spectrum of P7.

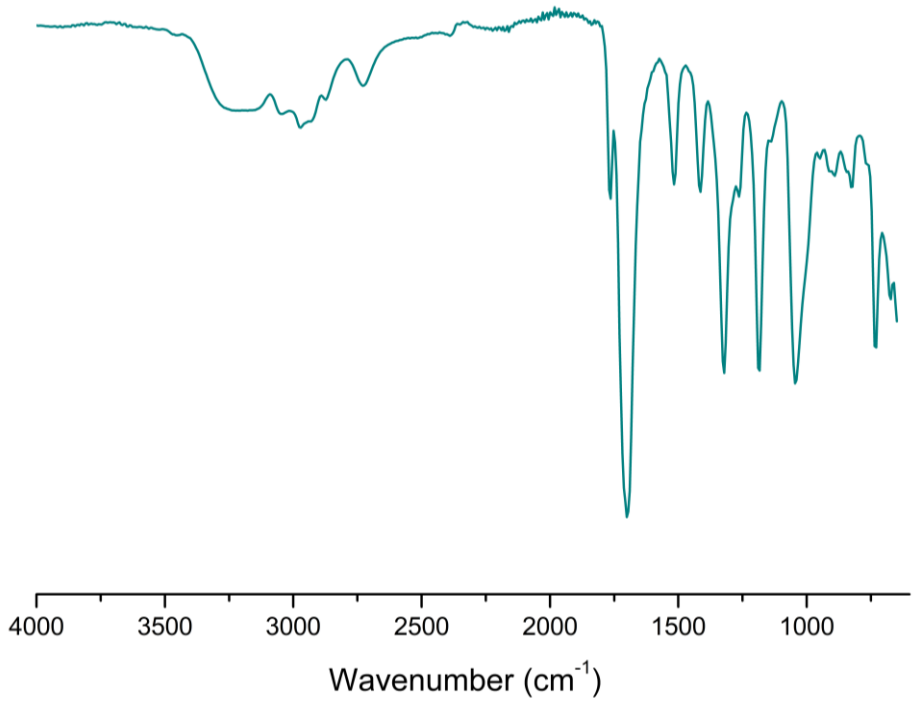

Figure A.32 : FTIR spectrum of P7.

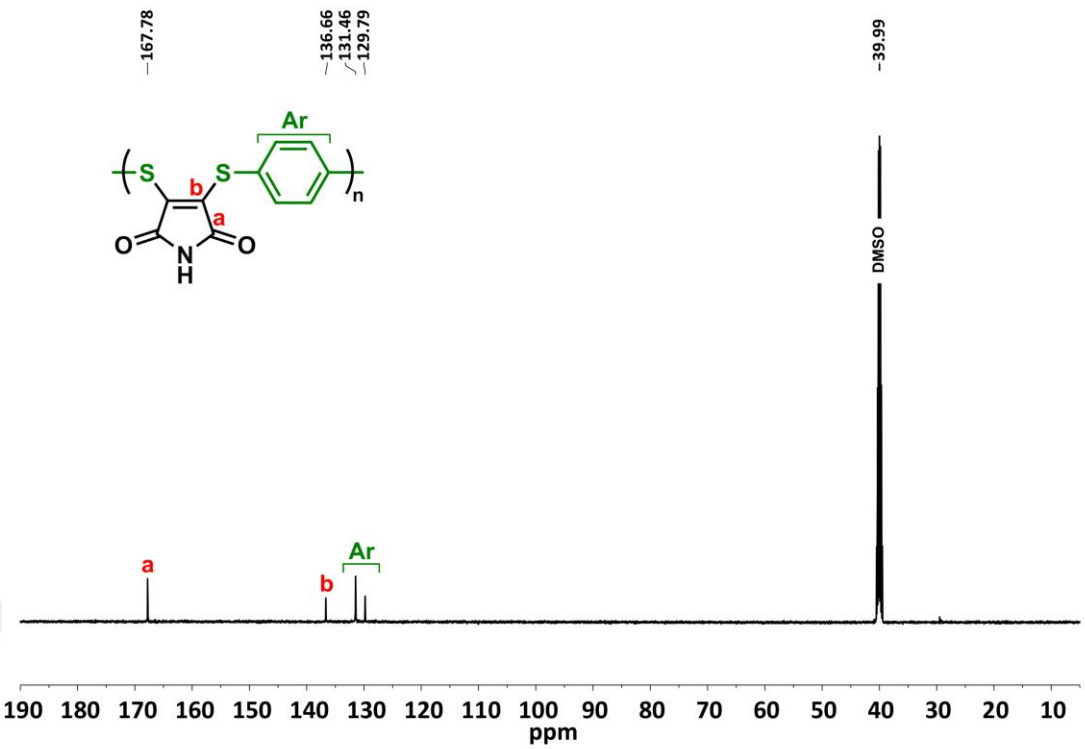

Figure A.33 : ^{13}C NMR spectrum of P8 in DMSO-d_6 (125 MHz).

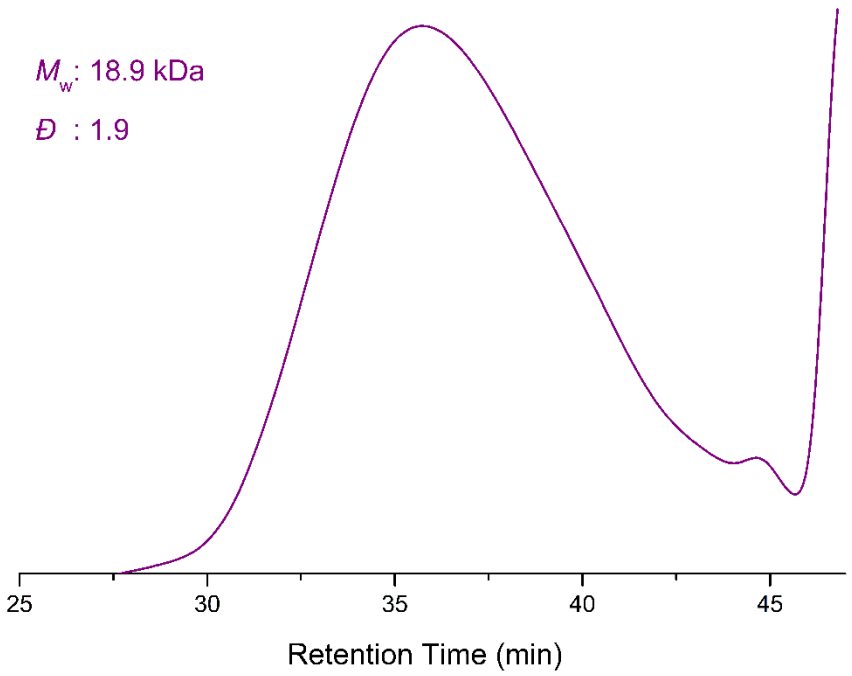

Figure A.34 : GPC trace of P8.

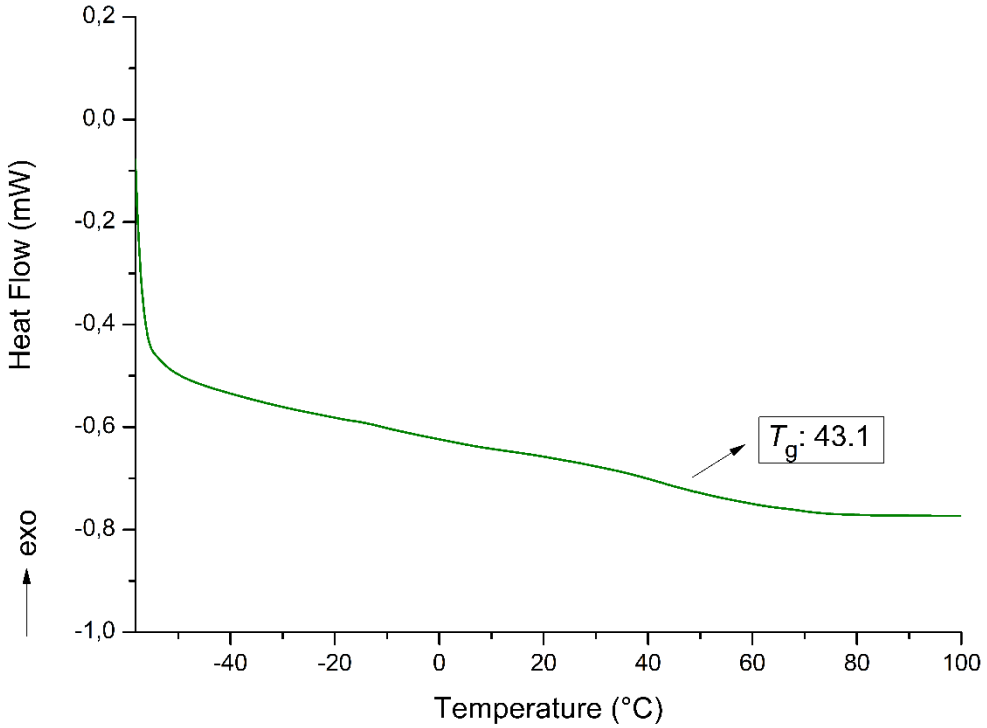

Figure A.35 : DSC spectrum of P8.

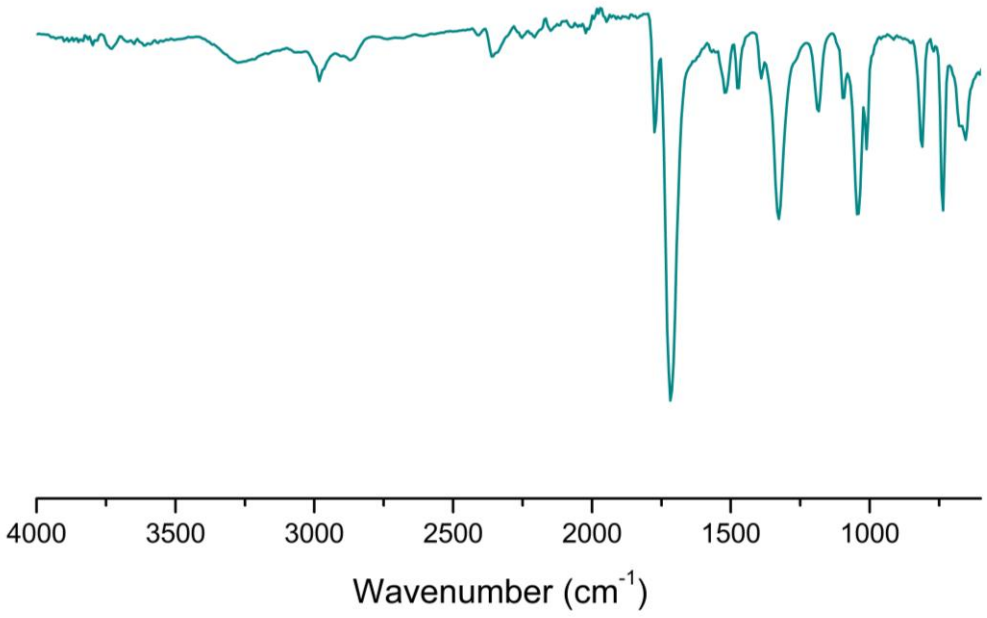

Figure A.36 : FTIR spectrum of P8.

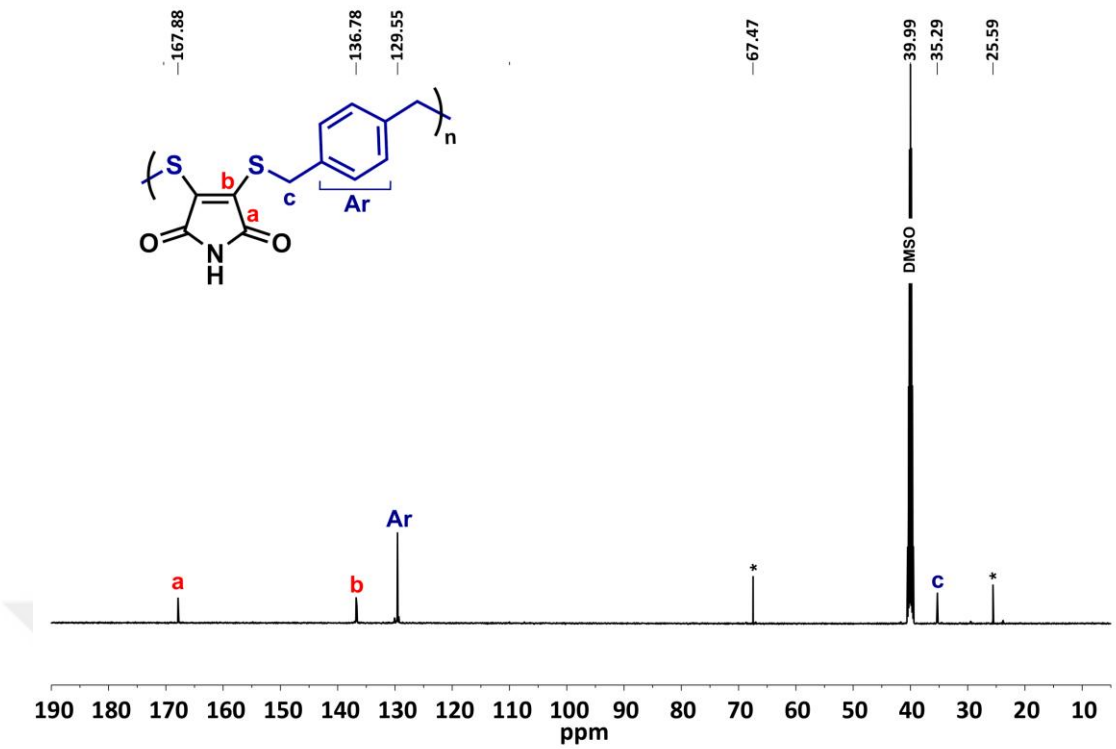

Figure A.37 : ^{13}C NMR spectrum of P9 in DMSO-d_6 (125 MHz). Residual THF peaks are marked with an asterisk (*).

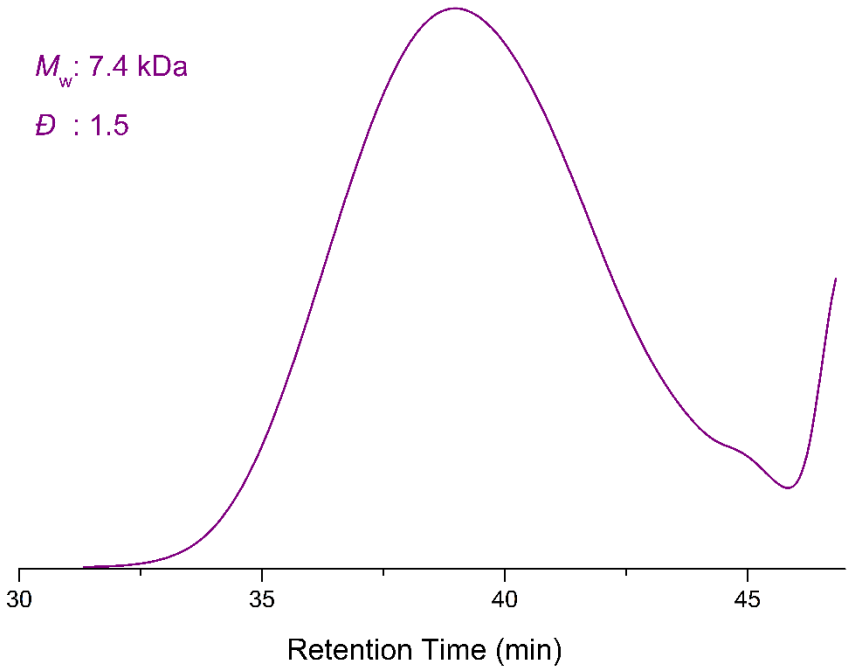

Figure A.38 : GPC trace of P9.

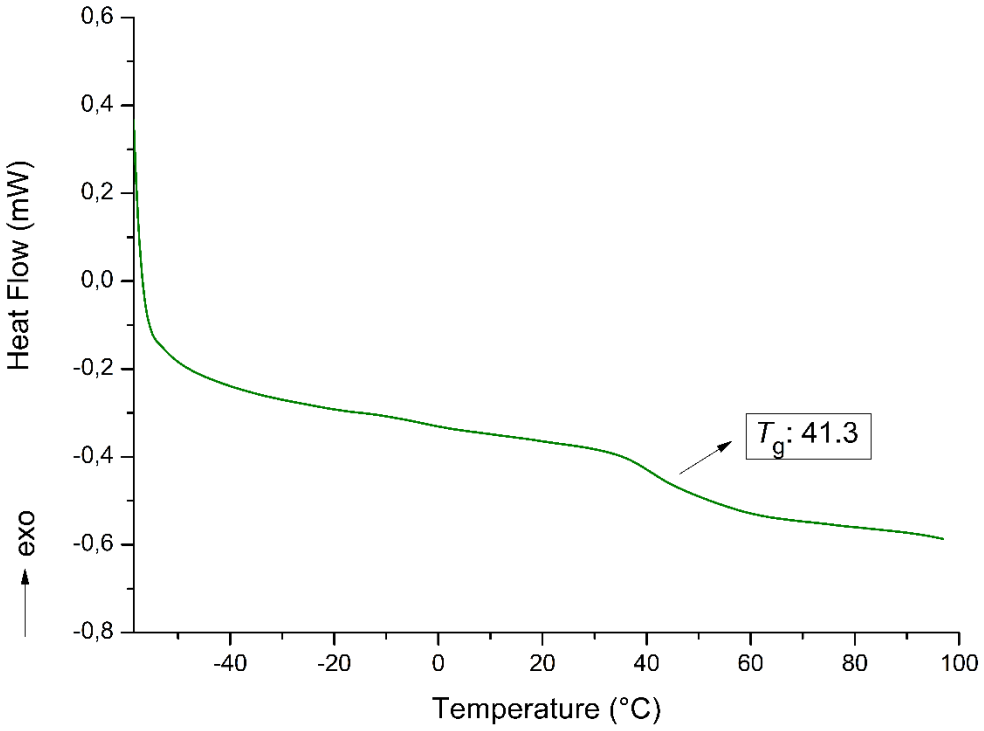

Figure A.39 : DSC spectrum of P9.

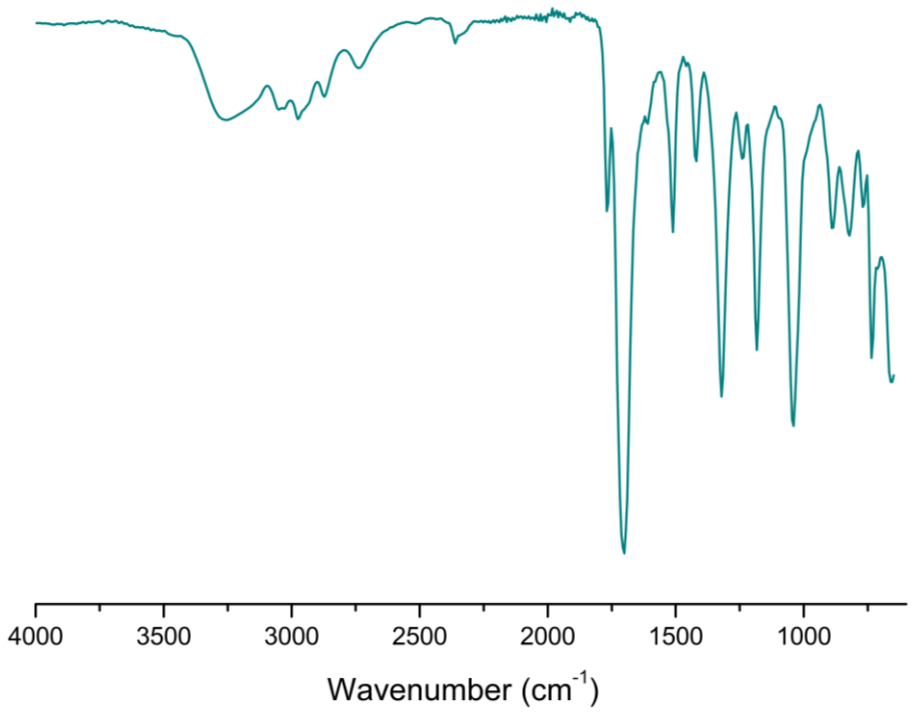

Figure A.40 : FTIR spectrum of P9.

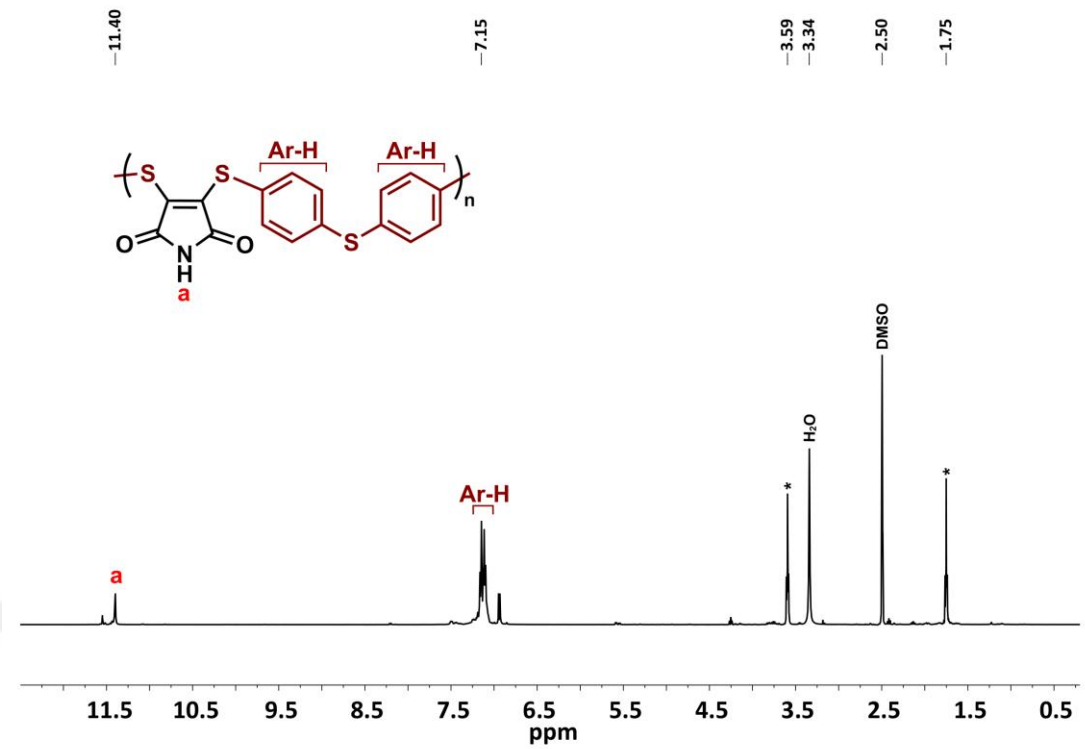

Figure A.41 : ^{1}H NMR spectrum of P10 in DMSO-d_6 (500 MHz). Residual THF peaks are marked with an asterisk (*).

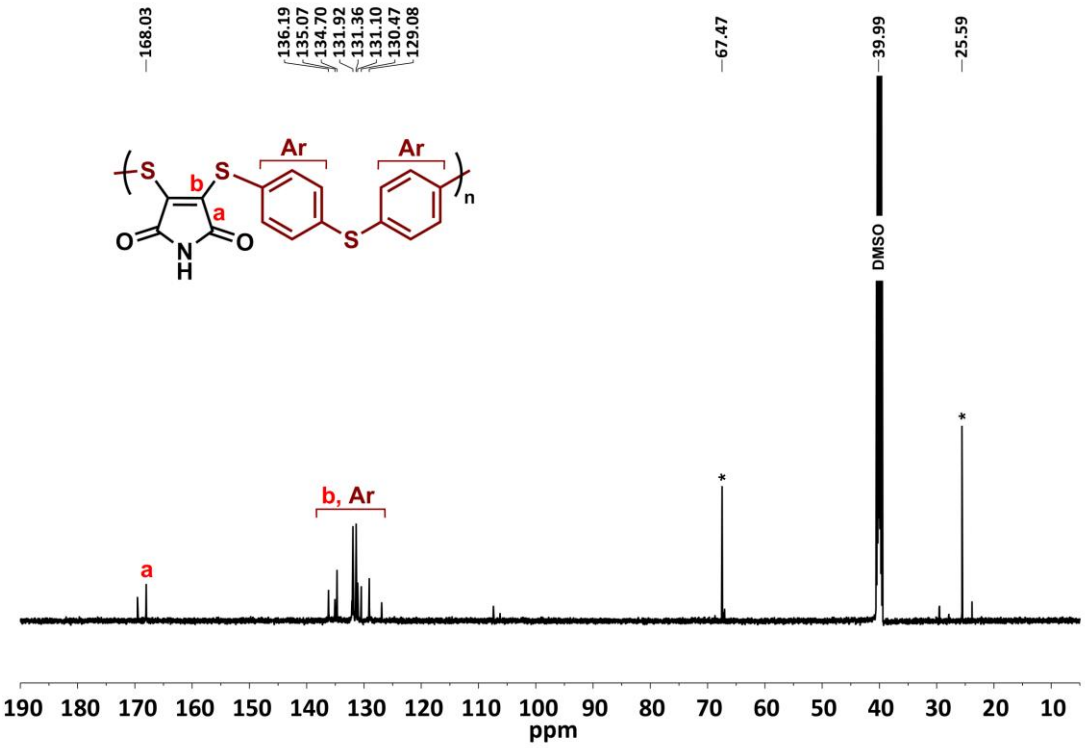

Figure A.42 : ^{13}C NMR spectrum of P10 in DMSO-d_6 (125 MHz). Residual THF peaks are marked with an asterisk (*).

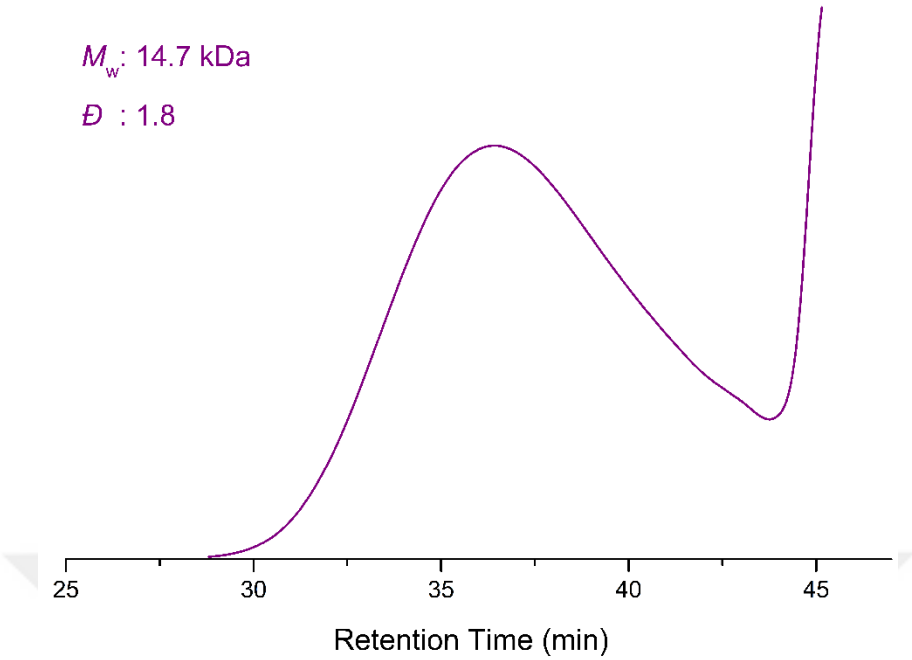

Figure A.43 : GPC trace of P10.

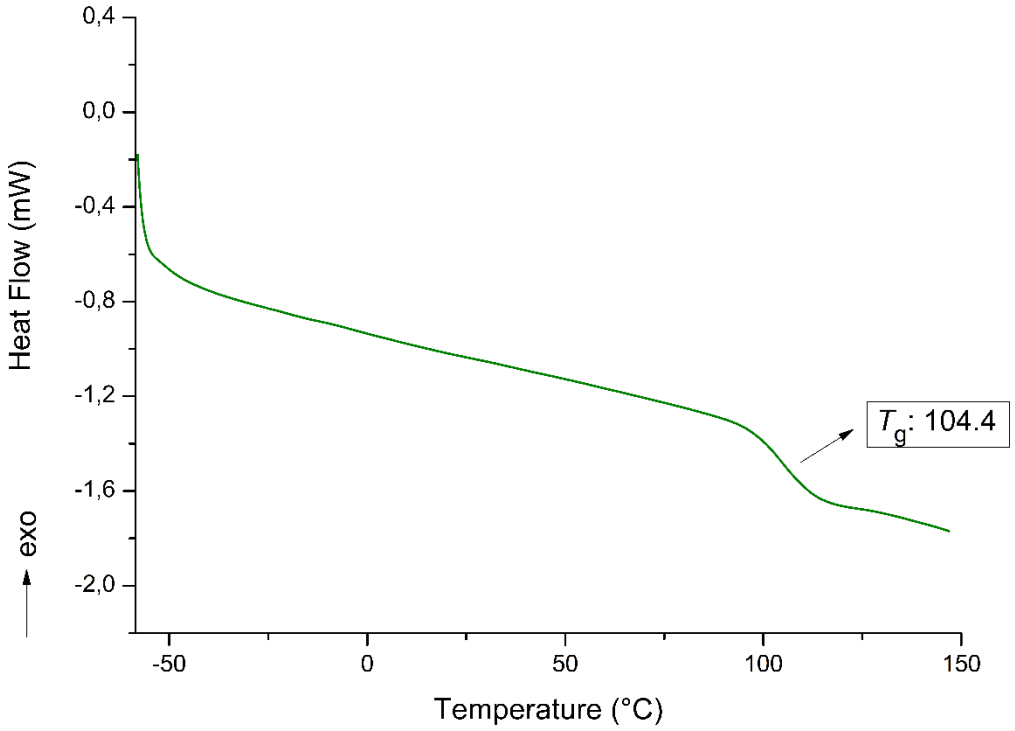

Figure A.44 : DSC spectrum of P10.

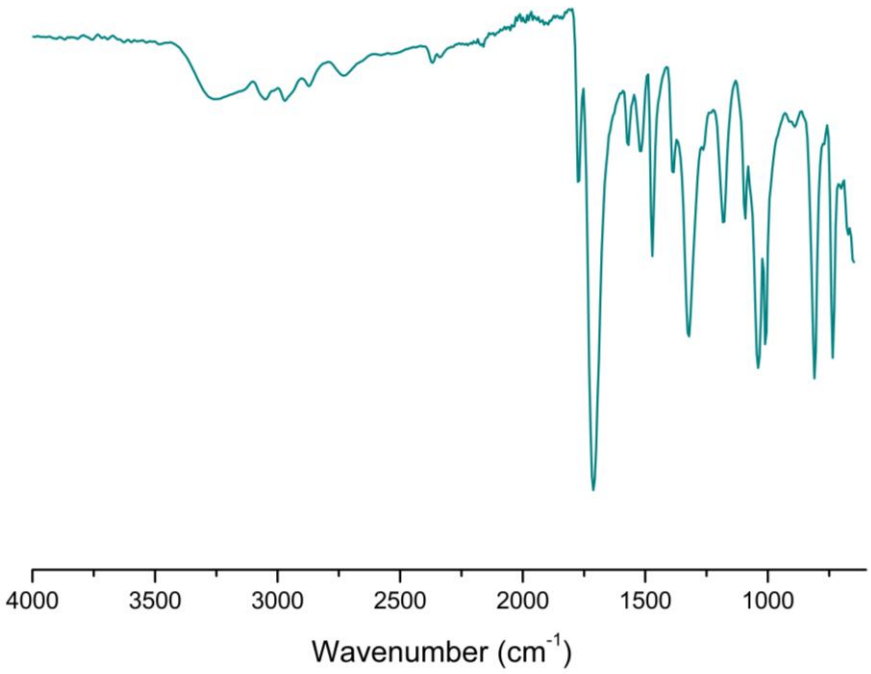

Figure A.45 : FTIR spectrum of P10.

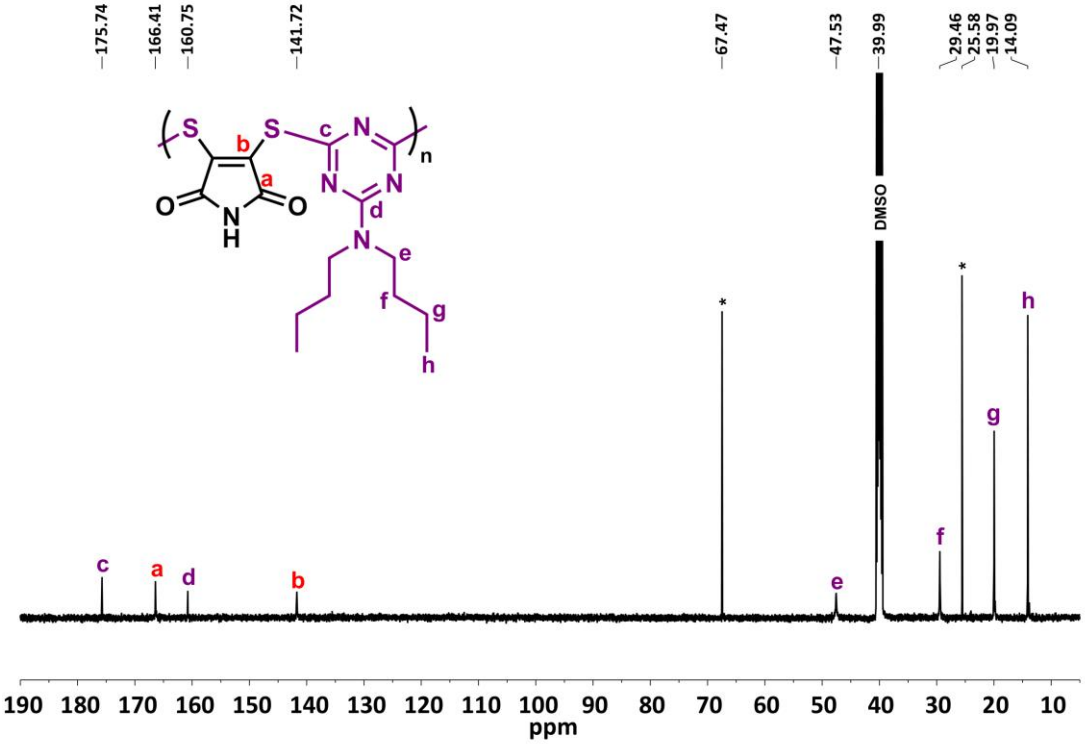

Figure A.46 : ^{13}C NMR spectrum of P11 in DMSO-d_6 (125 MHz). Residual THF peaks are marked with an asterisk (*).

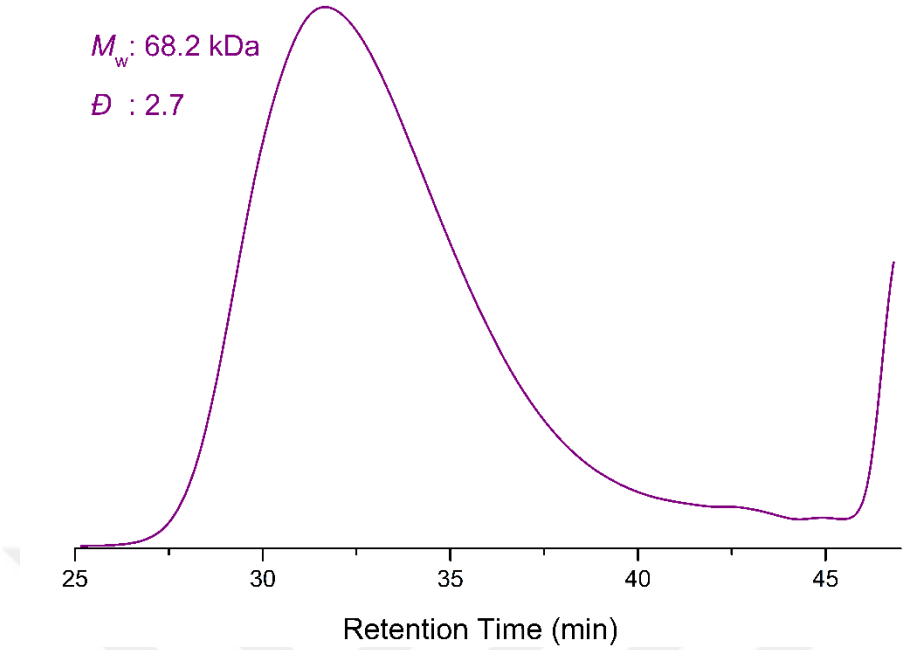

Figure A.47 : GPC trace of P11.

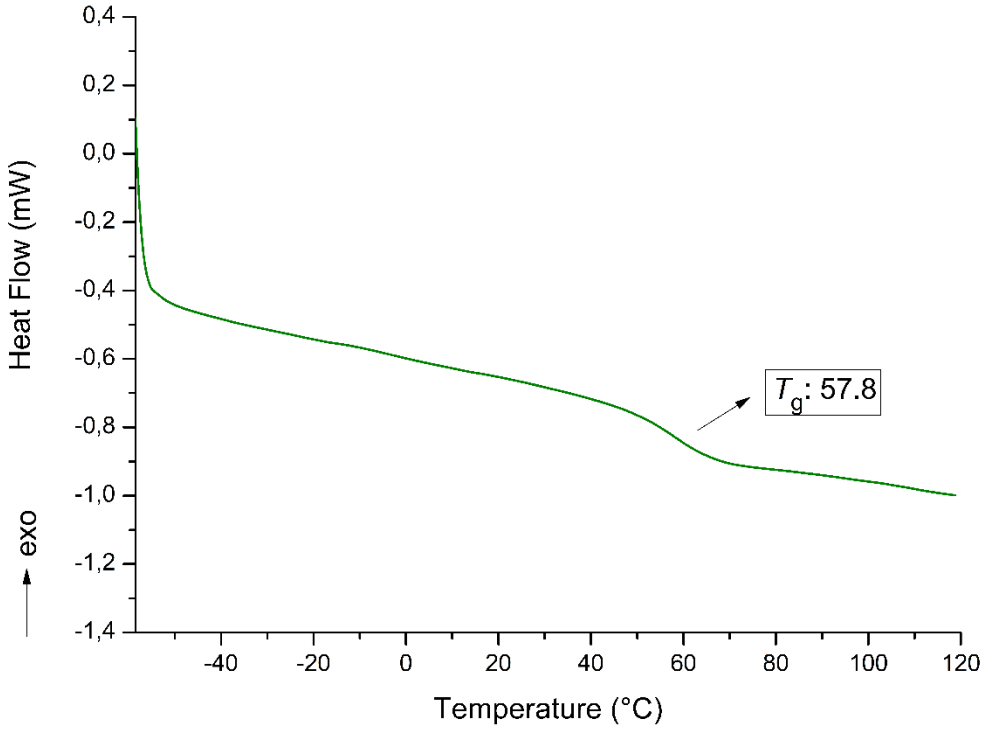

Figure A.48 : DSC spectrum of P11.

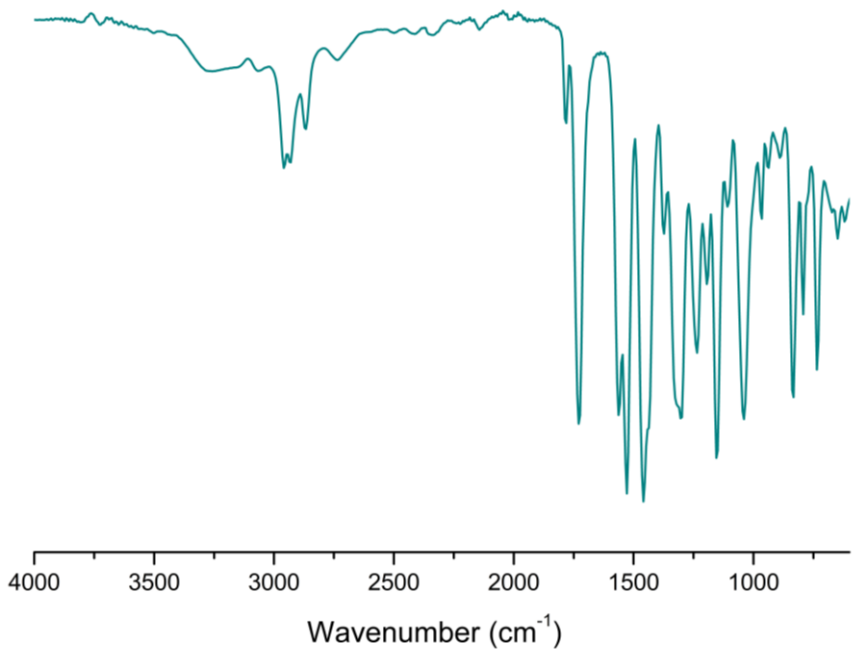

Figure A.49 : FTIR spectrum of P11.

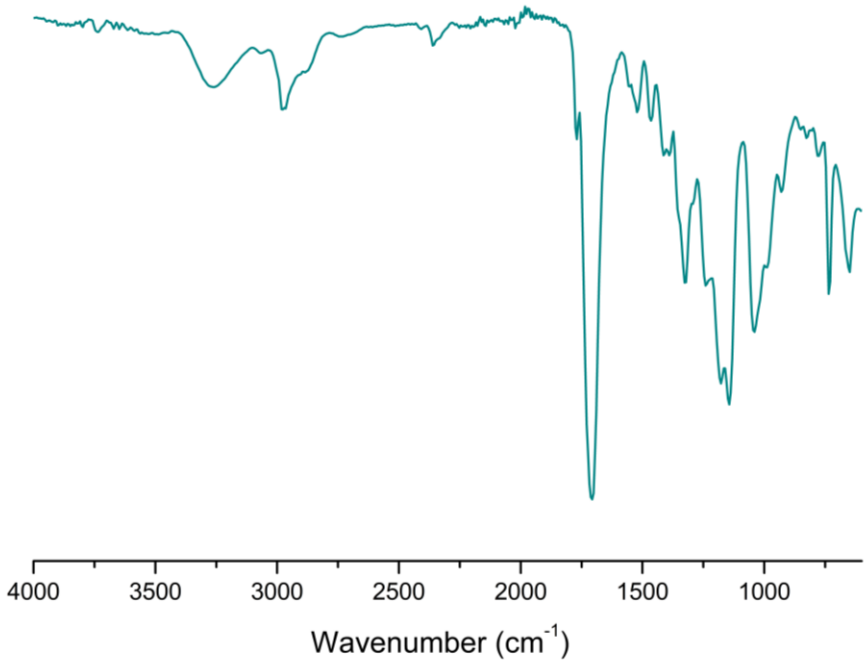

Figure A.50 : FTIR spectrum of cross-linked polymer.

APPENDIX B

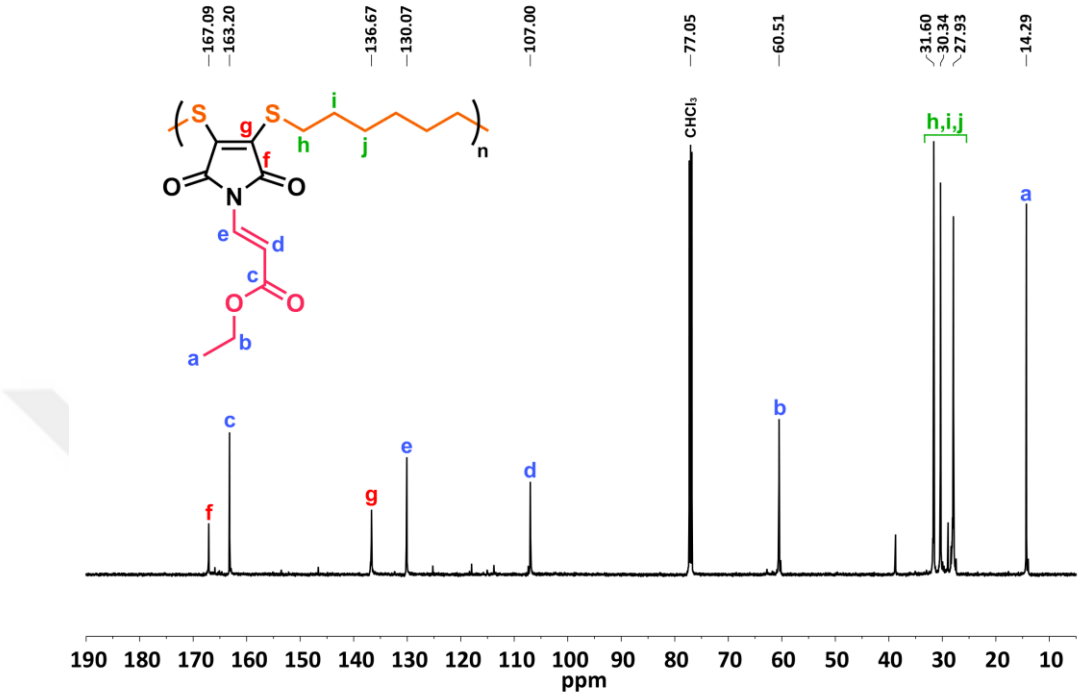

Figure B.1 : ^{13}C NMR spectrum of ethyl propiolate modified P1 in $CDCl_3$ (125 MHz).

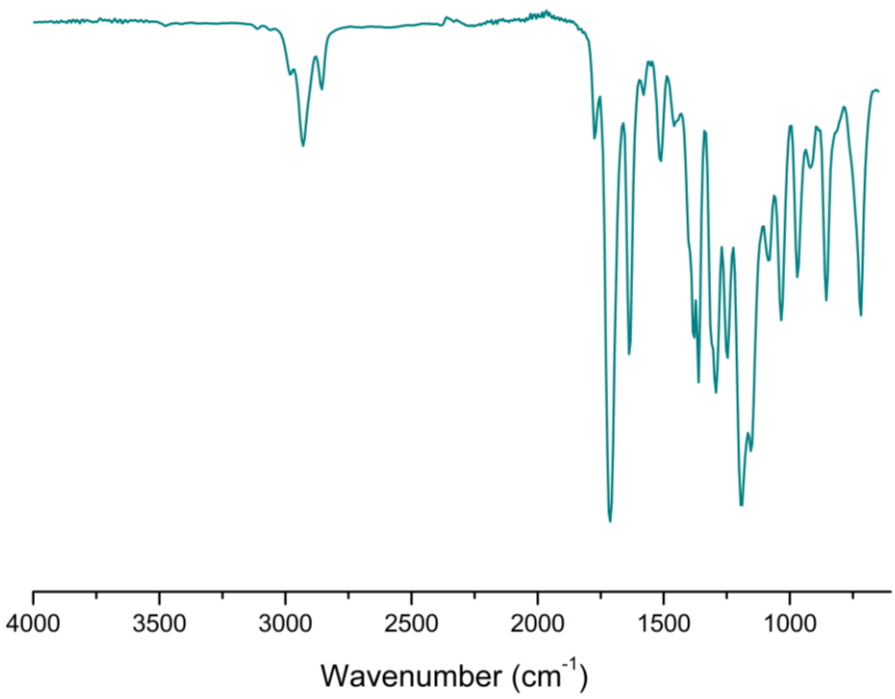

Figure B.2 : FTIR spectrum of ethyl propiolate modified P1.

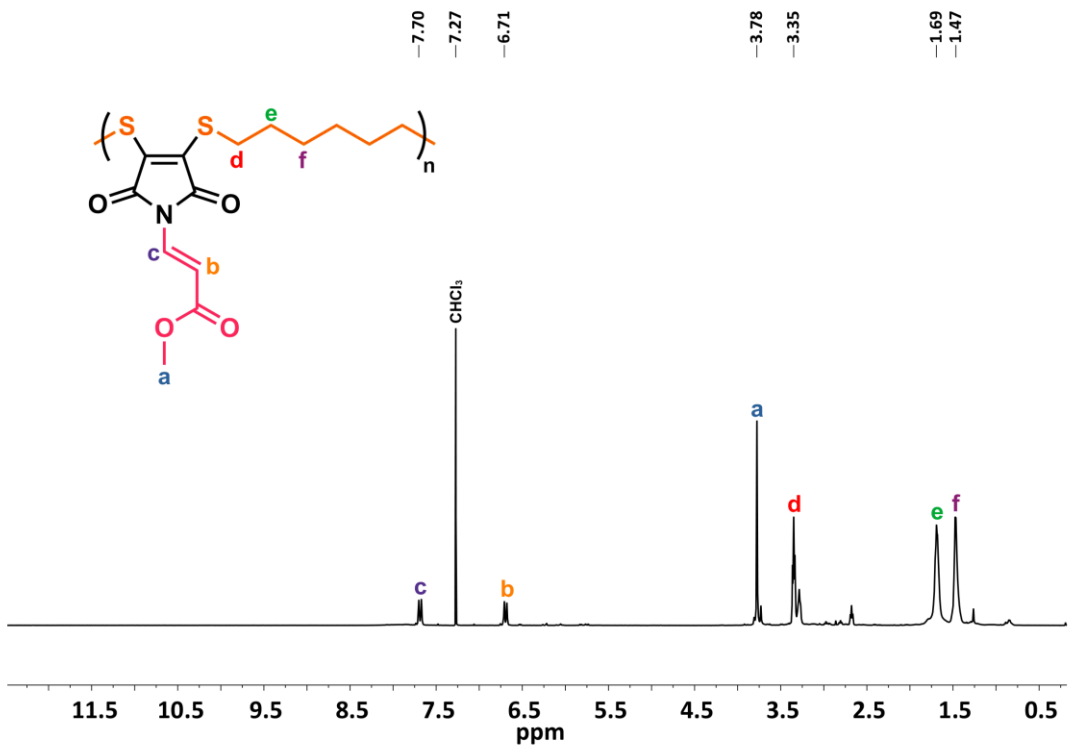

Figure B.3 : ^{1}H NMR spectrum of methyl propiolate modified P1 in $CDCl_3$ (500 MHz).

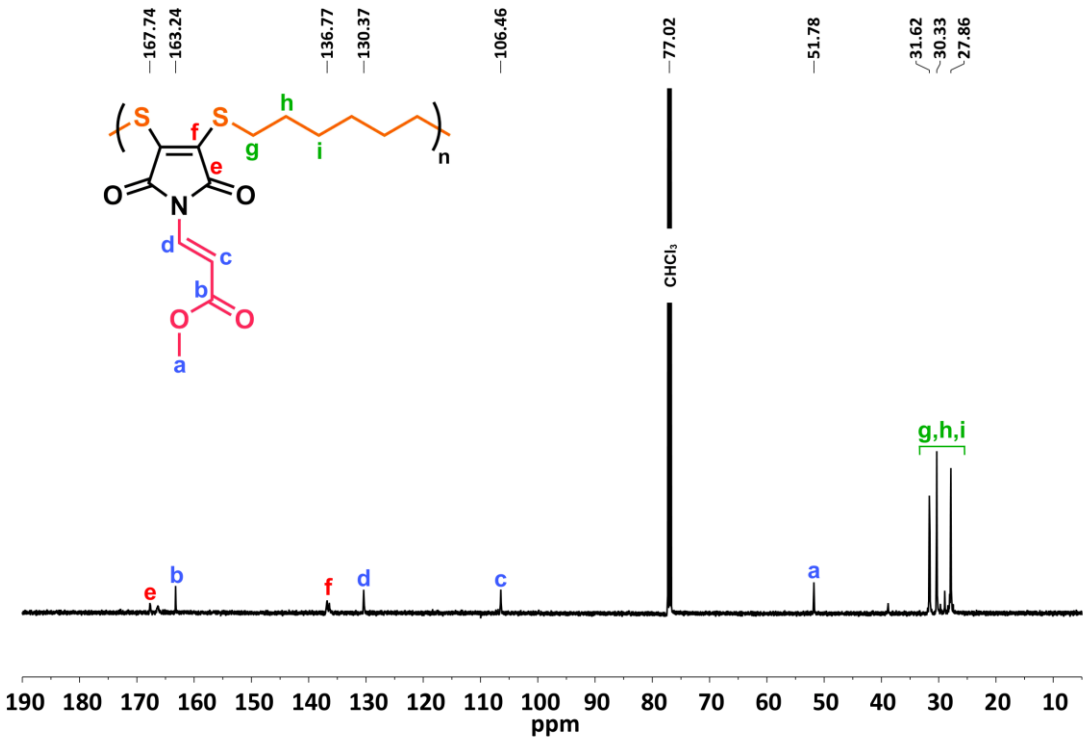

Figure B.4 : ^{13}C NMR spectrum of methyl propiolate modified P1 in $CDCl_3$ (125 MHz).

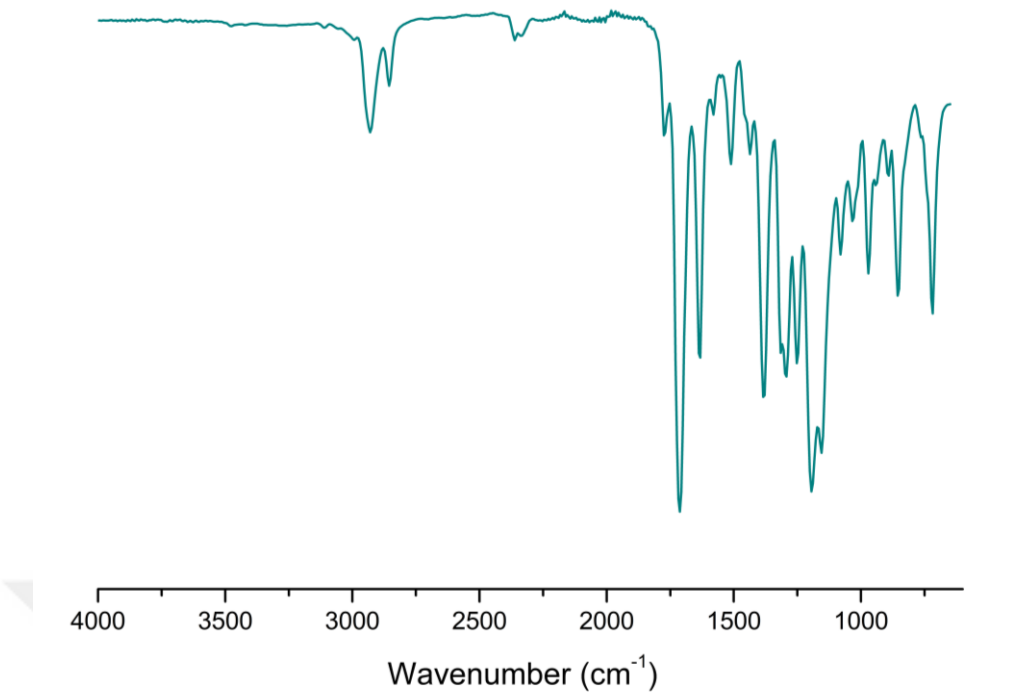

Figure B.5 : FTIR spectrum of methyl propiolate modified P1.

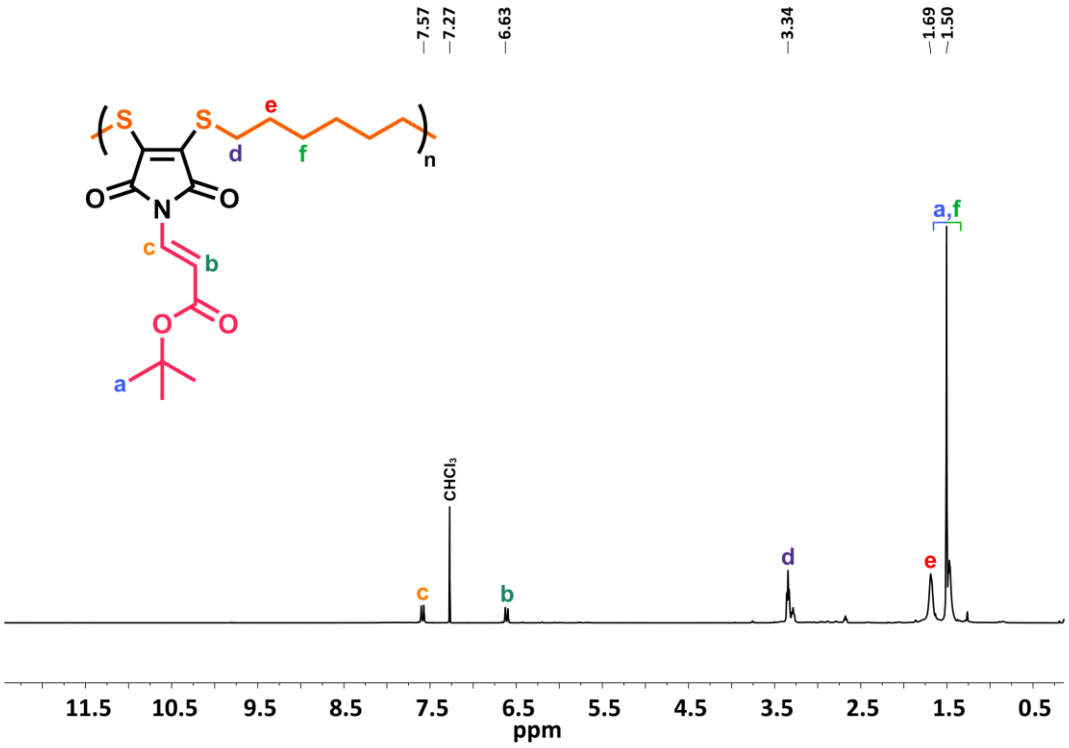

Figure B.6 : ^{1}H NMR spectrum of *tert*-butyl propiolate modified P1 in $CDCl_3$ (500 MHz).

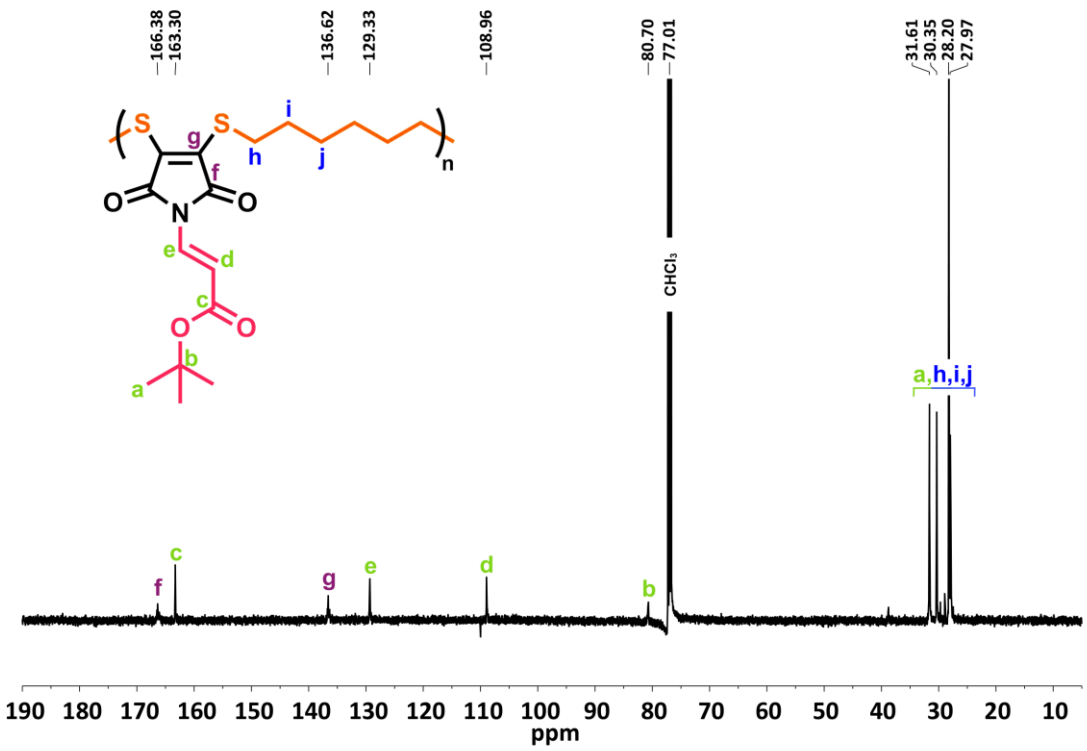

Figure B.7 : ^{13}C NMR spectrum of *tert*-butyl propiolate modified P1 in $CDCl_3$ (125 MHz).

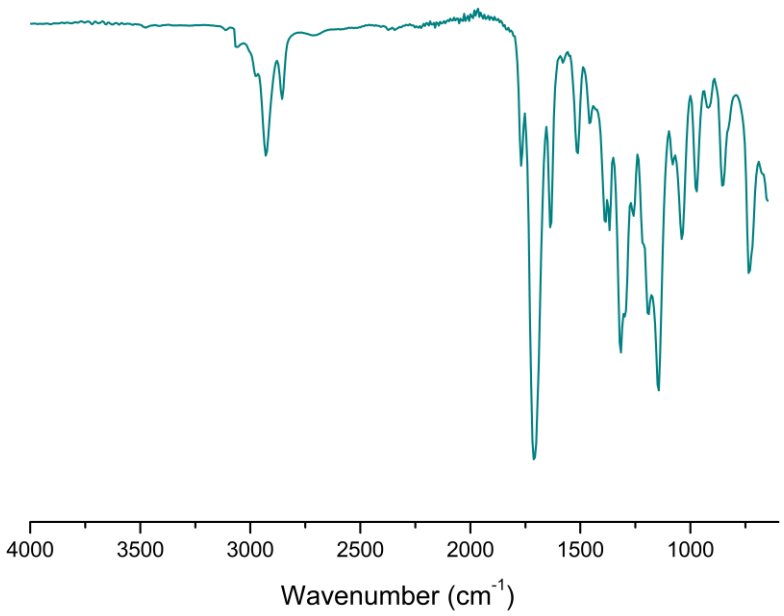

Figure B.8 : FTIR spectrum of *tert*-butly propiolate modified P1.

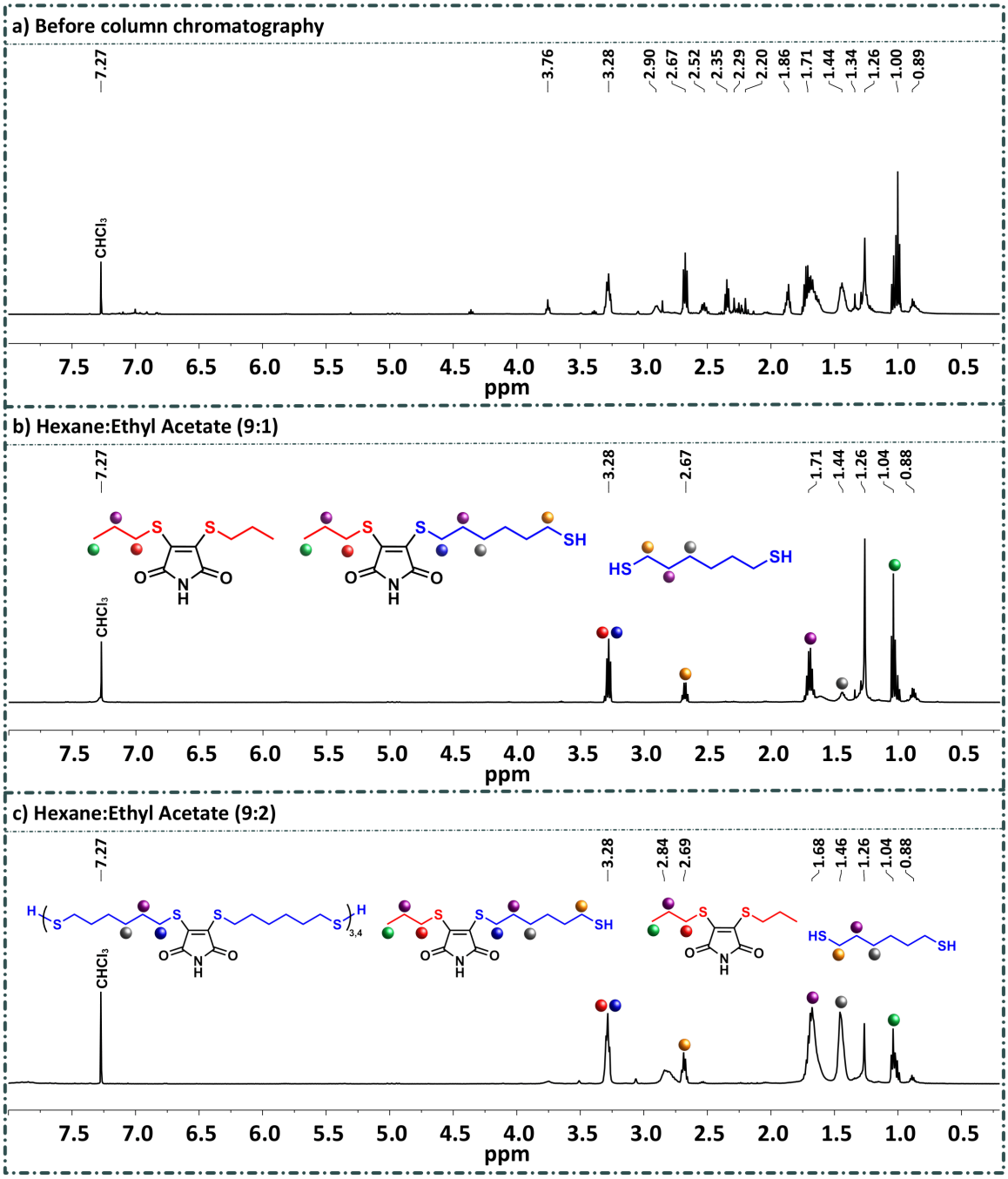

Figure B.9 : Overlaid ^{1}H NMR spectra of degradation products of P1: a) before column chromatography, b) eluting with hexane/ethyl acetate 9/1 (v/v), and c) eluting with hexane/ethyl acetate 9/2 (v/v) in $CDCl_3$ (500 MHz).

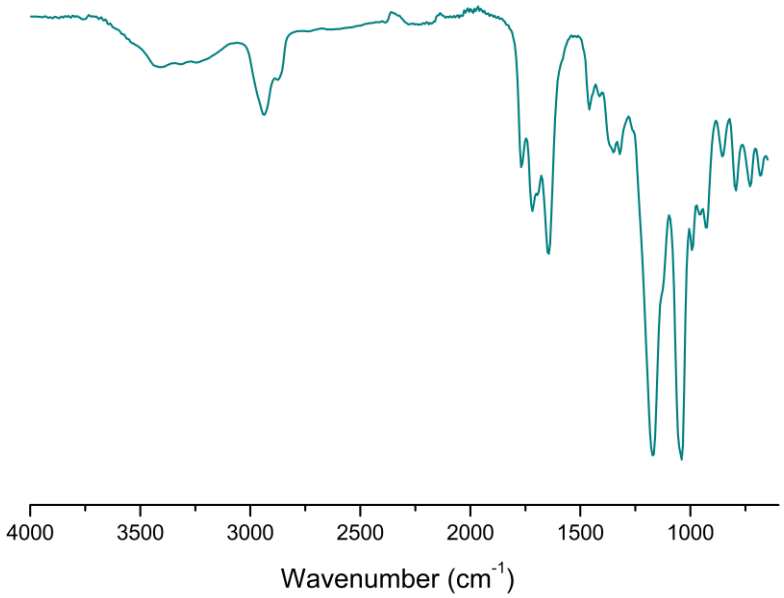

Figure B.10 : FTIR spectrum of degraded P1.

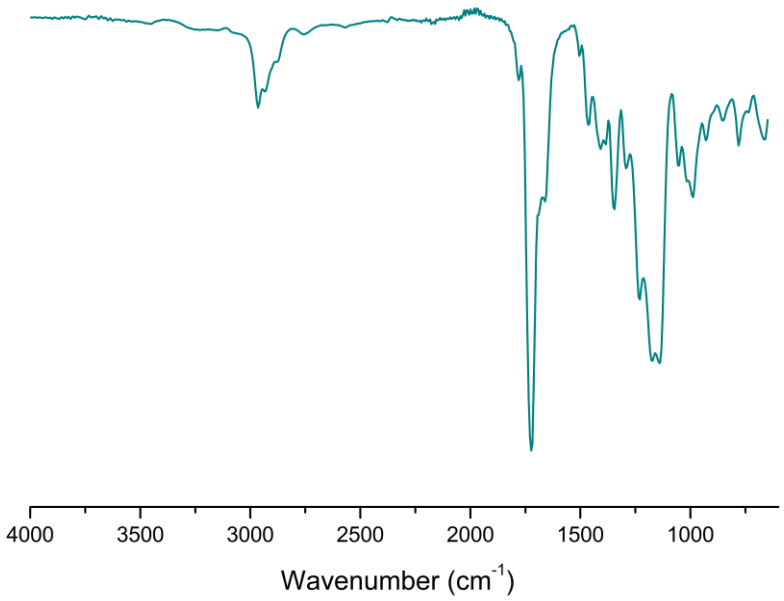

Figure B.11 : FTIR spectrum of degraded cross-linked polymer.

CURRICULUM VITAE

Name Surname **:** Gülşah İlayda TEZCAN

EDUCATION **:**

- **B.Sc.** **:** 2023, İstanbul Technical University, Faculty of Science and Letters, Department of Chemistry

PUBLICATIONS AND PRESENTATIONS ON THE THESIS:

- **Tezcan, G. I**., Aslanturk, O., Sagdic, G., Gunay, U. S. & Durmaz, H**.** (2025). Thiol-dibromomaleimide polymerization: a simple strategy for easily degradable and modifiable polythioether synthesis. *Macromolecules*, *58*(8), 3906–3915.